Electric Powered Jet Ski

March 25, 2021

Project Completed by:

Jacob Ciolfi
Electrical and Computer Engineering

Nathaniel DeSisto
Mechanical Engineering

Benjamin Cyran
Electrical and Computer Engineering

Brendan McClelland
Mechanical Engineering

Andrew Hunt
Electrical and Computer Engineering

Colin McNamara
Mechanical Engineering

Megan McCoole
Electrical and Computer Engineering

Aaron Whitehouse
Mechanical Engineering

Advisors:

Professor Mehul Bhatia
Mechanical Engineering

Professor Matthew Amissah
Electrical and Computer Engineering

A Major Qualifying Project Proposal to the Faculty of
WORCESTER POLYTECHNIC INSTITUTE
In partial fulfillment of the requirements for the
Degree of Bachelor of Science

Abstract

Jet Skis are recreational Personal Watercrafts (PWC), which have grown in popularity over the last decade. These are typically gas-powered and emit high amounts of toxic and potentially harmful hydrocarbons to species in lakes and waterways (Asplund, 2000). The Electric Jet Ski completely rids PWC's of hydrocarbon emissions and is relatively safer for aquatic ecosystems while additionally offering a significant reduction in carbon footprint. The Electric Powered Jet Ski project is an ongoing multi-year effort with the goal of reengineering a 1997 Sea-Doo SPX jet ski to run on electric power at performance comparable to the current gas-powered Jet Ski market. As part of this overarching goal, this project offers the design and successful prototypes of the following components: 1- an electrical drive consisting of a DC brushed motor and controller, 2- battery management system, 3- operator gauges and drive monitoring system, and 4- throttle control. This report outlines the Requirements Engineering, Architecture, Design, and Prototype testing activities and the resulting artifacts developed for the project.

Table of Contents

Table of Figures

Authorship

Jacob Ciolfi is responsible for the sections relevant to the Motor Controller electrical subsystem and editing the Abstract, Introduction, and Background sections.

Benjamin Cyran is responsible for the sections relevant to the Throttle Control electrical subsystem and editing the paper.

Nathaniel DeSisto is responsible for all sections relevant to drive shafts and the mechanical assembly.

Andrew Hunt is responsible for the sections relevant to the Battery Management System and Batteries and editing the Methodology.

Brendan McClelland is responsible for sections related to the motor and weight reduction and working on the background.

Megan McCoole is responsible for working on the introduction and background of the paper, as well as all the sections involving the user display. I also read through the entirety of the paper editing grammar and spelling

Colin McNamara is responsible for the sections relevant to impellers, battery casings, the introduction, parts of the background, and a majority of mechanical methodology section.

Aaron Whitehouse is responsible for sections related to the battery casings and overall assembly of the jet ski

1. Introduction

Polluted waterways increase the water's acidity and develop toxic conditions for marine life and surrounding fauna. These polluted conditions could lead to increasingly unsuitable habitats for aquatic species, potentially resulting in entire populations dying off at once (Hoffman, 2003). A third of marine pollution is caused by airborne emissions (Mackenzie, 2016). Personal watercrafts (PWCs) typically have engines that create greenhouse gas emissions and leak fuel into the waterways. An environmentally friendly jet ski would add a significantly less destructive option for those who want to enjoy personal watercraft and is one step towards creating a more environmentally sustainable future.

Personal watercrafts (PWC) have been around since they first launched in 1973. Since then, the PWC industry has massively grown. In 2000, it was estimated that 200,000 jet skis were sold in the United States alone (Asplund, 2000). As PWC usage increases throughout the country in waterways big and small, the ecosystems and marine environments are greatly affected. In the 1990s-2000s, jet skis mainly were powered with a two-stroke engine (Asplund, 2000). Two-stroke engines are notoriously known for producing highly concentrated hydrocarbon emissions (Morikawa, 1999). Two to three gallons of unburned fuel can be released into water bodies per hour because of jet skis. The water pollution and hydrocarbon emissions from the two-stroke engine in gas-powered jet skis have toxic effects on aquatic life in lakes, oceans, bays, and all bodies of water (Asplund, 2000). Hydrocarbons (HCs) can absorb light and affect plants and aquatic organisms' growth, which rely on the energy from the sun to develop. HCs also alter the water's pH levels, decrease dissolved oxygen, and reduce food availability for organisms that result in the extinction of underwater habitats (Hoffman, 2003). Within the past decade, most PWCs have transitioned to four-stroke engines, which emit less toxic hydrocarbon emissions but still negatively impact aquatic life. For the PWCs to become environmentally friendly recreational-use vehicles, the best option is to transition from gas-powered jet skis to electrically powered jet skis.

The development of electric jet skis has been underway in recent years, but none have yet come to market. Companies looking to try their hand in the electric jet ski market are the Nikola Motor Company, SeaDoo, and Taiga Motors. Universities such as the University of Western Australia have started taking steps toward creating a more sustainable world through PWCs; WPI recently began developing its own solution as well (Stacey, Braunl, Stott, & Knight, 2015).

In the academic year 2019-2020, five students at WPI began converting a stock gas-powered jet ski into an electric jet ski (Soltren, Duffy-Protentis, Quick, Hartwick, & Kolb, 2020). Our team's goal is to continue what they started: completing a first-generation working prototype of the electric jet ski. Additionally, we plan to implement a requirements-driven development process that will support our multidisciplinary project group as well as ensure future MQP's can access and improve on our designs with relative ease.

1.1.1. Prior WPI Electrical Jet Ski Work

The 2019-2020 MQP group ordered essential parts needed to get the jet ski prototyped. This parts list included batteries, an Arduino UNO, electrical jumpers (both Male-to-Male and Male-to-Female), a twist grip handle, an electric motor, a rotary encoder, and various other components as seen in Appendices A and B. They planned out the electrical circuits to use two Arduinos. The team also uninstalled original components from the jet ski, such as the combustion engine, gas tank, fuel system, oil injection system, and exhaust system. When their parts arrived, the Coronavirus had just begun.

The previous group designed parts of the electrical and mechanical systems for the jet ski. These parts included initial research, a functional design for the system, part selection, simulations, and recommendations. Due to the implications caused by the Coronavirus, the previous group was unable to begin physical work on the jet ski. Instead of physically creating the prototype, the group performed multiple simulations for each system.

Our group's contributions are focused on continuing their work to produce a fully functional prototype. Our team consists of eight engineering students, equally divided to work on the electrical and the mechanical system. We utilized the previous group's work and then created individual testing plans. To further advance our project's development, we broke the design phases into different sections: a functional design, a physical design, the finalized design, and the testing procedures.

1.1.2. Project Objectives

The focus of the current project is to manufacture the remaining mechanical pieces, as well as develop the electrical side: motor controller, battery management system, throttle control, and user display. To accomplish this goal, the following initial objectives were specified towards the completion of our project:

1. Understand the functions and components of gas-powered and electric-powered jet skis currently in the market.
2. Describe the functions of each of the subsystems and how they will interact with one another (the Functional Architecture).
3. Define the actual components of each of the subsystems, explore and select from a range of possible implementations for executing the specified functions
4. Design each of the subsystems and interfaces such that they meet specified requirements.
5. Build & test successful prototypes of the design.

1.2. Background

According to the United States Coast Guard, a personal warcraft is identified as a “Class A” boat that is less than 16 feet in length. The allowed occupancy is between one and three people on the watercraft. These boats are considered recreational but require the same amount of education as commercial sizes; however, they are restricted less than commercial sized watercraft due to their smaller size. This provides flexibility for systems such as the electrical system, the flotation requirements, and the power ventilations (PWC, 2020).

1.2.1. History of Jet skis

An inventor named Clayton Jacobson II created the first personal watercraft (PWC) in 1968, consisting of a stand-up craft with jet propulsion (Boating Tech Team, 2016). He secured the patent the following year for his “power-driven aquatic vehicle” ("Personal Watercraft", 2016). Jacobson partnered with Bombardier, a company that manufactures snowmobiles, with the idea to convert the company's Ski-Doo to be operable on water. With Bombardier, they began to work on creating what today would be known as the Sea-Doo. In 1971 after some disagreements in partnership, the patent and licensing rights were turned over to Kawaski before the Sea-Doo came to fruition (Travis, 2015). Kawasaki then released the invention to market in 1972, named the Jet Ski ("Personal Watercraft", 2016).

1.2.2. How Jet Skis Work

The main component that generates thrust in the jet ski is the jet drive. Newton’s third law is very much present and involved in the jet drive for a jet ski. The jet ski movement generated is due to Newton's third law. For every force an object exerts on a second object, there is an equal and opposite force exerted from the second object onto the first one. The impeller exerts a force on the water, which has low mass but very high acceleration, while the water, in turn, places a force on the jet ski in the opposite direction propelling the jet ski forward with obviously greater mass and a lower acceleration ("Personal Watercraft", 2016). Through an intake valve, water is sucked into the jet ski. In order to draw water into the jet ski, an impeller is used. The impeller is driven by the engine and consists of a propeller blade that has a specific pitch and diameter to optimize the flow of water through the jet ski. Having the propeller inside the jet ski prevents injuries that are more common with a boat that has an outboard or inboard-outboard motor because the propeller is contained. The water is then expelled out the back of the jet ski through a steering nozzle. When the handlebars are turned back and forth, the steering nozzle moves to the side and directs the water at an angle to turn the jet ski. If the jet ski is in motion gliding across the water and is not given throttle to spin the impeller, the jet ski can not turn because there is no water to be expelled at an angle from the steering nozzle.

1.2.3. Existing Jet Skis

To date, there are not very many companies manufacturing or even developing electric jet skis. Demand for gas-powered jet skis continues to remain very high, so companies already in the market continue to produce them. The reason electrical jet skis are not developed yet can be due to many factors, including having shorter driving ranges due to battery capacity and the need to charge the batteries, safety concerns with large batteries in close proximity to water, as well as the fact that gas-powered jet skis are easily produced where current electrical jets skis are more expensive (Lampart, 2020).

With recent success in electric transportation such as cars, more and more companies are looking to adapt their own vehicles to an electric version to get in on the up-and-coming market. Two such companies looking to try their hand in the electric jet ski market are the Nikola Motor Company and the jet ski company SeaDoo.

Nikola is one of the leaders in electric vehicles, powersports, and energy. In 2019, Nikola released an announcement for an electric personal watercraft called the Wav (O'Kane, 2019). The Wav features sportbike ergonomics, a 12” 4K user display, instant torque, and most importantly, waterproof components, but gives little other information regarding technical specifications. Nikola’s CEO describes the jet ski as the “future of watercraft” (O'Kane, 2019). The Wav is currently available for pre-order. The model year of the jet ski is 2022, with the exact release date not set, and currently valued at $90,000 (Nikola Corp, n.d.). On top of these two prospective models are the electric jet ski project completed by the University of Western Australia (UWA) and Taiga Motors’ “Orca”, which is currently available to preorder on their website.

The University of Western Australia (UWA) has a Renewable Energy Vehicle (REV) Project that focuses on revolutionizing the transportation sector by creating a fleet of zero-emission and driverless vehicles ("The REV Project", n.d.). They also focus on building charging networks that come from renewable sources. The REV project team consists of engineering staff and students at the university. In 2015, the team reconstructed a 2008 Seadoo 4-TEC into the first electric jet ski in Australia ("REV Electric Jetski", n.d.). The electric jet ski they created eliminated two typical factors in gas-powered jet skis, “excessive noise and heavy pollution of water and air” (Stacey, Braunl, Stott, & Knight, 2015). The team worked for two years to create the electric jet ski. The drive time of the jet ski is 30 minutes but, with more batteries, the team believes it can last for much longer. The largest obstacle the REV team faced was ensuring every component was watertight, keeping the user and everyone nearby safe. The UWA had a specially designed three-phase motor that was water-cooled and built by Submersible Motor Engineering (Stacey, Braunl, Stott, & Knight, 2015). Since 2015, more advancements have been made with the electric jet ski. In 2019, the REV team created the world’s first electric hydrofoil jet ski. With the partner Electro.Aero, the WaveFlyer was created (Reid, 2019).

The Taiga Motors company offers two models, sport and performance, capable of 60 and 65 MPH as well as 120 and 180 HP, respectively. The two models also boast total weights of 533 and 588 pounds, with the performance model having a capacity of three riders. Both Orca models can run for up to 2 hours of riding but are easily rechargeable and require zero maintenance (Taiga Motors, n.d.). The charge time of the PWCs is 3 hours for a full charge and 20 minutes to reach 80% charge using DC fast charge. Their user display consists of a 7" HD color center console and has many features, including GPS, LTE, Wifi, and Bluetooth (Taiga Motors, n.d.). The Orca is only currently available for pre-order, as it has not been released to market. The current release date is the Summer of 2021, and it costs $15,000 (Taiga Motors, n.d.).

Jet skis have just recently begun to be a part of the shift to electrical power. At the moment, there are only a few electric jet skis on the market to be pre-ordered by the consumer. Still, multiple organizations are currently working on them in an effort to reduce pollutants and create a more environmentally sustainable device. As more and more companies delve into the electric vehicle market, the traditional combustion engine is seeing less and less use as a means of power production.

1.2.4. Impacts of Electric Jet skis

Electric vehicles have been gaining more and more attention in recent years with the success of companies such as Nissan and Tesla in the field of electric cars. While opting for an electric motor instead of a combustion engine can have some drawbacks, such as a shorter driving range due to battery capacity and the need to charge the batteries, many benefits come with that decision. To start with, electric motors are more straightforward than combustion engines and have a generally longer life due to easier maintenance. The electric motor is more reliable to function properly and far easier to diagnose when not working. It is also far quieter than the internal combustion engine, making for a more enjoyable ride (Domonoske, 2019).

These watercraft vehicles have begun to be converted into electric vehicles partially because of their environmental benefits. Two-stroke engines leak millions of gallons of unburned fuel into the waters each year (Pearce, 1998). This fuel is detrimental to the organisms affected by it. Electric vehicles provide safety where significant leakages would never be considered an issue. If a watercraft carries 4 gallons of gas, roughly 1 gallon will leak into the water (Pearce, 1998). These gas leaks are hazardous to the environment. The Clean Air Act protects the public health by regulating the emissions of these harmful air pollutants. Burning fossil fuels releases gases and chemicals into the air. Air pollution is exacerbating climate change. An electric jet ski in comparison to a gas vehicle would reduce these negative environmental hazards.

The electric jet ski is a nature-friendly alternative for gas-powered vehicles. Electric vehicles are several times more efficient in converting energy into vehicle movement (Lambert, 2020). They can produce no emissions while also providing a much lower life-cycle emission level. When charging an electric battery through renewable energy sources, operating an EV is nearly emission-free. Heavy industries facilitate and complicate the transition to a net-zero

emission energy system. Vehicles have begun this transformation, leading the way for more companies to follow. Electric jet skis can have negative environmental implications when disposing of these unwanted batteries. These batteries require a large amount of additional work to ensure they are safe to dispose of. Batteries have to be sorted by type, discharged, disassembled, and removed from consumer products before they can be safely disposed of. (US EPA, 2016) Even with the additional complications introduced by the need to dispose of electric jet ski batteries, the electric jet ski is still much more environmentally friendly than gas-powered jet skis overall.

To create this transformation into an electric jet ski, exterior components had to be implemented in the jet ski. The jet ski originally purchased was a gas-powered jet ski, and conversion to an electric jet ski required additional electrical parts and systems. All of the parts purchased for the jet ski were purchased by two separate teams: the 2019-2020 electrical jet ski MQP team and our current 2020-2021 team. These purchases were made in 2019 and 2020, respectfully. Additional parts purchased in 2020 started with suggestions from the 2019 group. Extra features were implemented in 2020, which were purchased after our examination of the current state of the project.

1.3. Methodology

The System Engineering 'V' model shown in Figure 1. was adapted for this project. The left side of the V diagram is concept development and design. This area of the cycle focuses on the decomposition of requirements to individual functions and tasks to be designed and tested separately. The V diagram's right side represents integration and testing, where all components are combined into the final system.

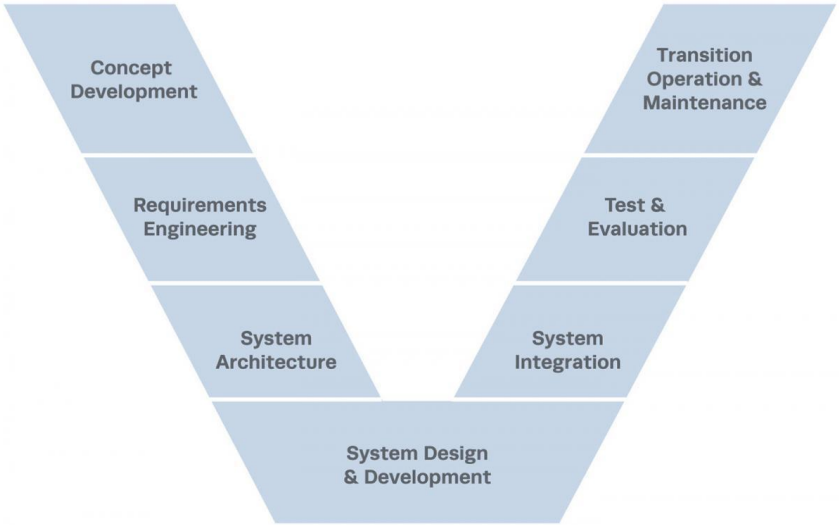

Figure 1. Methodology Process (Mitre, 2016).

With regards to this overarching approach, our MQP group proceeded from the system architecture phase. Due to limitations brought on by the Coronavirus pandemic, the project concludes with successful component and subsystems testing, falling short of a complete assembly and testing of the Jet Ski.

2. System Architecture

After considering the history of jet skis, how gas-powered jet skis are made, and what consumers' main priorities are, the system architecture can be determined based on all of this information. In this chapter, we discuss the high-level architecture of the electric jet ski. We consider the purpose of the Jet Ski primarily from the operator's perspective, referred to as the primary stakeholder. The following needs (given below) were identified as relevant to the main stakeholder:

- Operate in a safe manner
- Travel at a reasonably fast speed
- Have seating and controls be comfortable
- Easily rechargeable
- Waterproof
- Have the display be visually pleasing
- Easy to function
- Intuitive controls
- Operate for at least 2 hours at a time
- Fast response operation time during use

The jet ski is made up of electrical and mechanical components, with the jet ski operator also being a vital component of the system. The electrical components are seen in blue and made up of: the throttle control, motor controller, user display, BMS, and battery. The mechanical components are in red and consist of the drive shaft and impeller. The motor is what ties the electrical components to the mechanical components. The overall functional architecture for the jet ski system can be seen below in Figure 2.

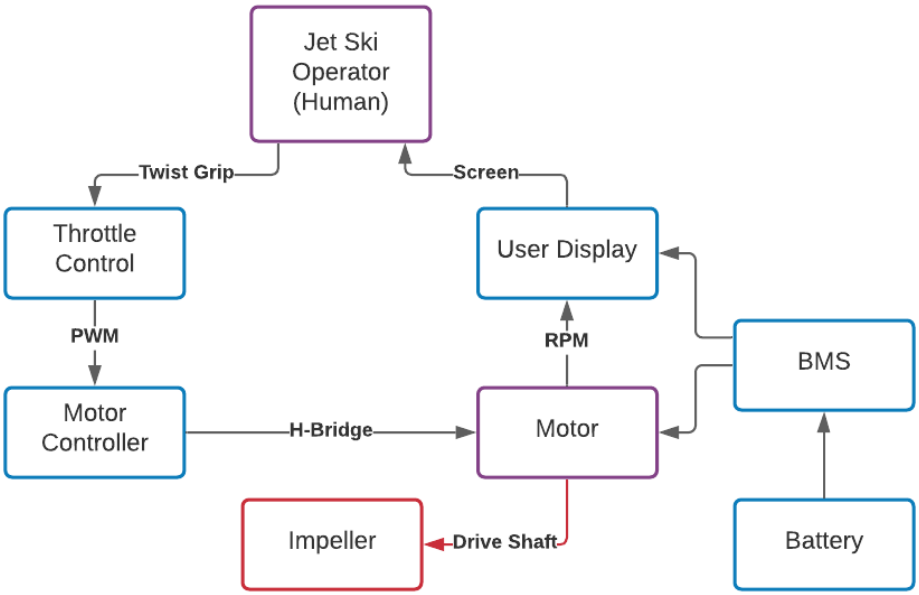

Figure 2. Overall Functional Architecture

Each block in the functional architecture adds a specific set of functions to the overall design. The throttle control gets the user speed input and drives the motor controller. The motor controller drives the motor using the H-bridge. The BMS ensures battery charging and discharging are done in a safe and controller manner; it also sends battery information to the user display. The user display communicates information about the jet ski to the operator. The motor then controls the impeller using the drive shaft. Subsequent sections further expand on the components illustrated in the functional architecture.

2.1. BMS

The batteries in the jet ski are responsible for powering everything in the jet ski, but mainly the motor. The electric motor will be drawing the most power, so the batteries must be large enough to power the motor through the motor controller. With large battery systems such as this, it is crucial to have a battery management system.

The battery management system, as seen in Figure 3, is responsible for multiple tasks to make sure that the system is electrically safe. The different responsibilities of the BMS are to measure battery capacity, state of charge (SoC), state of health (SoH), and temperature. In addition, the BMS is responsible for cell balancing. Cell balancing is important for making sure that each battery cell is producing the same voltage. This is done by setting a low voltage cutoff and a high voltage cutoff. When cell balancing is enabled in the BMS, it determines the battery cell out of a group to be the main balancing cell. This cell is chosen by having the highest voltage out of the selected group, having a higher voltage than the low voltage cutoff, and having a higher mean voltage than the group. The BMS evaluates the cells after a set time and makes sure that all of the cells are producing similar voltages.

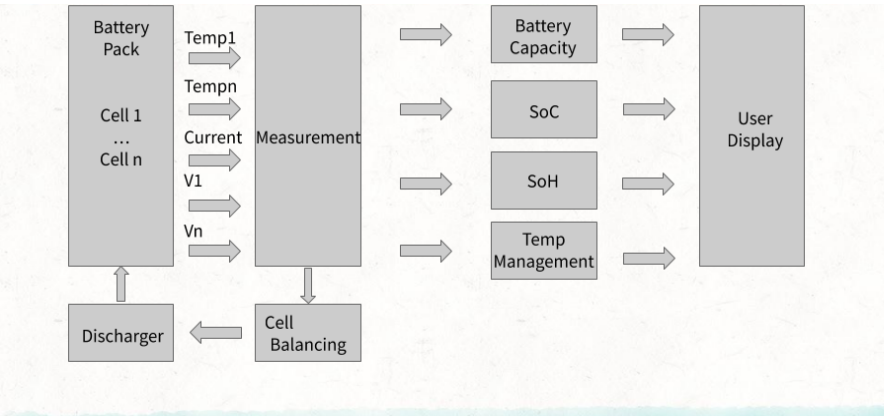

Figure 3. Battery Management System Diagram

Physically, the only requirements for the battery system are the overall size and weight of the battery. The previous MQP team determined the jet ski would have a performance goal of 50mph, including the jet ski, two passengers, and 22lbs of luggage. The battery system must fit in the given fuel compartment of the jet ski and must remain lightweight enough for the jet ski to remain power efficient. In addition to this, the display portion of the BMS must be able to fit on the dashboard of the jet ski and be waterproofed while keeping the touchscreen usage.

2.2. Motor Control

The motor controller, as seen in Figure 4 below, controls the speed and direction of the motor based on the user's input signal from the throttle controller. The motor controller also includes the dead man switch, which cuts power to the engine if the rider falls off. Additionally, the motor controller estimates the motor's rotations per minute in real-time, which is used in the user display. The user's only direct interaction with the motor controller is from the dead man switch; speed and direction are input by the user from the throttle control, which then signals the motor controller electrically.

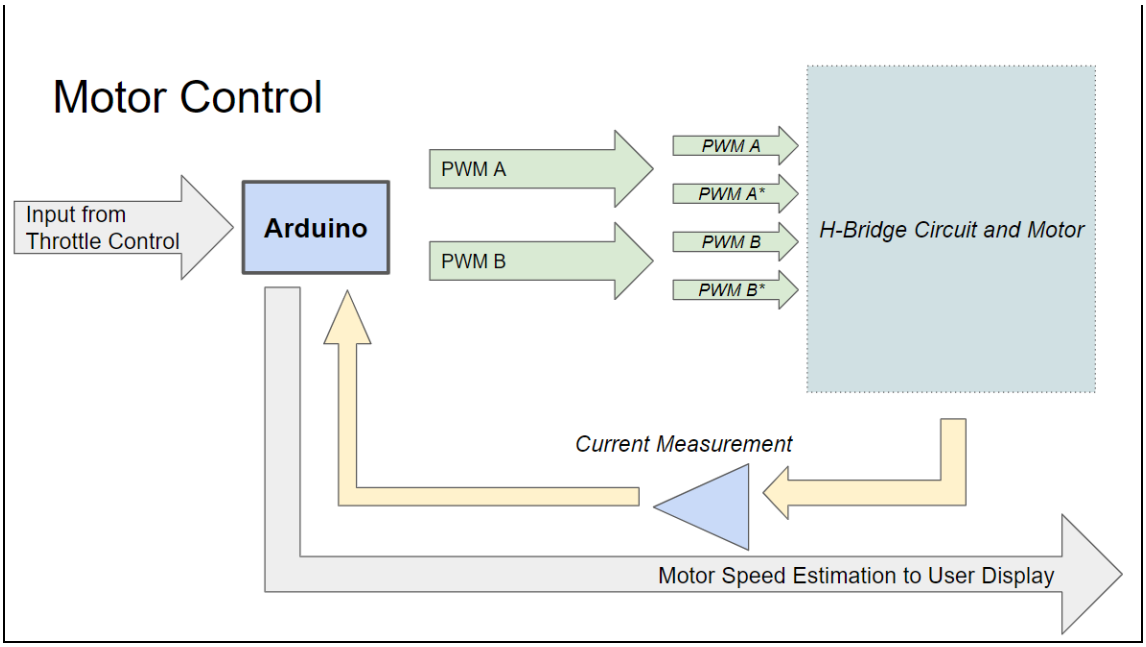

Figure 4. Motor Controller Block Diagram

The motor speed and direction are controlled by an H-Bridge circuit, which is driven by two pulse width module (PWM) signals from the Arduino. One signal drives forward motion, and one signal drives reverse motion, while the duty cycle of the PWM signal regulates the motor's speed. Each of the two PWM signals from the Arduino, PWM A and PWM B in Figure 4 above, are split and run through an inverter. This results in 4 final signals driving the H-Bridge: PWM A, PWM A* (the logical inverse of PWM A), PWM B, and PWM B* (the logical inverse of PWM B). By driving both left-side switches with PWM A and PWM A* and both right--side switches with B and B*, one side can never short out because both the top and bottom switches on one side can't both be closed at one time. To control forward and reverse, only PWM A or PWM B will be driven (pulsed) at one time; the other will remain tied off. The dead man switch is implemented as an Arduino interrupt, where if triggered, the Arduino will tell the H-Bridge controller to cut all current delivered to the motor. The motor's RPM is estimated using ripple counting techniques, implemented with a differential op-amp measurement taken across a current sense resistor between the bottom of the H-Bridge and ground. This current measurement is taken in by the Arduino and used to estimate the RPM of the motor.

The motor controller must be able to drive the motor to at least 2423 RPM and 90.25 Newton-meters and estimate the motor's RPM to within 25 rotations per minute. The dead man switch must be able to cut power to the motor within 0.25 seconds of being triggered. All electrical components will be powered from the main battery on the jet ski, requiring no additional power source.

2.3. Throttle Control

The throttle control is the physical connection between the operator and the jet ski's performance by controlling the operation of the electric motor in the watercraft. The throttle control consists of two physical components: the half-twist throttle grip and the Arduino UNO microcontroller. The main operation for the user is to signal how fast they want the motor to operate at a given condition by a twist signal.

The half-twist throttle grip is for the rider to choose an amount of power they would like to be sent to the motors. The further twist correlates to the further amount of power requested. The half-twist only rotates 180 degrees, as explanatory in the name. The half-twist grip has several types of similar products that would accomplish the objective. The 2020 group purchased an EBIKELING twist thumb throttle grip. A thumb grip only rotates on the right hand's thumb-side compared to the whole handle. This is preferred by most beginner riders, as only motorcycle riders are comfortable for the whole handle to rotate. This is because newer users are more likely to adjust their grip frequently, which could, by accident, change the twist. The half-twist throttle grip acts as a hall sensor. A hall sensor will detect the voltage difference created in the sensor when exposed to a magnetic field. This is way more preferable than a potentiometer, as a potentiometer has a resistance value. This resistance will lose energy in the form of heat and would release that heat into the twist grip handle; this can be shown by breaking the twist grip apart, as shown in Figure 5.

Figure 5. Half-twist grip hall sensor (Endless Sphere, 2016)

The 2019-2020 group initially planned to include a rotary encoder in the Arduino UNO. The rotary encoder sends two square waves, outputs A and B. Each square wave is 90 degrees out of phase with each other. The number of pulses for the square wave depends on the amount of rotation applied to the twist grip. Every time the A square wave goes from positive to zero, we read the value of the B pulse. When the encoder is turned clockwise, the B pulse is always positive. When the encoder is turned counter-clockwise, the B pulse is negative. By testing both

outputs with a microcontroller, we can determine the direction of the turn. By counting the number of pulses, we can determine how far it was turned. This was determined not to be necessary to the overall design as the half-twist grip could accomplish the rotary encoder's whole goal through code. It could provide use during the resting phase but was deemed unnecessary. The Arduino UNO will send a PWM to the motor controller. This Arduino UNO is the same one that is operating the user display and the motor controller.

There are not very many physical requirements for the throttle control. All specifications are based on convenience for the operator. The twist grip must have an accuracy of +/- 5 degrees in rotation. This ensures the operator does not have to understand the amount of power they are using; rather, it is subconsciously understood. The twist grip is a half twist grip, meaning it only rotates roughly 180 degrees. This specification is more impactful as the change in degree is half the amount of the planned 360 rotation initially set.

2.4. User Display

The user display was constructed in order for the operator of the PWC to have access to live data about their ride and watercraft. The user display shows the information seen in Figure 6: the user's speed, battery information, and water safety notifications.

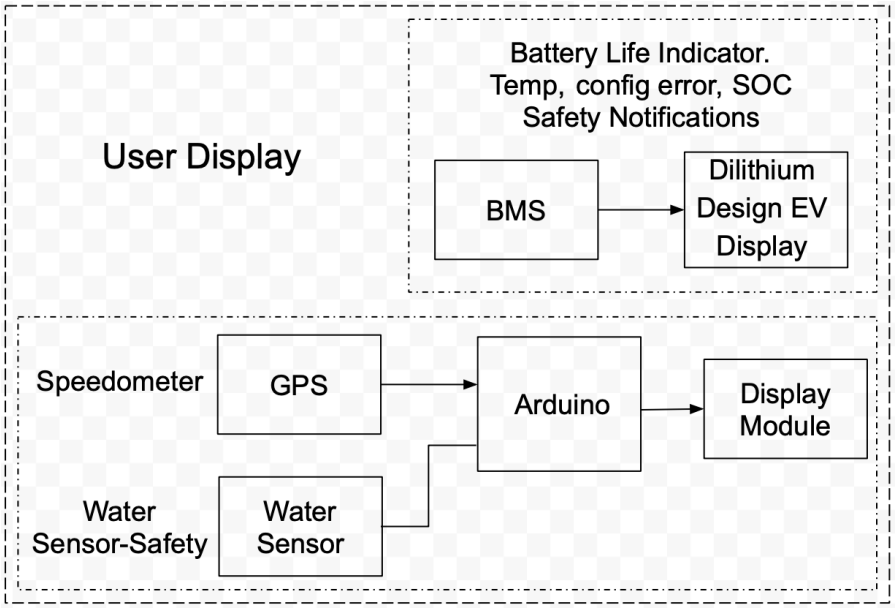

Figure 6. User Display Block Diagram

The purpose of the speedometer is to let the user know how fast they are going in order for the user to maintain a safe operating speed and meet any speed limits that are posted on the body of water that the PWC is driving within. The water safety sensor's purpose is to inform the user that waterproofing within the jet ski may have failed or water has somehow made it into the jet ski hull. Having water interact with electrical components is an imminent safety hazard for the user, passengers, or nearby water enthusiasts. An Arduino was coded to display all of the information modules, and the information was displayed on an OLED display. The purpose of

the battery information display is to show how much power remains in the battery before the PWC stops running; therefore, the user will know when to charge the PWC, as well as SOC and other safety warnings.

There are functional requirements that must be met by the different components of the user display. The speedometer needs to be able to display the speed within +/- 2 mph at a steady speed and display fast enough that when the user is operating the jet ski on the water, there is not a visible lag in the speed. The water safety sensor needs to notify the user that water is present within the PWC when it comes in contact with water 98% of the time. There are various features within the battery information display, but the main component is the battery life indicator. The functional requirements for this were previously stated in the battery management section. The functional requirements set for each of the components were utilized and kept in mind when designing the overall user display.

Along with the functional requirements, there are physical constraints for the user display that would have to be met to maintain the jet ski's manufactured design; otherwise, the jet ski display design would have to be altered. The reasons for choosing to maintain the current physical design as much as possible are to reduce the cost and time of restructuring the display area to fit the new components. The manufactured design of the inherited jet ski includes three holes to display the user data. Each hole is roughly 3 inches in diameter and must be waterproof, as it is exposed to the outdoors. Although there are physical restrictions to the user display based on the inherited jet ski design, the physical architecture can be altered if the following criteria are met:

- There are funds to restructure the user display area
- The new dimensions can fit within the dash area of the jet ski
- The display is either waterproof or made waterproof
- The seal from the new hole in the jet ski is sealed to be watertight.

2.5. Shafts

Shafts are important components of almost any mechanical system. They are used for many reasons, such as transmitting power, support, and transporting a load. There are four main categories of shafts: posts, rods, linear shafts, and rotary and drive shafts. Rotary and drive shafts are used for power transmission applications. They transmit torque and can withstand heavy torsional forces.

For our application, the drive shaft is used to transfer torque and engine rotation to the impeller. Drive shafts require high tolerance standards because they need to rotate accurately without causing unnecessary vibration. The length tolerance needs to be high as well because drive shafts can be used for direct mounting.

Drive shafts transmit torque, serving as a connection between two parts. For the jet ski, it will connect the motor and impeller. There are many types of alterations that can be made to

make sure there is a precise fit. Some examples of alterations to accommodate mating the parts include: wrench flats, keyways, retaining ring grooves, threaded, and tapped.

2.6. Battery Casings

Of course, when conceptualizing an electric jet ski, the first thing that comes to mind is the battery. The batteries are the source for all power of the jet ski, specifically the motor and display modules.

Because the jet ski will be powered fully by the battery, one must think of the battery type and its capabilities. For our project, we will be using 24 Nissan Leaf batteries, which were purchased by the 2019 MQP group. Although these are not the most capable batteries on the market, they are suitable for our project as they are cheaper than competitive batteries and fit within our project's budget. Additional benefits include that they are lightweight and easily interchangeable.

One of the main concerns when conceptualizing an electric-powered jet ski is the waterproofing of the electrical system, and in particular, the batteries themselves. Batteries for watercraft are made to get wet; however, a battery that is well maintained and kept dry will have a much longer lifespan. The top and bottom half of the hull are held together by a strong epoxy (polyester resin) that creates a watertight seal between the two hull pieces (Kelly & Kelly, 1991). Even with this watertight seal, we still need to account for any small leaks or hull breaches, and extra protection for our battery system will lead to the longevity of our batteries.

The main difference between electric and gas-powered jet skis is in the way with which they need to be recharged with fuel or electrical energy. Gas-powered jet skis have user-friendly methods for refueling their jet skis. It is as easy as pouring fuel into an outlet on the outside of the jet ski. The electric jet ski needs to charge each battery within the PWC when power is low. This can be a very strenuous and complicated task. The user's ease of accessibility of the batteries for recharging is crucial to the performance measurements of the battery casings.

The main performance metrics of the battery casings for our electric jet ski are based on their level of waterproofing, degree fit of the batteries (do the batteries move around in the box), and user-friendly accessibility for recharging of the batteries.

2.7. Impeller

The impeller is the mechanical component of the jet ski at the back of the hull that is connected to the motor and rotates, creating a stream of water that propels the jet ski. The pump impeller generates a pressure difference due to the pushing out of the water by the back face of the blades on the impeller and the pulling in of the water on the front face of the blades as they rotate. The positive/negative pressure differences due to centrifugal forces are the mechanisms that allow the water to be controlled and pushed out at high speed, which in turn launches the jet ski forward.

The pitch of the impeller blades is a key property of the impellers that helps with controlling the acceleration, centrifugal force, and velocity of the water and, therefore, the jet ski. Pitch describes the angle of the blades within the impeller. As the pitch decreases, the top speed decreases, and acceleration increases. As the pitch increases, the speed increases, and acceleration then decreases. In order to get the best of both worlds in having good acceleration and speed, most jet skis have progressive pitch impellers. This means that the angle of the impeller blades changes as the blade extends to its outer edge. This will help increase acceleration without having to sacrifice the top speed.

The pump impellers used in jet skis have been mainly manufactured in stainless steel. The material is very strong, very dense, and does not need much volume in order to generate strength. The disadvantages of using stainless steel for impellers are that they are heavy and can wear over time.

Newer materials are becoming prevalent in place of stainless steel that are much lighter, similar in strength, and have much better wear resistance, which is carbon-fiber composite impellers. The carbon-fiber composite impellers will also help with cavitation within the blades, which is a common cause of failure for pump impellers in jet skis. Carbon fiber has a similar elastic modulus to steel, and even a higher modulus in some cases, while also having a much lower density, making carbon fiber parts much lighter than their steel counterparts (Liu, Zwingmann, Schlaich, 2015).

2.8. Project Management

To accomplish a detailed design of the components discussed, sub-teams were created, and each group member was tasked with the design of a subsystem/component. The table below shows the team member and component design task allocations.

Electrical and Computer Engineering	
Battery Management System	Andrew
Motor Controller	Jake
Throttle Control	Ben
User Display	Megan
Mechanical Engineering	
Battery Casing Design & Manufacturing	Aaron
Battery Casing Design & Manufacturing	Colin
Motor Mount & Drive Shaft	Brendan
Motor Mount & Drive Shaft	Nate

Table 1. Component Allocations

To ensure that all parts work well together when assembled, they are first each individually tested and verified to meet their own required specifications. Once components meet specifications individually, adjacent components are assembled and tested, ensuring that the interfaces between the components were correctly implemented. This component-by-component combination and test method will be followed step by step until the entire jet ski is assembled, tested, and verified as an overall unit.

3. Design

After defining the systems architecture, our fourth goal of the project is, “Design each of the subsystems and interfaces such that they meet specified requirements.” In the designing process, the system architecture is utilized. The functional and physical requirements laid out in the previous section must be met when developing the overall design of each of the components.

In this chapter, we discuss the analysis, design, and development of components for the electric Jet Ski. The design of the electrical jet ski began last year with the 2019-2020 Electrical Jet Ski group; therefore, the continuation of the design this year utilized and expanded on the inherited parts. The list of inherited electrical parts from the previous MQP group is given in Appendix A and B. In the following subsections, we outline the rationale, analysis, and final design outcomes for each of the subcomponents of the Jet Ski discussed in the previous chapter.

3.1. BMS

Most components for the battery system were selected by the previous MQP group. Their selection was based on a value analysis that was conducted. The batteries chosen are Nissan Leaf Lithium-Ion batteries. The analysis done to pick these batteries compared the life span, performance, specific energy, specific power, and cost. These batteries are rated at 7.6V, 500W 66Ah. The determined configuration of the batteries was to use 12 cells in series that are in parallel with another 12 cells in series. Each series of 12 cells produces 91.2V, 6kWh at nominal voltage.

The BMS chosen was the Dilithium Design Battery Management System. This BMS is capable of controlling 24 cells, which fits the design needed. This BMS is also used in electric cars, so it suits the usage of an electric jet ski. The BMS is also capable of adding more satellites (BMSS), which allow for another 24 cells to be added to expand power if needed. The main controller (BMSC) consists of a BMS processor which holds the firmware that provides interfacing for 12V power, CAN bus, cell loop, serial port, and LED. This processor communicates between the measurement boards, which are Linear Technologies LTC6811 multicell battery monitor chips. These measurement boards are each capable of monitoring up to 12 battery cells each and are measured in less than 2.5ms with an accuracy of ∓ 1.2mV. The LTCs also support diagnostics, which will identify any physical/wiring errors such as short/open circuits to help minimize any damage that can be caused by user error. In addition to this, they are responsible for cell balancing and are designed to minimize power consumption during long-term storage. The full BMS architecture can be seen below in Figure 7.

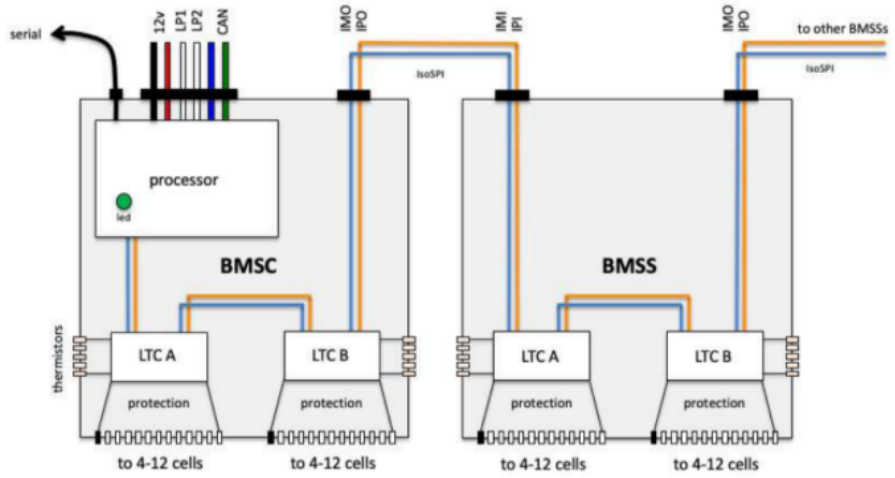

Figure 7 BMS Architecture (Thunderstruck, 2019)

The BMS system also consists of a Dilithium Design Electric Vehicle Display. This display is a touchscreen display that is 2.55” tall and 1.91” wide. This display allows for the user to quickly monitor the battery voltages, SOC, and can also be used to configure many of the voltage settings, such as the high and low voltage cutoffs. When used with the EVCC, the display can also be used to monitor the charging history of the batteries. The display is also used with an optional Hall Sensor. This sensor is connected using a given 4-pin connector. It is connected directly to the display using +5V, GND, Vo, and Vr connections. This sensor is supplied with a PCB made by Thunderstruck to allow for easy connections. The display also has a 5-pin connector to connect to the BMS. This consists of +12V, GND, CL, CH, and GA. These connections can be seen in Figure 8 below, showing the EV Display Architecture.

Figure 8. EV Display Architecture

3.2. Motor Control

The motor controller drives the ME1002 motor and is run by an Arduino Uno using the schematic in Figure 9 below. The H-Bridge consists of two IRFP4468PBF N-channel MOSFETs for the bottom two switches and two SUP70101EL P-Channel MOSFETs for the top two switches, driven by two PWM signals from the Arduino; one PWM signal drives both left-side switches (A_{TP} and A_{BT}), and one PWM signal drives both right-side switches (B_{TP} and B_{BT}). The PWM signals are digital logic and are HIGH at 5V and LOW at 0V. The top switches are preempted by a BJT-based inverter circuit, such that the top switches remain open when the PWM signal is HIGH and close when the PWM signal is pulled LOW. In this way, a left-side HIGH PWM signal closes the bottom switch and opens the top switch, while a LOW PWM signal closes the top switch and opens the bottom switch. This BJT circuit has a very low current and voltage through it, so it is based on the commonly available 2N5550 NPN BJT. When PWM1 is LOW, the BJT is biased on, connecting the bottom of R_{BOT} (R2 and R5) to ground and forming a resistive divider between Vbatt and this BJT ground. R_{TOP} (R1 and R7) and R_{BOT} make this resistive divider, and their values dictate the voltage that the PMOS gate is biased to. When PWM is pulled HIGH to 5V, the BJT is biased off. The bottom of R_{BOT} is floating, there is no voltage drop across R_{TOP} or R_{BOT}, and the PMOS gate voltage is equal to its source voltage, turning it off. With R_{BOT} value of 25kOhm and R_{TOP} value of 4.4kOhm, Vgs is pulsed ON at

0.15*Vbatt. With a datasheet-specified maximum threshold voltage of 2.5V, the circuit should work as intended with a Vbatt voltage as low as about 16.67V. Vbatt must not exceed 100V, as this is the breakdown voltage of the PMOS, and both top switches may fail and short.

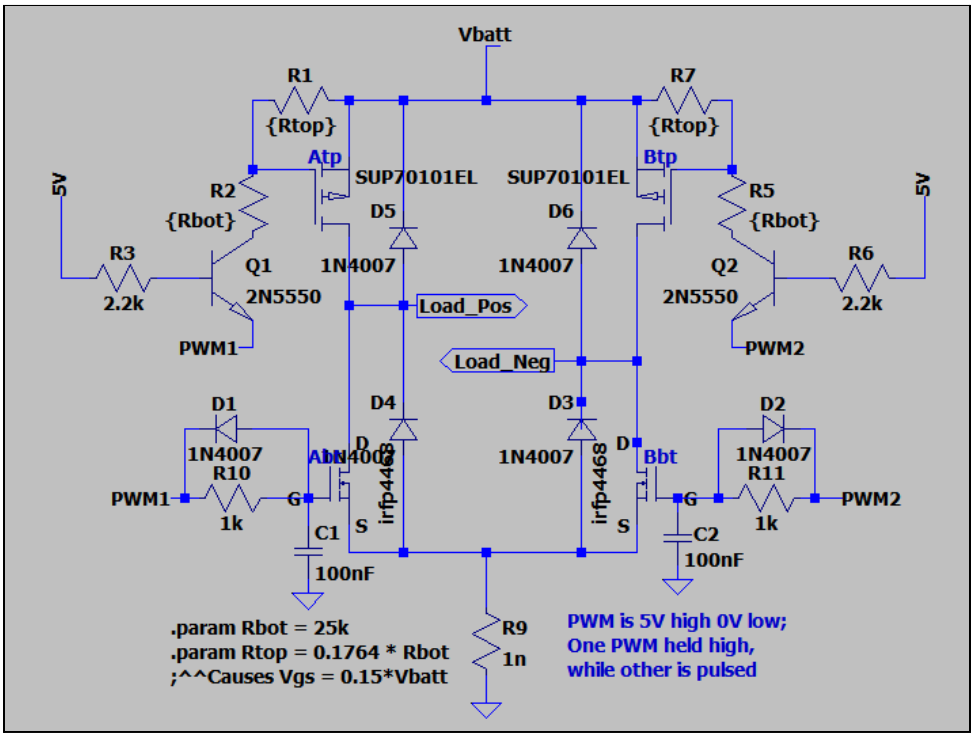

Figure 9: H-Bridge Architecture

The bottom side switches are more straightforward; NMOS sources are tied to ground, and gates are tied to PWM. When PWM is LOW at zero volts, the switch is open due to a gate-source voltage of zero. When PWM is pulled HIGH at five volts, the switch is closed by a gate-source voltage of five volts.

PWM	Top Switch	Bottom Switch
PWM High	OFF (open)	ON (closed)
PWM Low	ON (closed)	OFF (open)

Table 2. Single PWM Example

The table above shows switch positions by PWM state for a single side of the H-bridge. PWM1 controls top and bottom switches on the left side, and PWM2 controls top and bottom switches on the right side. To prevent both top and bottom switches on one side from being closed at once during the PWM transition, creating a short from battery to ground, a small delay circuit is created at the gate of the bottom switches using a resistor, capacitor, and diode. The resistor and capacitor act as an RC delaying circuit when turning on the bottom switch, ensuring the slower top switch has enough time to fully turn off before the bottom switch turns on. To

prevent delayed turn off for the bottom switches, the RC circuit is bypassed by a diode biased such that the bypass is only enabled when turning off the bottom switches, meaning that while the bottom switches have a delayed turn on, there is no delay when they are turning off.

Below, the two graphs in Plot 1 show the operation of the circuit in simulation while PWM 1 is used to modulate one side of the motor from V_{BATT} to ground, and PWM 2 is held HIGH at 5V in order to keep the other side of the motor grounded. The top graph shows PWM 1 and PWM 2, with PWM1 being the green line modulating between HIGH of 5V and LOW 0V, while PWM2 is held LOW. The bottom graph shows the voltage across the load in red, modulating from V_{BATT} (99V, shown in teal) to ground, in phase with PWM 1's modulation. These two graphs show the simulated H-bridge operating as intended, as the load has the full V_{BATT} voltage across it when PWM 1 is pulled LOW, and there is no voltage across the load when PWM 1 is pulled HIGH.

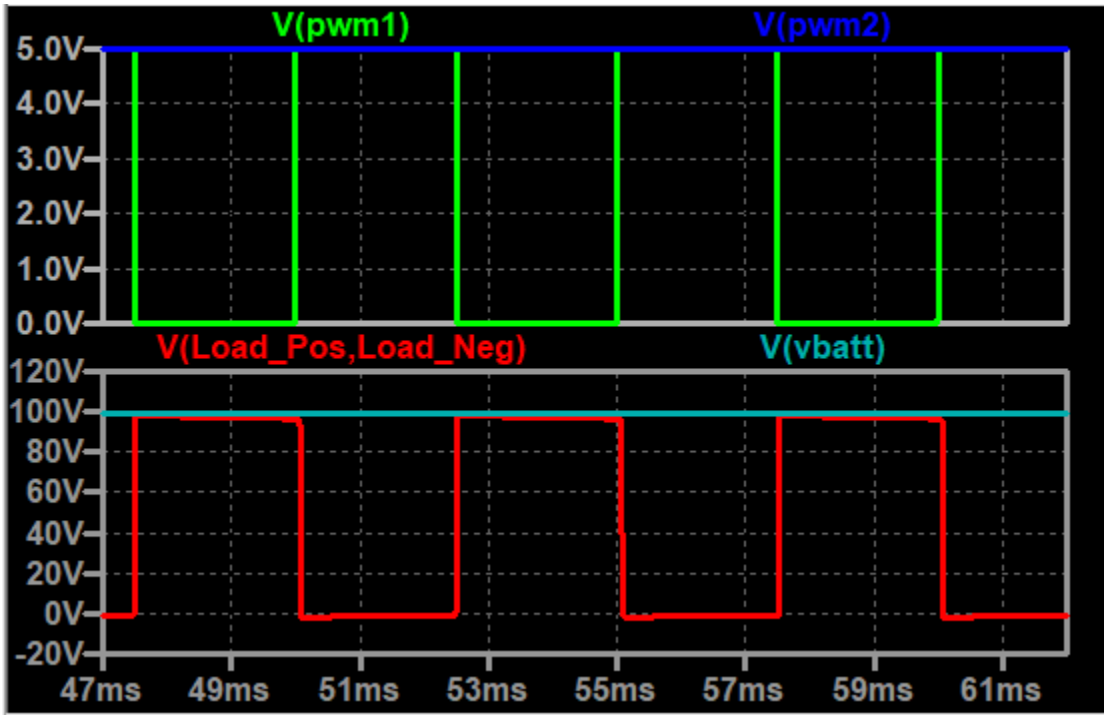

Plot 1. H-Bridge Simulation

To estimate the RPM of the motor, the current generated by the motor could be sensed by an MCP6024-E/P operational amplifier, measuring the voltage drop across a small sense resistor. The sense resistor is seen as R9 in Figure 9 above, with the current sense circuitry not depicted. Power to the Arduino should be delivered with a buck switching power supply, powered by the main battery, and still to be designed.

3.3. Throttle Control

All components for the throttle control were selected by the previous MQP group. Their selection was based on a value analysis that was conducted. These parts consist of a half-twist grip handle and an Arduino UNO. The half-twist grip purchased consisted of three signals; an enthode, +5V, and a signal source. This signal source pin allows a generated value to be sent from that pin. That value, when decreased or increased, will allocate the direction of the twist grip. A value of 1023 is correlated to a full twist, and a value of 0 is sent when it is at rest.

The simulation for the throttle control had to be altered as the component of a half-twist grip is not already created. Several companies that make similar components were reached out to, and no datasheet, nor manual, had been found. The twist grips use electromagnets to control the voltage and create a signal. How the twist grip operates can be illustrated in the simulation shown in Figure F.

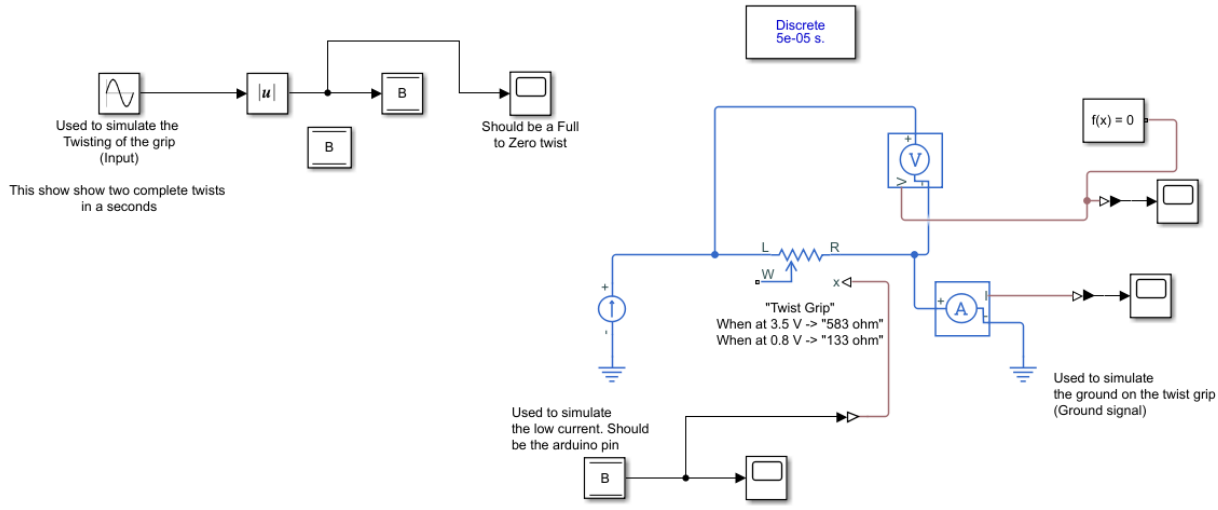

Figure 10. Twist grip simulation

On the left side of Figure 10, we have the operator twisting the twist grip. This is done by having an absolute value sine wave pulse from zero to one. This serves as a perfectly symmetrical amount of twist on many attempts. This input is then sent to the twist grip specifications as shown on the right. The parameters for the twist grip are: V_{IN} = 4.3V, V_{OUT} = 3.5V - 0.8V, & I = 6mA. To achieve this, a constant current source of 6mA is fed into a variable resistor. This variable resistor changes values slightly due to the twist grip input. The resistance of this variable resistor is altered depending on the desired voltage. As V_{OUT} ranges, the imputed resistance ranges as well. The twist grip operates as a hall sensor. A magnetic field is generated inside the twist grip to alternate the output voltage and the PWM desired. The power dissipation

that appears in this simulation will not be accounted for. This is because the twist grip used does not act as a potentiometer.

The circuit shown in Figure 10 is a simulation based off of the specifications of the twist grip. As there is no twist grip function block in the simulink library, it had to be represented in a different way. Plot 2 illustrates the current used by the twist grip electrical component. Plot 2 illustrates the current when the twist grip is not in operation. As the current is shown at a constant 6mA, the twist grip uses little current.

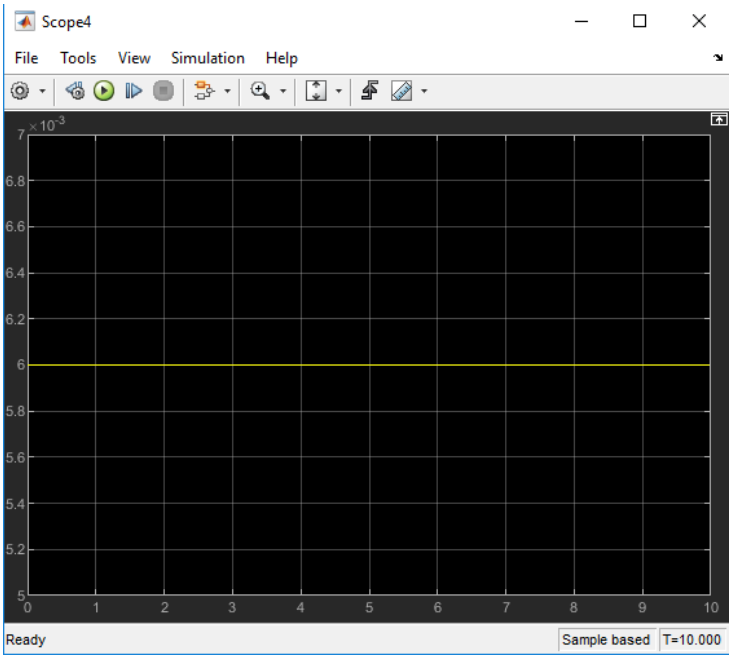

Plot 2: Twist grip current when not in operation

To view the voltage when the twist grip is not in operation, this can be shown below by Plot 3. There is a very brief spike, but when the twist grip is not in use it remains less than 0.8 volts. The very brief spike is essentially negligible.

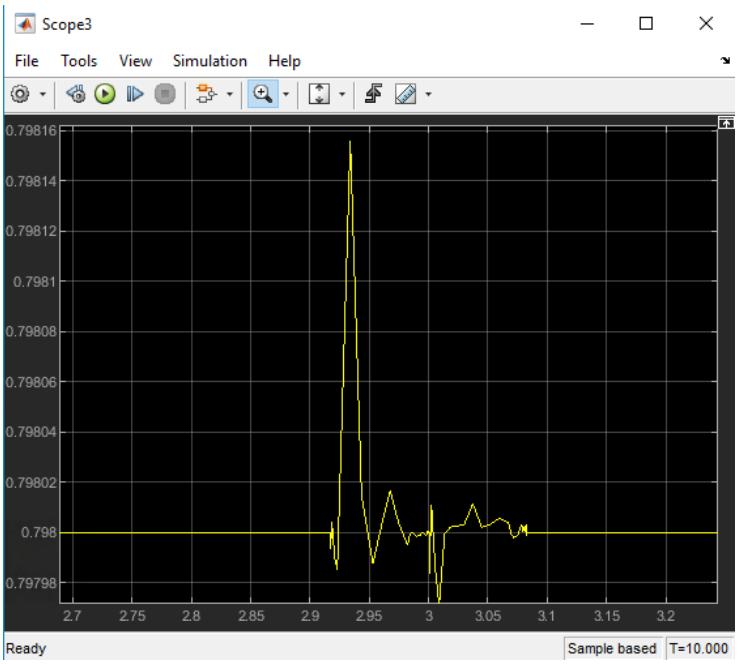

Plot 3: Twist grip voltage when not in operation

The twist grip's data stated that the device operated at a constant 6mA during all operations. Therefore, Plot 2 also describes the twist grip during a full twist. Plot 4 below shows how a full twist of the twist grip affects the voltage of the device.

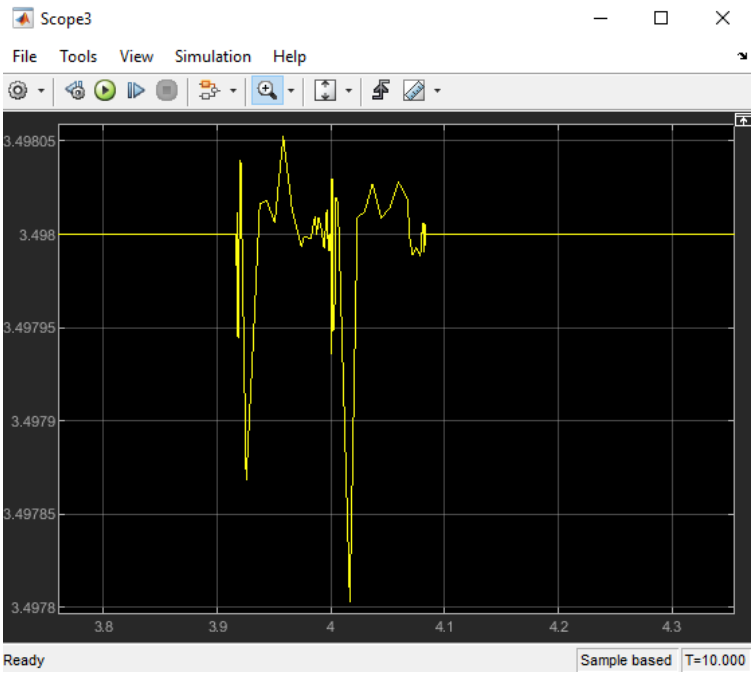

Plot 4: Twist grip voltage when in full twist operation

The twist grip ranges from 0.8 volts to 3.5 volts during operation. The voltage will vary depending on the amount of twist provided. This is due to it's electromagnetic properties of the magnetics inside the twist grip. Connecting circuit elements utilizing Figure 10 will describe how the whole circuit will act when conjoined.

3.4. User Display

The design of the user display consists of implementing multiple features such as the speedometer, water sensor, and battery information. There are various ways to implement a speedometer and water sensor. A speedometer can be based on how many times the wheels have turned and how much ground has been covered in a typical land vehicle. When on water, the relationship between how much the propeller turns is not directly related to how far the PWC travels; therefore, the design chosen for the speedometer is based on a GPS signal. The GPS gives information such as longitude, latitude, speed, and satellite count. In order to determine if there is water within the jet ski, which is a safety hazard to the user and bystanders, a water sensor is used. There are many water sensors on the market, but for the design of this jet ski, a water sensor was chosen based on affordability, accuracy, and compatibility with an Arduino; This being one of our design constraints, because the Arduino was already purchased by the previous MQP group. The different components and the schematic used in designing the user display are below in Figure 11. The battery information display and schematic can be found in the BMS design section. The circuit schematic was created using Tinkercad and images of the pieces used, and the specific connections that were made are discussed further in this section.

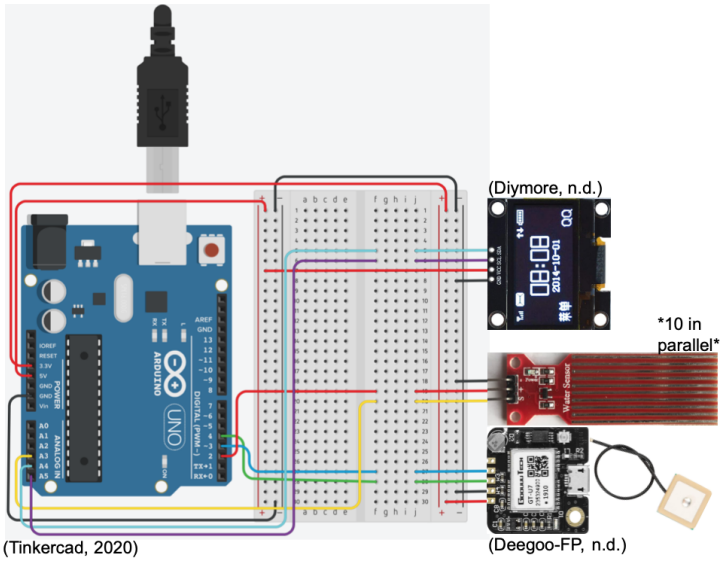

Figure 11. User Display Schematic

The overall design of the user display consists of an Arduino UNO, GPS module, antenna, ten water level sensors, dilithium design EV display, and an Arduino compatible display module. The user display components were chosen in order to meet the physical and functional

requirements outlined in the previous sections. The user display was developed using the parts purchased in Appendix D. The specific parts purchased to create the user display consist of a 'Rain Water Level Sensor Module', 'GPS Module Receiver: Navigation Satellite Positioning NEO-6M', and 'Diymore 1.3 in OLED Display Module'. The inherited part that was utilized to create the user display was the Arduino Uno. The user display components' specifications are tabulated in Appendix E, including their voltage requirements and current draw. Using the purchased components, along with the Arduino, the user display was then built and tested to create the final results.

The display module was the first component to be selected and connected. The display module is an I2C; therefore, there are only two connections needed other than power and ground, unlike SPI displays which require more substantial wiring. The reason for picking the 1.3 in - I2C display is to limit the number of connections which would have to be waterproofed; As well as it is the largest screen that could be found at a reasonable price, to allow the user a more "visible" screen. The display module is compatible with two specific libraries, the Adafruit_SH1106 and the U8glib. The libraries set up classes and functions that simplify the coding for setting the position, size, color, etc., of the text on the display. The design choice for picking one over the other is based on the amount of space/memory that the libraries use. The U8glib library uses much less memory of the Arduino; therefore, it was chosen in the design process for the display.

The first step in order to construct the speedometer was to make all the necessary connections. The antenna must be connected to the GPS module, which has 50 different channels and has a Time-To-First-Fix (TTFF) of under 1 second (Goouuu Tech, n.d.). The Neo-6M has four connections: VCC, GND, Rx, and Tx. The GPS voltage range is between 3.3V and 5V, but after research, it is recommended that when connecting it to an Arduino, the VCC is connected to the 3.3V power supply. Once the GPS module was connected to the Arduino, it was coded to display the speed from the GPS module onto the serial monitor. The Neo-6M and Arduino are compatible with the TinyGPS++ library (Hart, 2013). The library has the capability to read the National Marine Electronics Association (NMEA) data signals the GPS module produces, which consists of numbers and symbols, and converts the data to understandable information such as longitude, latitude, knots, etc. Once the speed was displayed correctly in the serial monitor, it was then coded to be sent to the display module.

The parts utilized for the water safety sensor are a 'rainwater level' sensor, an Arduino, and a display module. The display module, in the end, will be displaying both the water notifications and the speed. The schematic of this component is shown in Figure 11. The (+) pin of the water sensor is connected to a digital pin instead of the 3.3V or 5V pin because the power is not constantly being drawn into the sensor, reducing the corrosion rate of the sensor and extending the lifespan (Last Minute Engineers, n.d.). When water interacts with the sensor, it acts as a varying resistor or potentiometer. When the level of water increases, the resistance decreases, and when the level of water decreases, the resistance increases. A lower threshold Arduino rating needed to be determined in order to decide when the user will be notified on the

display of “No water” or “Water on board.” The display would then warn the user about water on board as a safety feature for the jet ski.

Once all three components were correctly working individually, the code was combined in order to display and view all components at once. The water safety sensor and the speedometer were coded to be displayed on the same display. The design choice for this was because the display is large enough where both information can fit where they are both still “easily readable” for the user.

3.5. Understand the Mechanical Functions

The first objective prior to working on the 1997 Sea-Doo jet ski was to become an expert on personal watercraft and learn about the mechanical functions and systems within electrical and gas-powered jet skis. Our team researched scholarly articles, review papers, books on gas and electric jet skis, and current electric jet ski company websites. Through this, we have gained a greater knowledge of each individual system and how we can improve gas-powered jet skis as well as the current and future electric jet skis in the market.

Each mechanical engineer has researched a mechanical component that we are going to design ourselves or outsource from outside manufacturing companies, including the drive shaft, motor, impeller, and battery casings.

For the impeller, our team researched the optimal material, shape, and size that should be used for the impeller connecting to the drive shaft and motor. The battery casings, dimensions, and specs were determined through the research of an ideal, waterproof material for the outside of the casing that is lightweight, yet strong and cheap. Research was also conducted for the optimal material for the battery casings to provide a soft, yet durable, layer of protection that can equally distribute the forces caused by the usage of the jet ski and transfer the heat so that the batteries do not overheat. Lastly, our team researched the most efficient way to mount the battery casings into the hull. Furthermore, online research was conducted through google scholar and the WPI library database to educate ourselves on the ideal weight distribution of a jet ski and areas where we can reduce weight so that the electric jet ski can travel at similar performing speeds as the gas-powered jet ski.

A major constraint for the drive shaft is that it needs to be clear of corrosion. The Jet ski will be submerged in water for extended periods of time, which causes corrosion. This is a problem for most Jet skis since, over time, corroded parts need to be fixed or even replaced. Finding the optimal material and treatment that will minimize the need to fix or replace parts is essential in the optimization of the propulsion system. When deciding on a specific material, we accounted for weight, strength, corrosion, and wear resistance properties the drive shaft needed in order to decide whether to add a surface treatment. Obviously, there are basic corrosion inhibitors like WD-40, but there are more advanced coatings and treatments that provide good wear resistance, good corrosion resistance, or both. Some treatments include Hard Chrome Plating, which is especially good for wear resistance, while Low-Temperature Black Chrome

provides good corrosion resistance. There are many other treatments that include: 52100 Bearing Steel, 440C Stainless steel, Electroless Nickel Plating. Further research will be necessary as we get closer to manufacturing and implementation.

For the battery casings, we researched waterproofing methods and seal tight methods to boxes/casings and materials that would be beneficial to have as a battery casing box. Our team made basic measurements of the inner hull to determine possible fits for the casings. The former gas-powered jet ski was not designed to secure battery casings for 24 batteries. Our team had to figure out how to design the casings in order for them to fit in the jet ski. Also, we needed to figure out how many casings we could make, how many batteries each casing will carry, where in the jet ski the casings will sit, how we will secure them in the inner hull of the jet ski and how to design each casing so that the user can easily access all 24 batteries. We agreed that the most cost-effective, lightweight, and feasible option for constructing the casings would be through additive manufacturing in the WPI Prototyping lab.

3.6. Design of Mechanical Components

Objective two launches our team into the design, ordering, and construction of each mechanical part. Based on the research conducted in objective two, our team was able to formulate multiple design ideas and agree on a final design or model for battery casings, motor, impeller, and drive shaft. Parts were constructed through 3D printing, machining on the minimill, laser cutting, and outsourced from manufacturing companies outside of WPI.

3.6.1. Impeller

For the impeller, the team will converse with companies to see what impellers are available within our price range that match the optimal material and sizing that would work best with our jet ski for a possible impeller donation. We are going to compare the current impeller from the 1997 Sea-Doo SPX with jet ski impellers currently out in the market. Based on the comparisons, the research on optimal impeller material and sizing, and the current company's impellers available, we will make a decision on which impeller will give the best blend of cost efficiency, lightweight, and high RPM.

After failing to come to an agreement with companies about donating a composite impeller to our project, we began looking at all the parts that we have left over from the original 1997 Sea-Doo model and determined all the systems that we need moving forward for the electric jet ski and the systems that only apply to gas-powered watercrafts. The main system we focused on was the propulsion system. Our team began ordering all the missing parts of the propulsion system from the old 1997 Sea-Doo model. From there, we determined what parts of the model we needed to modify due to the impeller fitting change between the old engine and the new DC motor. After discussion with the manager of the machine shop at WPI, we came to the conclusion that our best method of connection between the 1997 Sea-Doo model drive shaft and DC motor was a coupler with a spline connection on one end for the shaft and a key fitting on the

other to fit with the DC motor. This option allowed our team to limit the error involved with machining our own drive shaft with very fine and exact spline cuts. Fatigue analysis on the coupler, motor, and drive shaft connection will be conducted.

3.6.2. Motor Mount

Since our project is a continuation of a prior MQP, we already have the DC motor that last years' team purchased and planned to use in their jet ski modifications. Since we are using a formerly gas-powered jet ski for our project, the hull is not designed to mount our current electric motor inside of the jet ski. Therefore, we will manufacture a motor mount out of aluminum that can be bolted to the hull of the jet ski and is strong enough to withstand the forces of the movement of the jet ski. Not only did last years' team purchase the motor, but they also designed a custom motor mount and created the CAD files necessary to machine the different components out of aluminum. The next step is to create simulation files in a program called Esprit that is used for computer-aided manufacturing. Esprit is a software that is capable of simulating machining processes on a 3D model, showing you what the process looks like, the final product, and whether or not the machine will crash when actually machining the part. This lets the operator know when they are ready to machine their part and provides confidence that the part will be manufactured as desired. Once the files have been created and the aluminum stock is delivered, we will be able to machine the components and have the motor ready to be installed in the jet ski.

3.6.3. Drive Shaft

To summarize what last year's MQP team did with the drive shaft, they designed a drive shaft to fit the motor but did not get to the fabrication stages. The final design they chose is shown in Figure 1, in an exploded view.

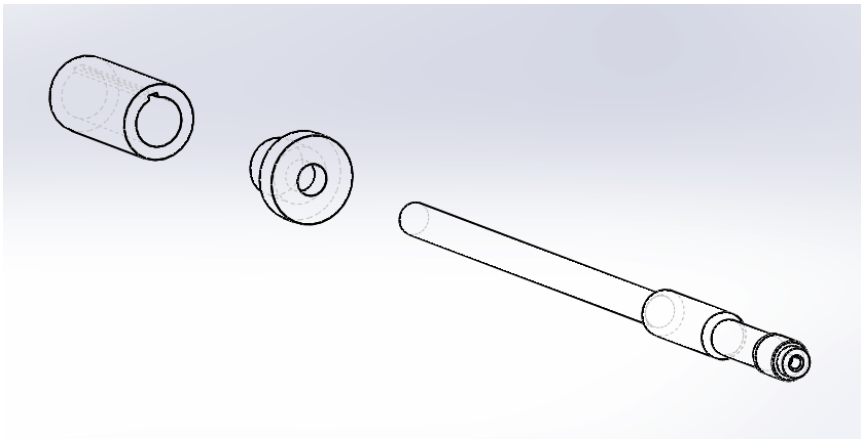

Figure 12. Drive Shaft

The sleeve is a long cylindrical piece of 316 steel, which is bored out to the size of the motor's shaft with a tolerance of .002" for an interference fit. A keyway alteration was designed to lock the motor to the sleeve. Two threaded holes are machined perpendicular to the keyway on the sleeve for the installation of securing grub screws. The sleeve was designed long intentionally so that once the proper motor-drive shaft connection was made, they could see how much material they needed to machine off (Electric/Solar Powered jet ski 2019). A second piece was designed, seen on the bottom right of the figure, to attach the impeller.

Before fabrication, we need to find the optimal mates for the motor and impeller. Research and trial and error methods will lead us in the right direction. The lab monitors in Washburn Shops were helpful as well and gave us good advice to make sure our connections and tolerances are correct.

To get a better understanding of the fits of the shaft, the team ended up ordering a used drive shaft from the original model gas-powered jet ski (SPX 1997). The spline fit of the impeller end fit very well after a deep cleaning. We manually tested the fit by spinning the shaft while attached to the impeller blade. It turned smoothly, which we deemed functional for the time being.

Figure 13: Impeller/drive shaft configuration

Initially, the team inspected the drive shaft to impeller connection. Next, we tried to come up with methods to alter the shaft to ensure a fit with the motor. The motor shaft has an outer

diameter of 1.25” while the drive shaft itself has a diameter of .75”. There is not enough material on the drive shaft to create a fit with the motor shaft, so some sort of additive process is necessary. We were initially thinking either to weld an attachment piece or to order an entire new drive shaft. We thought the stress points created from the weld would cause a problem for a high speed and torque system. A number of weld defects are bound to happen in every weld; typically, weld defects create additional stress concentrations. Welding introduces residual stresses into the weld and surrounding structure. Even mildly restrained welds develop peak residual stresses at or near the yield strength of the metals being welded (M.H. Johnson).

To gain further expertise, I ended up meeting with Sr Lab Technician, James Loiselle. We discussed options, and he mentioned that a weld is stronger than we think and that it is potentially an option. A good weld is very strong, and WPI has the resources to make it happen. However, a different option also came up in discussion that was a splined-to-keyed flexible shaft coupling. These are used in gearboxes, pumps, and other high-speed systems as well. The coupling is made from two hubs and one spider. The hubs fasten onto the shaft without causing any damage and also have clamping screws to tighten if necessary. The spider sits between the two hubs and is made of Hytrel or Polyurethane, which provide good vibration damping and chemical resistance.

The team measured the spline fit on the drive shaft to see which spline size we are working with. The spline standard is SAE, where sizes range from A to E. Our measurements came out as a spline size between A and B. The x value of the spline was .75” while their value was .6”. Even though we do not have the correct SAE size at the moment, to find the right coupling, we looked up the necessary RPM and torque constraints. The iron hubs can withstand a max speed of 3,600 RPM and a maximum torque of 1,860 in-lbs (McMaster Carr). The Hytrel spider does not meet the torque requirement, but the polyurethane does. These constraints are within our threshold of 2,423 RPM and 796 in-lbs.

Figure 14: Shaft Coupling system

The spline standard ended up being the wrong size and did not fit well. Problems would arise as the SAE standard coupling would not be able to transmit the required torque to effectively turn the impeller. Because there were no design specifications for the drive shaft, the

only way to create a custom coupling was by reserve engineering. Reverse engineering is the process of recreating the design of a physical body without the design specifications.

The process began with research on spline design. There are requirements specific to each spline standard, which was another obstacle to overcome since we did not know our standard spline. The tooth interlock of the internal and external spline connection is determined by the number of teeth, pressure angle, pitch, etc. We measured all the dimensions possible with the tools in Washburn Shops and created the tooth profile in Solidworks. We referenced the DIN standard to make sure our dimensions were reasonable. They ended up being accurate and were ready for manufacturing.

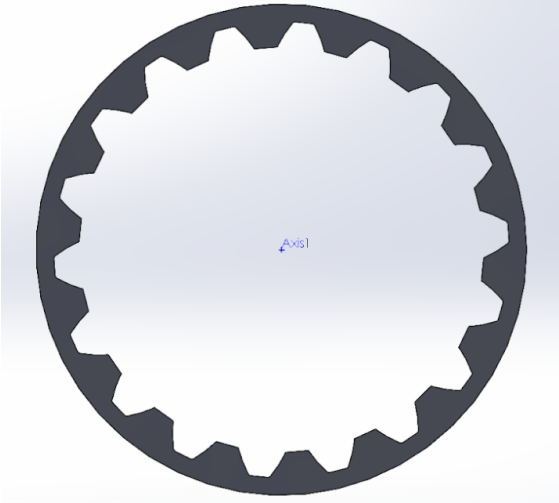

Figure 15:Internal Spline Design

We chose to use the Wire EDM (Electrical Discharge Machining) because we wanted the tightest possible tolerance to create an interference fit. The machine uses a thin, single strand of brass wire that is submerged in deionized water and creates an electric current through the wire, which can cut hard conductive metals. This process has impacted the manufacturing industry greatly because of its precision accuracy. We created the CAM file in Esprit and cut out our spline from a spare coupling found in Washburn.

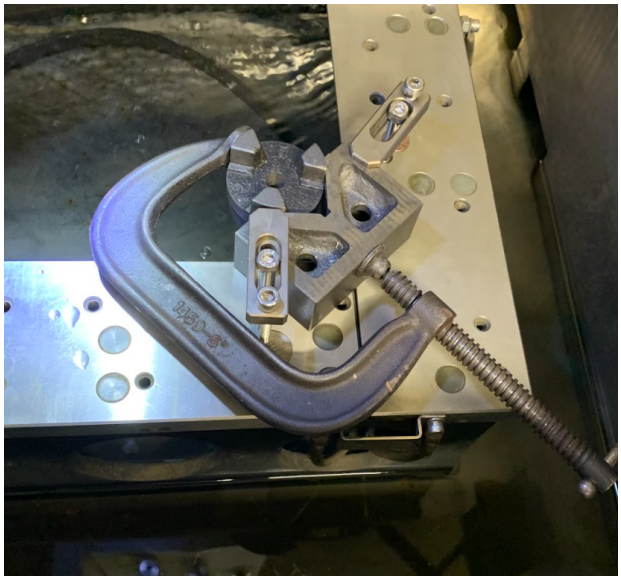

Figure 16:Wire EDM Configuration

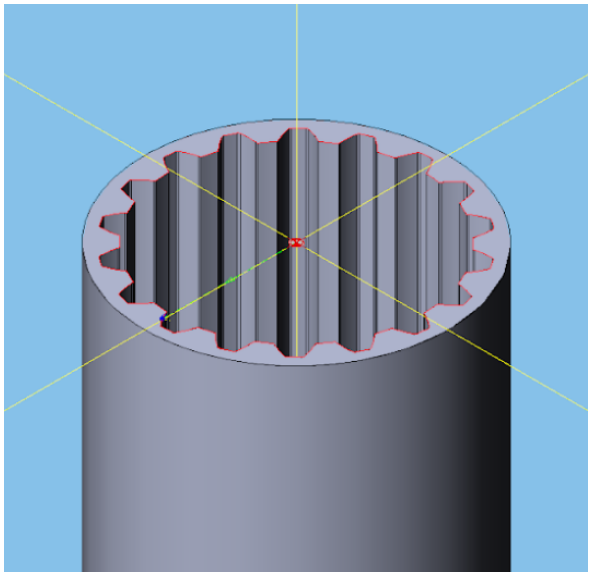

Figure 17:Internal Spline CAM

The Wire EDM cut the spline without any issues. The interference fit was good, and the coupling was pressed into the drive shaft with the assistance of an arbor press.

Figure 18:Coupling/Drive Shaft Mate

3.6.4. Battery Casings

The battery casings are a crucial part of the success of the jet ski system as a whole. The battery casings ensure that the Lithium Ion Batteries are secured in a dry, sturdy area where the batteries are able to output voltage and current at levels needed for the motor and propulsion system to function at their desired Torque and RPM. The housing design for the Lithium Ion

batteries are critical in determining whether the accessibility of the batteries for recharging is user friendly or not. Since an electric powered jet ski needs to recharge their batteries frequently, the accessibility of taking the batteries in and out of the casings for recharging is very important.

In order to achieve proper housing of the batteries, we must first alter the previous design of a waterproof casing that will not allow any water to penetrate the hull inside of the casings and come in contact with the batteries or wiring. Secondly, the battery casing must be able to protect the batteries against the constant forces being applied by the use of the jetski, including the force of the water on the jet ski and the vibrations of the motor on the hull. Lastly, the casing must ensure that the batteries will not overheat due to the usage of the jet ski. The material chosen for the casings must meet the previously stated requirements, as well as limiting the amount of weight used up by this extra material.

There are 24 batteries total in the jet ski system. The casings need to be positioned in the jet ski such that the weight distribution is even.

To begin the design process, the team conceptualized last year's SolidWorks model and made some minor adjustments to best fit the battery's dimensions while also reducing the weight and space taken up inside the hull. The 2019 team had designed battery casings to house a total of three batteries. However, we felt as though we could limit the amount of weight caused by the casings even more. The previous years MQP team's battery casings that housed 3 batteries had dimensions 9.5"x5.625"x13" with a material thickness of half .25" and the other half .5". Their 3D print must have had a higher layer density than our team because the difference in weight between last year's casing and our first iteration was significant. Below in figures 18-21 show the battery housing unit created by the 2019-20 MQP team.

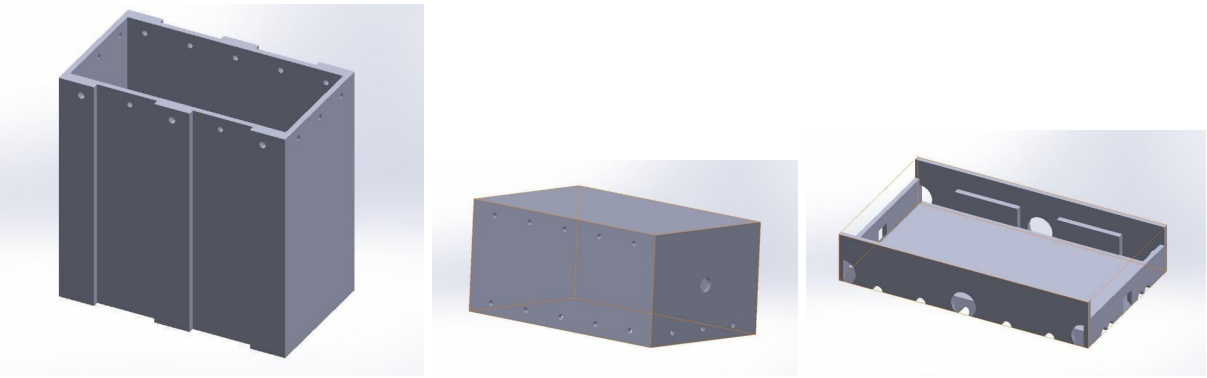

Figure 18,19,20: SolidWorks Designs of Battery Casings from 19-20 MQP team

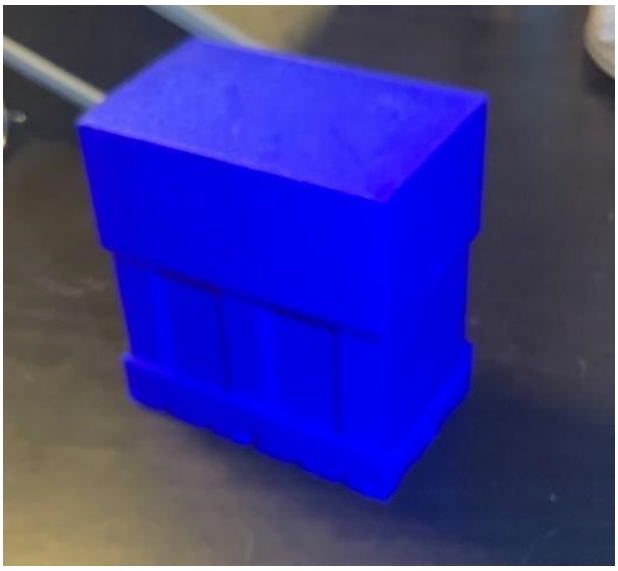

Figure 21: 3D Print of Battery Housing Unit

Based on their design and our measurements of the inner hull, we realized that we wouldn't be able to fit 8 boxes of 3 batteries each that pack an unfavorable size and weight in the jet ski. Our team initially decided to pursue a similar design which was suited for four batteries per casing as seen in figure 4. The reasoning behind a 4 battery box was that we could make an even number of boxes that could all hold 4 batteries which could equally distribute the weight throughout the jet ski. The design would decrease the boxes needed by 2 which simplifies the system more. Also, the initial box design was .25" thick throughout the casing compared to last year's casing design that had half of the box .5" thick and the other half .25" which significantly reduced the weight of the box. We decided to separate the box in two pieces to include a rubber lining along the rim of the bottom half of the box along with store bought latches on either side to ensure a perfectly sealed box as well as allow for accessibility of the batteries. Because of our

budget and weight limitations, we decided to utilize the 3D printers available through WPI and additive manufacture PLA boxes. This design satisfied the capability to limit the weight while maintaining the basic protection and waterproofing of the batteries. The first iteration design was more geared towards fitting the batteries into the jet ski with less boxes which increases the ease of use for taking out batteries for charge. The first iteration's main goal was to make sure that we had a box that had the right dimensions to fit a certain number of batteries with little tolerance and limit vibration.

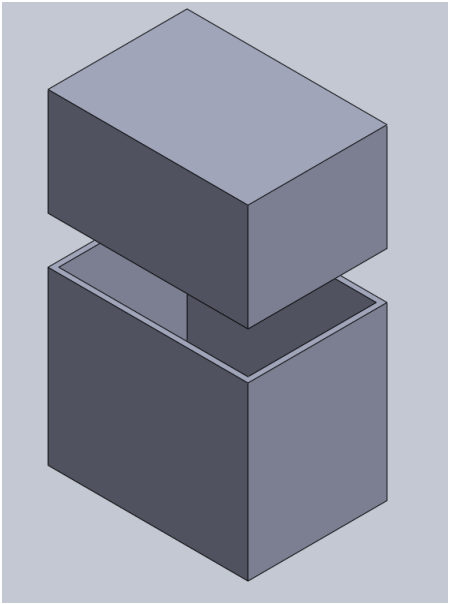

Figure 22: SolidWorks Design of Battery Casings

After reviewing the initial design of the casings and further analyzing the layout of the inner hull of the jet ski, we altered iteration one to generate a more innovative, secure and feasible fit for the battery casings in the jet ski.

Our team inspected the inner hull and figured out the areas where the battery casings would fit best within the jet ski. Our team looked for areas with a flat plane where the casings would be able to be secured in an upright position and not be fastened in a crooked configuration. Furthermore, our team looked into areas with the most height from the bottom of the inner hull to the top which allows for easier access to the batteries. The batteries need to be taken out of the casing for charging and in order for the batteries to be taken out of the casing there needs to be ample room between the top of the casing and the ceiling of the inner hull so the user can feasibly charge the batteries. Lastly, our team looked for ways where we could evenly distribute the weight of the batteries throughout the jet ski so that the jet ski weight wasn’t favoring one side and the weight distribution was even. Figures 23 and 24 show the layout of the inner hull where the casings will be.

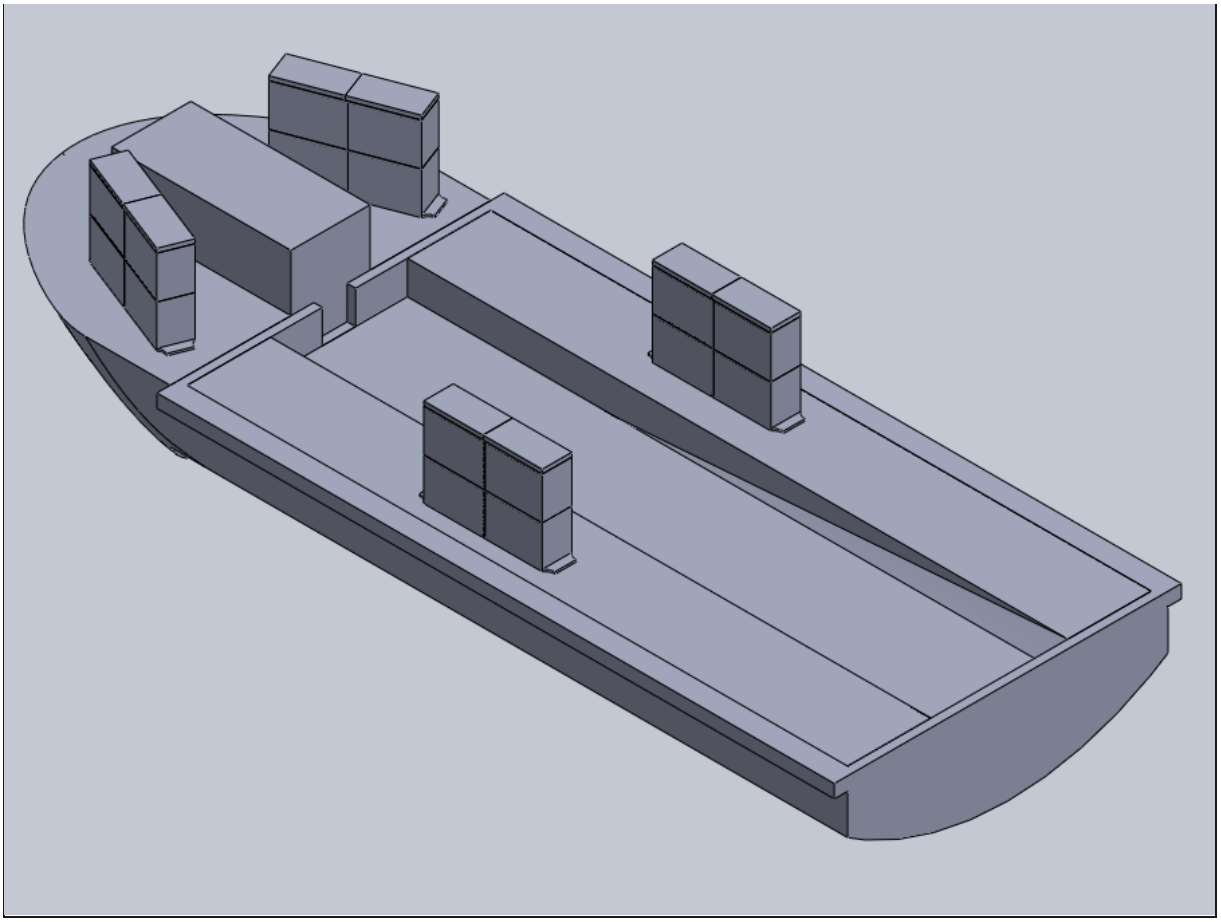

Figure 23: 3D Model of Battery Casings Configuration

In our second iteration of the design, we decided to separate the battery casings into 5 casings: one casing of 16 batteries oriented vertically and four casings of two batteries each oriented horizontally on the side.

In order to divide the 24 evenly throughout the jet ski without compromising the weight distribution of the jet ski, we decided to utilize the long cavity in the front of the hull to house the group of 16 batteries (Figure 23). The four casings of two batteries were distributed with two casings on either side of the motor and two more in the front end of the jetski on either side of the 16 battery housing unit Figure 23). The cavity in the inner hull gave us a lot of room to work with vertically. We would have enough space to implement a battery casing in the cavity with a height of 13”.

The layout of the inner hull has a cavity in the center that was measured out to be 26.6” and a width that was nearly a perfect fit which was 9.4375” (Figure 23). Two batteries lined up next to each other had a combined thickness of 3”(Figure 24). With the casing needing a thickness of .75” on each end due to screw length for the latches, the casing inside of the valley could fit 16 batteries with an extra ⅔” of space for the wiring.

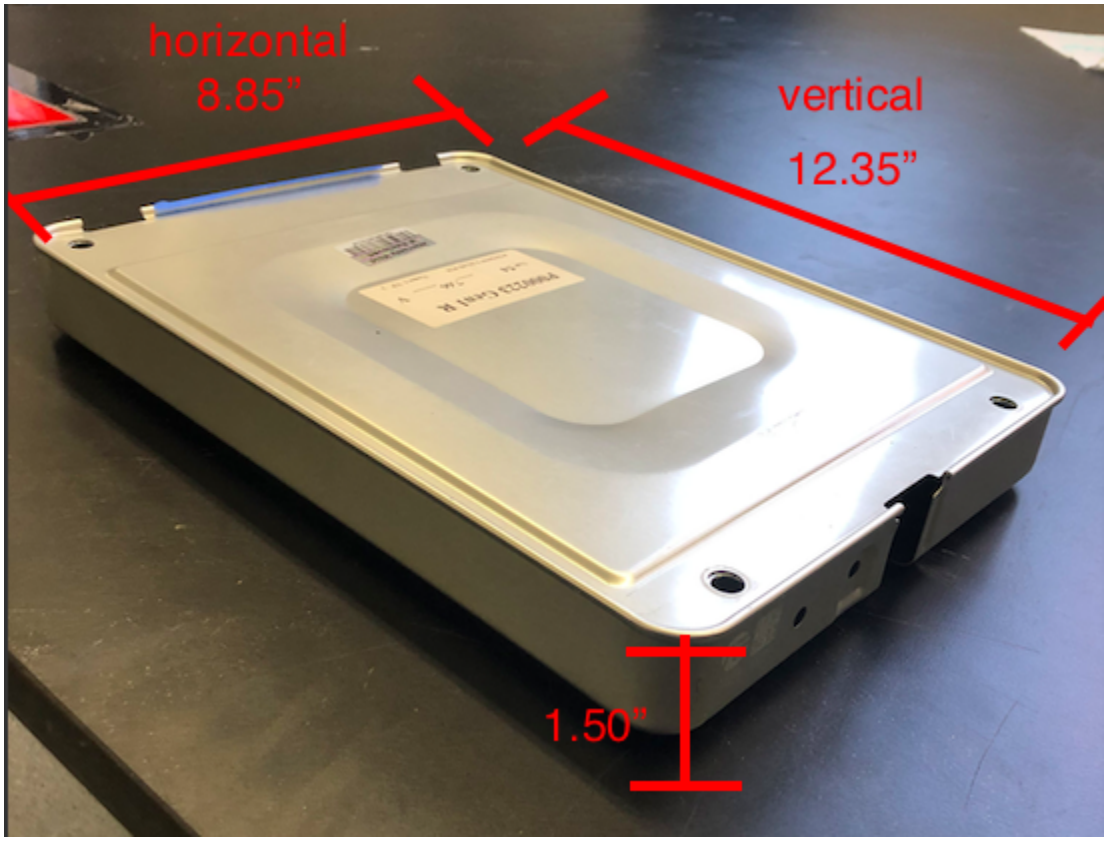

Figure 24: Battery Dimensions and Configuration

In designing the 16 battery housing unit and preparing it for 3D printing, we broke the casing into 10 separate parts in order to fit the available 3D printers printing capacity in the WPI prototyping lab. To further improve the water proofing capabilities of the box, we added the “step” design, as shown in figure 26. We epoxied the pieces of the box together in the area of the step connection or also known as rabbet joint fixture.

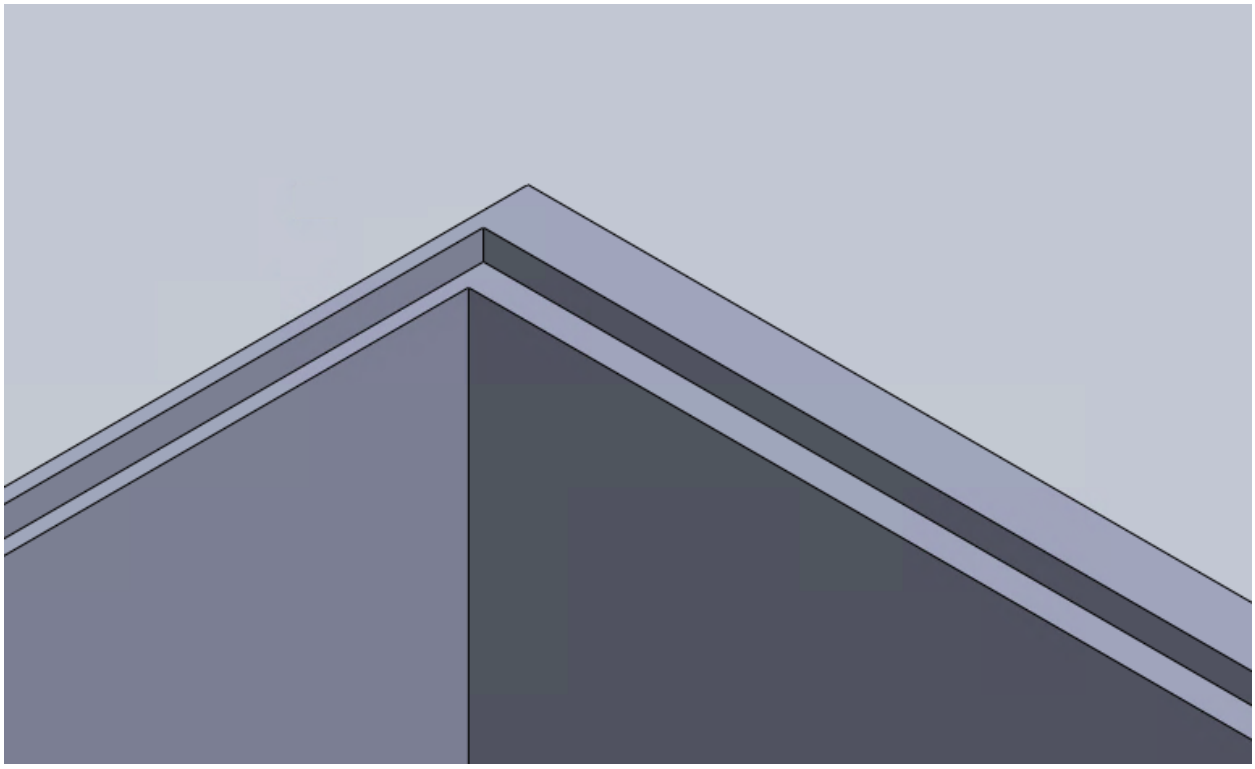

Figure 25: Step Design (Rabbet Joint Fixture) on 16 Battery Casing

The step design allowed for each piece of the casing to attach to one another using an interference fit. The reasoning behind this design was because the step idea adds an extra barrier of defense against water entering the casing at each connection point. The epoxy secures the pieces together and once the whole base was constructed, we waterproofed the connection points between each part with flex seal, a spray-on rubber coating, to waterproof the outside of the casing. The top piece (3 piece configuration), which is acting as our removable lid to the box and shown in figure 26, was broken up into 3 pieces that will also be epoxied together. In order to secure this box to the jetski, we were required to acquire store bought legs to connect the casing to the inside of the hull of the jetski. Similar to this, the four casings of two batteries were designed with similar concepts with different dimensions. However, these casings were able to be designed with legs to be screwed into the hull of the jetski, as shown in figure 27.

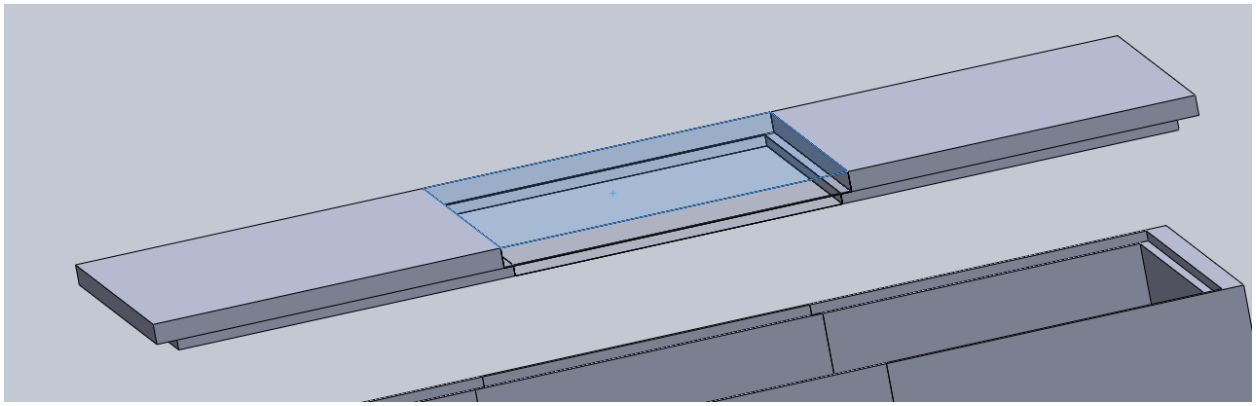

Figure 26: Removable Lid for 16 Battery Casing

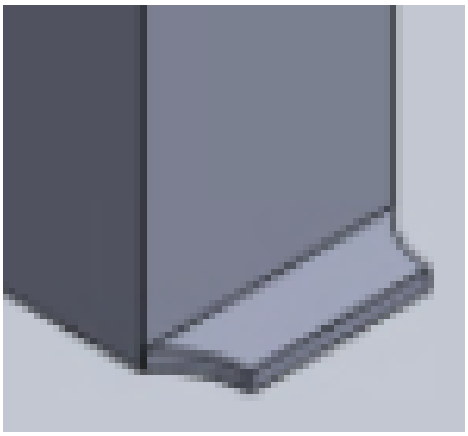

Figure 27: Legs on the end of 2 Battery Casing for Fixturing into Hull

Each casing was designed using the step connection or more known as the rabbet joint approach. In order to waterproof the connection between the top and the base of each housing unit, our team decided that we would use staple safety hasps where we would attach the hasp to the top plate and screw the hasp onto the top of the lid with material thickness of .75" to account for the screw length. The hasp will be able to rotate at a 90 degree angle which will allow for the hasp to rotate down parallel to the base where the hasp will slide through the loop fastener where the hasp can be secured and the lid can compress into the base of the casing. The bottom of the lid, that will submerge into the base of the casing via the rabbet joint approach will be covered in a rubber coating of flex seal which will allow for the rubber to compress and generate a waterproofed casing around the lid-base connection.

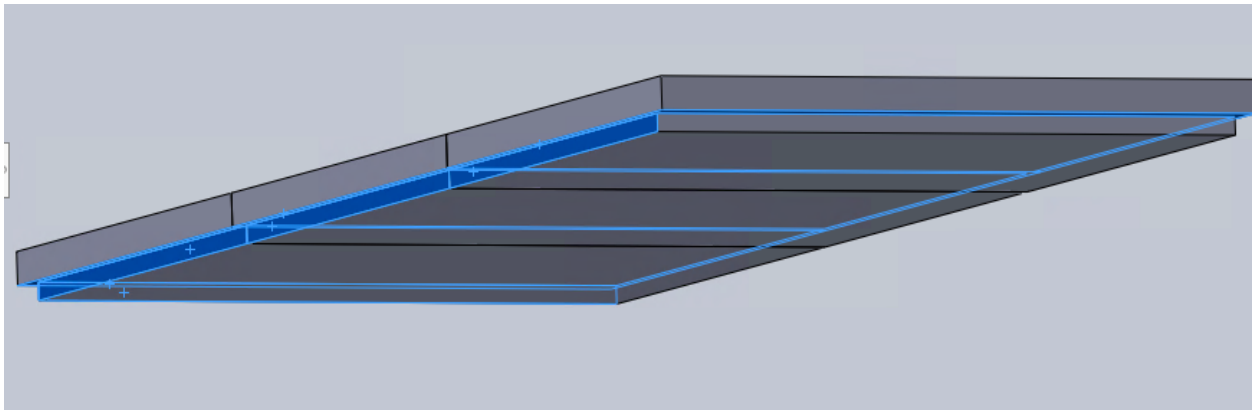

Figure 28: Flex Seal Region Highlighted in Blue

Figure 29: Staple Safety Hasp Configuration on Casings

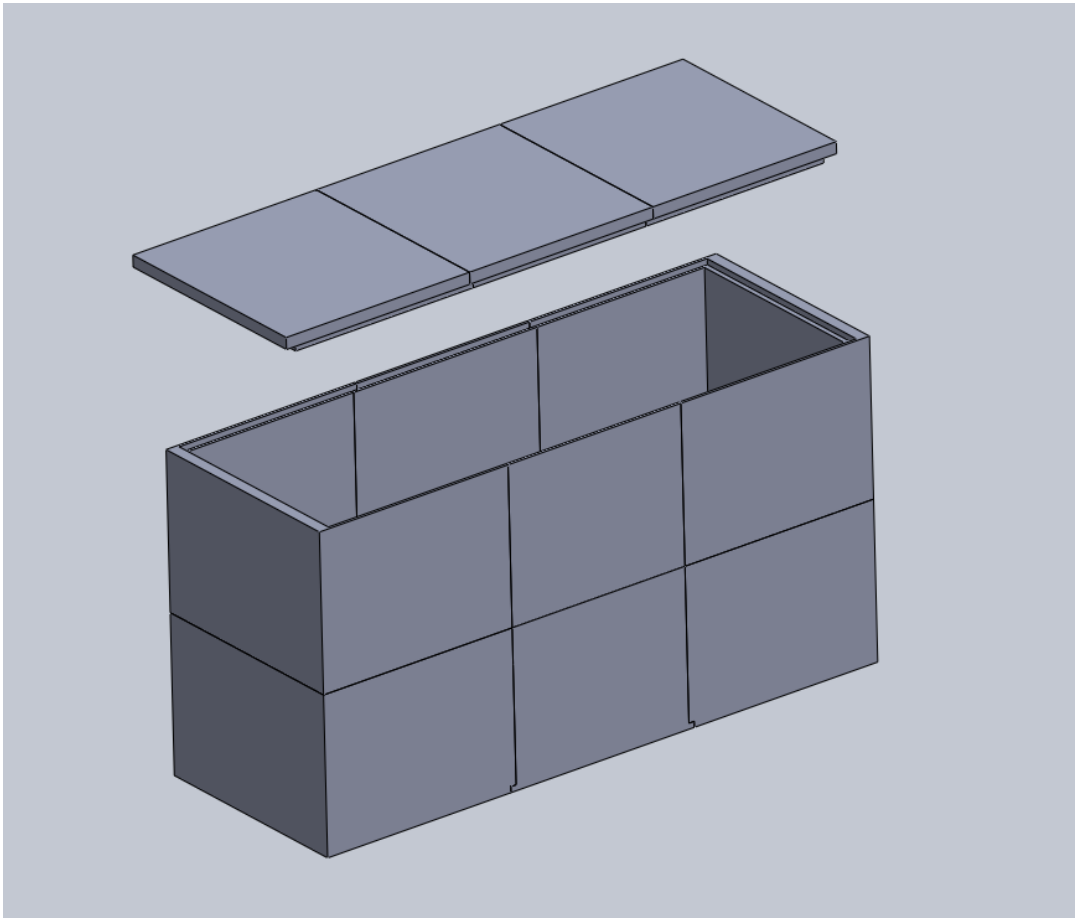

Figure 30: Full Lid-Base 16 Battery Casing Configuration

Much like the 16 battery casing, the four casings of two batteries were designed with similar features. In this design, our team separated each casing into 6 different pieces; four pieces for the base and two pieces for the removable lid to allow access to the batteries. These pieces were epoxied together using the same step design as the 16 battery casing as well as including the legs, as presented in figure 27, to secure the box into the hull. Due to the sloped walls of the inside of the jetski thus the limited height for the top to be taken off, our team decided to orient the batteries horizontally, the design is shown in figure 31. This allowed for the total height of the box to be reduced. This allowed us to easily have access to the batteries by removing the lid. The lid will be attached using the latches shown in figure 29. The connection points between each individual part of each casing was sealed with epoxy and Flex Seal to ensure a secure and waterproof casing for the batteries.

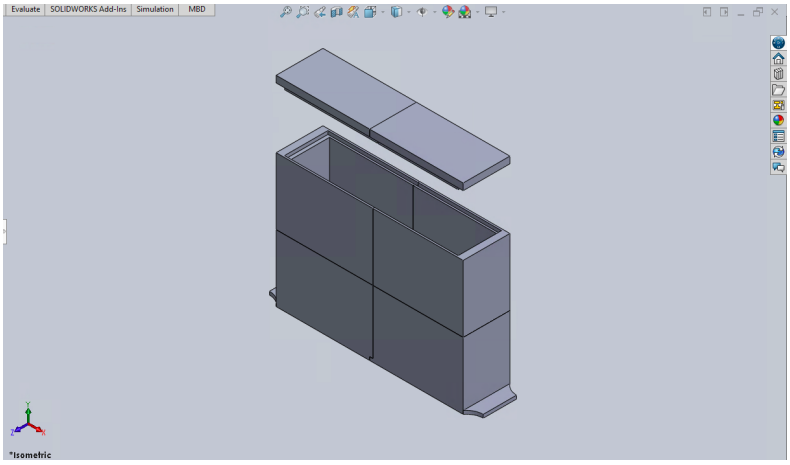

Figure 31: Full design of two battery casings

3.6.5. Weight Reduction

Due to our budget limitations and the substantial weight of the current motor we have available, we need to find other areas of the jet ski to cut down on weight in order to improve the overall performance of the vehicle. Many commercial jet ski companies use carbon fiber parts for their hull since carbon fiber is very strong and corrosion-resistant but also lightweight. Carbon fiber is a very good substitute for the current plastic hull pieces that comprise the jet ski to ensure the strength of the hull but also to remain lightweight. Besides the body of the vehicle, our team can potentially save weight in other mechanical components of the watercraft, such as the impeller and drive shaft. Graphite composite is also utilized in watercraft impellers, commonly made from stainless steel, to ensure similar strengths but also greatly decrease the weight. Similarly, most drive shafts are manufactured from stainless steel and add a lot of weight to the overall system. Again graphite composite would serve as the best substitute if it is a feasible option and readily available.

As mentioned prior, our team researched and called companies for their services with little luck in determining a quick, cost-effective method for weight reduction in the jet ski that could offset the increased weight of the motor and batteries. Our team moved in a direction more geared towards generating and configuring a working propulsion system that can then be tested. Dwelling on weight reduction aspects delayed our configuration of the propulsion system after the lack of beneficial dialogue with impeller companies, so we moved away from weight reduction and focused on configuring the propulsion system after all the 1997 Sea-Doo parts were delivered. Another aspect of reducing the weight came from the battery casings. The previous team had decided to put three batteries per casing. Our team decided to go with four batteries per casing to reduce the total amount of 3D printing plastic in the jet ski.

Furthermore, We could not gather the resources needed to optimize our weight reduction of the impeller and major mechanical components. Our main areas of proposed weight reduction to compensate for the added weight of the DC motor and electrical batteries were to trim off weight from the hull and impeller. For the hull, we wanted to see where there was excess

material that was not needed and could be modified. We also wanted to use a different impeller with a composite material that was six times lighter than the stainless steel impeller that we currently have. The company that manufactures these graphite composite impellers would not entertain the idea of donating an impeller to our project. The fiberglass hull is very lock tight, sturdy and stable. Cutting out areas of unwanted fiberglass will cause waterproofing problems, instability, and unknown consequences to the jet ski, so our team decided to leave the hull as is and focus on our work inside the hull, including the battery casings, the positioning of the casings, the motor, motor mount, and the rest of the propulsion system.

4. Testing and Integration

Once the design had been created which met the system requirements, the next step was to test the components and integrate the systems. The fifth goal of the project is, “Build and test successful prototypes of the design.” Having a thorough testing plan and strategy before implementation allows for a more safe, smooth, and effective implementation. Throughout this section, the testing plans and simulations are discussed, with the results of the testing included in Chapter 5. In this section, we discuss the development and testing of prototypes for the jet ski components. The electrical systems will first be built and tested independently and then integrated together once the individual components are verified to be working as intended.

4.1. BMS

The battery system build-and-test procedure is split into three different modules. First is battery testing, followed by the electric vehicle display, and then the BMS module. Battery testing is a quick task. The assembly requires the batteries to be cased within the battery housings. To test the Nissan Leaf batteries, it required the use of a multimeter. Using this tool, the battery terminals were checked to show each cell is outputting around 7.6V. After each battery was measured, the actual voltage can be recorded of each cell.

The second part of testing is with the electric vehicle display. To connect the display to the BMS, the CANH and CANL cables connect between the display and the BMS. The CAN jumper is then connected to the JP3 terminal. From here, the display is powered up using a 12V source. Normally, the 12V source would come from the charge controller also supplied by Thunderstruck. We did not have the charge controller, so during initial testing, a 12V power adapter was modified. Using this power supply, the wires were cut and tested using a multimeter to ensure a 12V output. They were then modified to have two outputs for each +12V and GND. These were connected to both the BMS and the EV Display. With the display on, the BMS and cells are visible, and it can be confirmed that they are powered correctly. A hall sensor was also used in the testing of the BMS. This sensor was connected to the EV display using the given connector from Thunderstruck. To determine the polarity of a current sensor, the motor can be manually spun. If the current sensor is showing a negative value, the sensor is flipped. After this step, the only thing left to test is the charging port. This is simply done by plugging in the charging cable and seeing if the charging icon appears on the screen.

With the display setup, the BMS can also be tested. The physical setup of the BMS was done by first routing the power, CAN, and IsoSPI datalink cables and then forming the cell loop wiring seen in Figure 22 below. Using the wiring harness, the cells are connected and tested via the harness verification tool. This tool is a PCB used to test the voltages of the cells in their configuration to make sure they are outputting the correct voltage before connecting them to the BMS. This is done to ensure the safety of the BMS module. With the wiring complete, the next steps were using the Thunderstruck BMS software. The terminal drivers and terminal emulation

program are installed first and connected to the computer being used to set up the BMS. From here, the cells can be seen by the program to confirm they are connected properly. To safely test the cells without risking damage, one cell will be tested at first. If this cell is discovered and working as intended, more cells are added and tested. Using the BMS software or the EV display, the low voltage and high voltage cutoffs can be tested. Optionally, cell discharging can be enabled, and cell balancing can be tested.

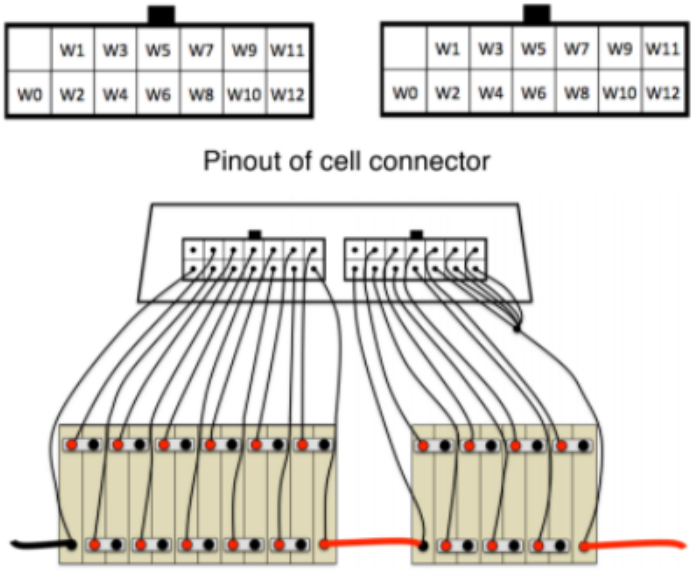

Figure 32. Cell Wiring (Thunderstruck, 2019)

4.2. Motor Control

The H-Bridge is the main part of the motor controller, and so was built and tested first. The H-bridge, H-bridge driver, and motor were all simulated in order to verify the intended operation of the H-bridge circuit, ensuring there were no shorts from power to ground and the maximum voltage drop across the load. Then, the H-bridge circuitry was breadboarded for initial testing with low voltage (Vbatt of 30V) and low current (below 100mA) conditions using a much smaller motor as the load and a signal generator to drive PWM inputs. Once H-Bridge integrity is verified in this way, it will be transferred to perfboard, and soldered, and tested in the lab at high voltage (90V) and high current 100+ Amps). Finally, the circuit will be tested with the full-size motor as the load, and the motor's RPM and torque will be measured and verified to meet the necessary specifications of 2423 RPM and 90.25 Newton-meters. The motor is the most expensive electrical component, and doing tests in this progressive fashion ensures that it is not damaged due to a faulty H-Bridge circuit. Once fully tested, the H-Bridge will be integrated into the design overall by powering it with the battery controlled by the BMS, attaching the full motor as the H-Bridge's load, and driving the H-Bridge with the Arduino that is taking the output of the throttle control. This Arduino then uses the input from the throttle control to determine the

duty cycle of the PWM signal driving the motor, effectively allowing the Throttle Control to determine the speed and direction of the motor.

The ripple counting could not be verified in simulation due to the motor's ripple not being generated in simulation; therefore, it will be tested in practice with the motor once the H-Bridge is fully functional. This should be first done by using an oscilloscope to measure the current ripple seen by the current sense resistor and manually estimating the RPM from this signal. Once this can be done to within 25 RPM, as verified by a tachometer, a ripple counting Arduino sketch will be created and implemented to estimate motor rotations and report RPM. This sketch can then be verified using the tachometer. The ripple counting component is integrated into the system overall by ensuring the ripple counting software is active and working on the Arduino also running the user display, so this same Arduino can display the estimated RPM on the display panel.

The dead man switch will be tested by adding the functionality to the Arduino to cut power to the H-bridge driver as soon as an external interrupt is triggered. This is then tested by adding this interrupt feature to the previous Arduino sketch, which drives both the H-bridge driver and implements ripple counting while testing the time from triggering the dead man switch to there being no power supplied to the motor. A working Dead Man switch is integrated into the system by ensuring the necessary code is active on the Arduino that's sending the PWM signals controlling the motor.

The buck converter shall be built first in simulation, where it is verified that it will be able to supply the necessary current to power the supplementary electronics while staying within the Arduino's input voltage range. After verifying performance in simulation, the buck converter can be built and verified using a power supply and an electronic load. Finally, the buck converter can be integrated with the rest of the electronic parts by using it to convert high voltage battery output (65V - 99V) to a stable low voltage output usable by the rest of the electronic components.

4.3. Throttle Control

The purpose of testing the throttle control is to ensure that all components used work as intended before being combined with the remainder of the electrical team. As the throttle control mainly corresponds with the motor controller and the user display subsections, ensuring that the throttle control is functional alone is crucial, so the other subsections are not affected. Testing the twist grip did not raise concern for an electrical hazard, as it operates at roughly +5VDC at 6mA. The twist grip could be damaged in several ways during the full combination if not properly tested. Mechanically, as in broken terminal legs, or with excessive hard vibrations. Electrically, the twist grip could be damaged over large voltage inputs, current shorts, or from reverse polarity. Some twist grips are not waterproof unless specified; contact may cause a short circuit.

To properly test the twist grip, tests need to be run electrically and mechanically. To begin testing, we 1st: individually tested the twist grip without the Arduino UNO. To test this, we attached the leads of a digital multimeter to the ends of the +5V signal and the ground signal. We

can do this safely by placing the twist grip on a breadboard and testing the voltages there. Unlike a potentiometer, the twist grip uses the hall effect to alter its voltage. So measuring resistance will not work. We will measure the voltages as the twist grip is turned. Through research, it is determined that the twist grip inputs between 5 and 4.3 volts. The output voltage is between 0.8 and 3.5 volts. We then let the twist grip remain at rest and measure the output voltage. After, we twisted the twist grip fully as expected to remain within the boundaries of 0.8 and 3.5 volts.

After a successful expected outcome, we then 2nd: Code the Arduino. Here, we coded the Arduino to see the twist grip ratings appear in the console display. These numbers were ranging from 0 (when the twist grip is at rest) to 255 (when the twist grip is fully turned). An important aspect to watch out for in this testing procedure is to ensure noise is not present. A jet ski operator would not like the motor to begin slightly turning when there is no twist of the handle present. The code here must also account for human error when their hand is on the twist grip, but they do not turn. This test was performed visually. To test this, we held the twist grip without intentions to twist it and see if the console display provides an output.

Following, we must 3rd: connect the twist grip to simple electrical components and observe its operation. We attached the twist grip to a simple component to allow the Arduino to operate using the twist grip. A simple example of this is to use an LED. The twist grip & the Arduino UNO were connected to the LED, as shown in Figure 33. The objective of this testing was to ensure the LED could dim and change its brightness based on the amount of power given to it by the twist grip. This simple element demonstrated the amount of voltage the LED was receiving. This can be extended in the laboratory to test the amount provided to the LED.

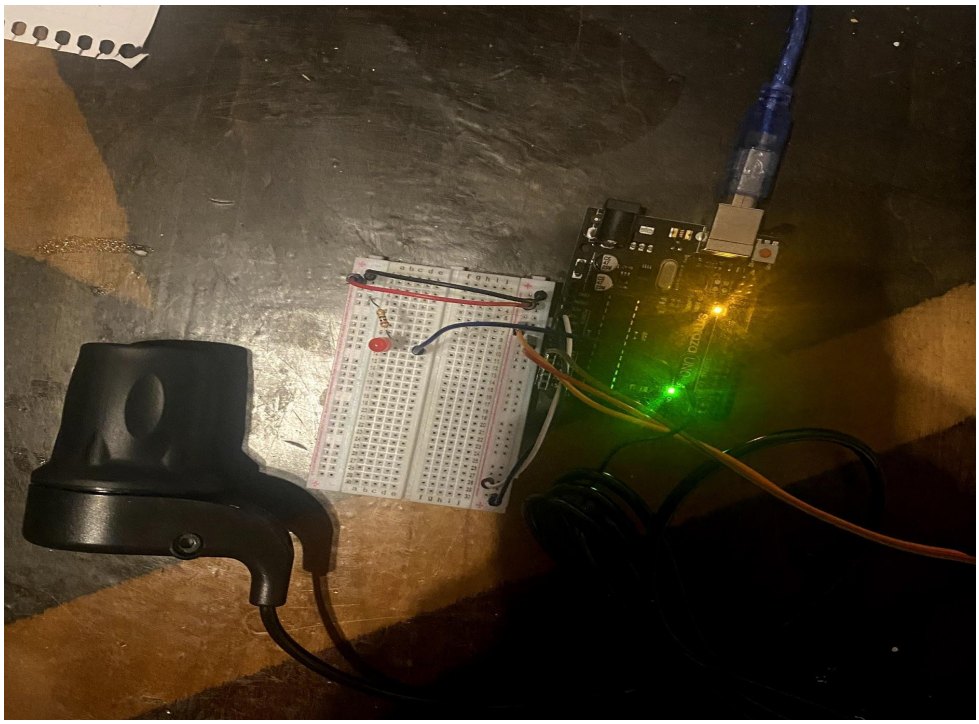

Figure 33: Arduino Uno/LED connection

This LED was receiving a pulse width module sent from the twist grip. We can use an Arduino UNO to create this PWM through code. As seen in Appendix F, the analogWrite() function writes an analog value, a PWM wave, to a pin. These lines of code sent the PWM to the motor controller. This is a simple solution for the PWM. It is simple as the analogWrite() function operates only at 60 Hz. To operate at the frequency of the motor, we need to set the bits on the embedded code for the Arduino.

Once all the programming in Arduino is complete for the twist grip, we then have to 4th: test the pulse width module. The pulse width module was created through Arduino code, and afterward, the testing was completed using the LED setup, as shown in Figure 33. The pulse width module must correctly send the information of the twist amount to the motor controller. This pulse width module was examined using an oscilloscope in the lab. The oscilloscope reading must correctly match the amount of twist provided in the twist grip. As simple as it sounds, this must also look like a pulse width module. The output on the oscilloscope is what will be sent to the motor controller. This proved to be no issue as the Arduino would create a pulse width module due to the rotation value, mapped to be a value from 0 to 1023. By mapping the twist value out on a larger range, testing would allow the twist grip to be sturdy and only send the pulse width module past a certain value. This is used so a signal is not sent because of noise or while the operator is attempting to hold the grip and not twist.

The twist grip is then almost finished its individual test. 5th: we must ensure the twist grip is waterproof enough. The twist grip will be tested with water by spraying the component. The wiring of the twist grip appears very secure on first notice; however, it is better to test this now than when fully configured. We will get the twist grip slightly wet around the space allocated for the twisting of the device. The twist grip hopefully will never be submerged during operation, and further testing during submersion can be performed if deemed necessary. For the majority of its operation, the twist grip will only have to deal with splashes and wet hands by the operator. Again for safety, this will not be electronically connected until after both tests are done. After getting wet, it will be connected electronically. If failure would occur and the device would short circuit, a new one can be Amazon primed within a couple of days for a minimum price seen in the bill of materials.

Lastly and 6th: the throttle controller will be tested in conjunction with the other subsystems. For the user display, we will test that the Arduino UNO can handle all operations. This includes for the user display, the GPS, the water sensors, and for the twist grip. The Arduino should be able to listen for all of the following devices and should prioritize the twist grip. Any lag in the twist grip could serve as a hazard or an inconvenience to the operator. For the motor controller, we will test that the PWM is received by the motor controller and operates the motor accordingly to the twist grip.

4.4. User Display

There are four main components that must be tested for the user display. One of the components is the battery information display. How the battery information display will be tested is discussed in the battery management system testing section above. The other three components consist of the display, speedometer, and water safety sensor. After the components were chosen and the circuit was designed and built, the next step is to test the components individually and then combine them.

The display module was the first component to be tested. Once it is connected correctly, it is tested by running a simple code through the Arduino and determining if the expected output was produced. Two displays were purchased to utilize one and have one as a backup, so both displays were tested using the U8glib library, which is compatible with the displays. The “Hello World” and “Graphics” examples were used to test the Displays. The text’s font and size were tested by standing back five feet to see if the display was still visible. Once both displays were tested to see if working properly, it was time to move onto the next test.

After the speedometer was connected to the Arduino, it was time to test it. Once the GPS module was connected to the Arduino, code was first written to read the NMEA data coming in from the GPS module to the serial monitor. To test if the GPS was reading in the NMEA data, the code in Appendix H was first run. Next, example code from the TinyGPS++ library, compatible with the NEO-6M GPS module, was used for testing in the serial monitor. The “Full Example" code from the TinyGPS++ was used for the testing. Once the expected outcome from this test was performed, code was then written to display the number of satellites and the speed to the serial monitor. Once the speed was displayed correctly in the serial monitor, it was then coded to be sent to the display module for more testing.

To test if the device was operating correctly, the device was driven in cars to test various aspects of the speedometer. The main component needed for testing is a car. The first test performed is the ‘steady speed test’. The car was put on cruise control at various speeds to see if the speed on the display matched the car. The next test was the ‘accelerating test’. The car was accelerated to see if the speedometer was incrementing fluently and accelerating equally to the car. Finally was the ‘hard stop test’. For this test, the driver of the car slammed on their breaks to a complete stop, and the time difference between the car hitting zero and the GPS speedometer was compared. Two other tests were performed to test the accuracy based on location and antenna strength. The speedometer was tested at various locations to see if this had any effect on the speedometer. The antenna was placed under various conditions, such as in the windshield and in a box within the car, to determine where the optimal place in a jet ski would be for the antenna. Once the speedometer tests passed, it was time for the water safety sensor tests.

Initially, all the water sensor tests were only performed with one sensor before adding all 10 in parallel. In order to test for the lower threshold voltage (analog readings) of the water sensor, it was placed under various water conditions. The sensor was submerged 1 cm in water, removed from water (but still had water droplets), and with one water droplet. At each of these

points, the Arduino analog value was determined. Once the lower threshold was determined, the Arduino was then coded to display “No water” when the value was below the lower threshold. When the level is above the lower threshold, the display warns the user, “Water On Board.” Once the display was coded, a few more tests were performed by adding water droplets to the sensor, submerging the sensor, and drying it off. All ten sensors were then placed in parallel and were tested one at a time with a droplet of water to see if the display changed to “Water On Board.” Once the tests were completed with the expected results, the user is now able to see whether water is inside the jet ski.

Once the individual tests passed, the code for the speedometer and water safety were combined in order to display and view both at once. The same tests were then performed again for accuracy to determine if they transferred correctly in the combining process. Once all were approved and accurate, the next step would be to install the module into the jet ski with waterproofing, which will be passed on to the next group.

4.5. Testing Mechanical System

Our individual mechanical components will require testing to ensure they perform properly when tested as an entire assembly. The specs of the motor can be tested by performing what is called a speed-torque test using a machine called a dynamometer. The speed-torque test requires coupling the shaft of the motor to the dynamometer and attaching the motor terminals to a power supply. By varying the speed of the motor using the power supply, we can measure the torque being produced through the dynamometer. This will give us an accurate representation of the torque being produced by the motor and powering the impeller.

Furthermore, fatigue simulation on the propulsion system, including the motor/drive shaft connection as well as the impeller, will be conducted to determine the abilities of our system. To run the simulations, our team needs three-dimensional models of all the components that we have a concern with regarding fatigue failure.

Some of these mechanical components include the motor mount, drive shaft, impeller, and the coupling we will use to connect our drive shaft to our motor. The motor mount will experience constant vibrations while the jet ski is moving, so it is susceptible to fatigue failure over so many cycles. The drive shaft, impeller, and shaft coupling will experience constant rotation while the jet ski is moving, so these components are also susceptible to fatigue. Our team will use a simulation software called Ansys to simulate fatigue of our components over a large number of cycles. The different parts will be fixed in the software where they would actually be fixtured in the jet ski to simulate those parts being connected to something else. For example, the drive shaft will be fixed on both ends when simulating because it is connected to the impeller on one side and to the motor on the other side. The corresponding CAD models are shown in Appendix G.

We need to ensure that our battery casings are completely waterproof to protect the batteries from any water damage. To test our battery casing design, we will expose the finished

casing itself (without the battery) to water in two ways. Using a hose, we will spray the casing from every direction to try to simulate water getting into the hull of the jet ski while it is maneuvering. Next, we will submerge the casing in a small amount of water for a period of eight hours to simulate if the jet ski hull had taken on water and not been used for a period of time. These tests will reveal where any potential leaks may be coming from and if our casing design is feasible for long-term use.

Lastly, our team is determining how we will test the whole jet ski. We have three different ideas where tests could be conducted on RPM and overall performance. The first idea is to reach out to the athletic department and see if we could use their pool facility to conduct our first stage testing. The second is to design our own box/mini pool where the jet ski will be suspended by cables on every corner of the box made out of wood and filled with water. The box will be covered in a tarp-type material that will be able to hold the water. The jet ski will be stationary due to cable suspensions but able to run at max RPM during testing. Lastly, our final test option would be depositing the jet ski in open water in a pond or lake in or around the Worcester area.

4.6. Assembly of Mechanical Components

Our team was able to perform simulation testing on the new battery casing configuration. Finite element analysis was performed in Ansys on the casings to evaluate the total stress analysis on the battery casings. The stresses that the casings were taking on that our team analyzed were the forces of the weight of the batteries on the base of the casings and the random vibration stress analysis on the battery casings from the vibrations of the motor and the vibration of the jet ski in motion on the water body. These were the two most pertinent forces that would cause stress on the casings. We used these testing parameters to determine whether or not our final design would be able to withstand these static and vibration forces, including the shape of the casings, the thickness and the material selection.

We integrated one of the 2-battery casing boxes into the jet ski to show that it is easily accessible and would be user friendly in terms of opening up the casing and removing batteries. Below is our final 3D print of the 2-battery casing and its implementation into the jet ski. The lid of the design which is shown in red below is unlatched on each side and can be removed with only inches of excess space. With the caving in walls and low ceiling in the inner hull of the jet ski, the design needed to be able to open up for battery access with as little space as possible.

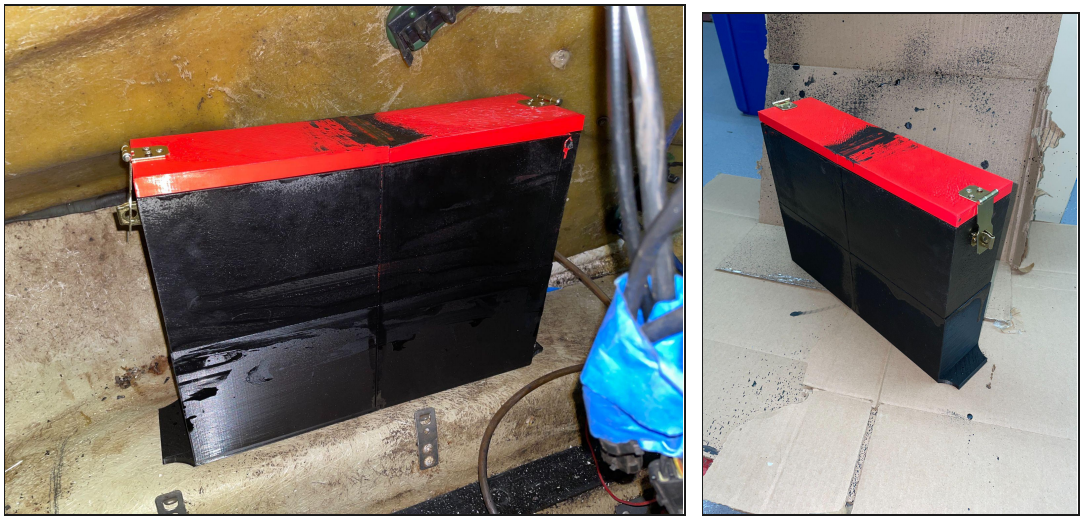

Figure 34 A,B: 2-Battery Casing Configuration & Implementation

4.7. Assembly of Mechanical Components

Once each mechanical component, including the motor, drive shaft, impeller, and electrical casings, are either ordered and delivered or manufactured through various production methods, our team will proceed to assemble the components together within the jet ski.

We will begin by mounting the motor to the jet ski with the machined aluminum mount parts. Once the motor is mounted, the drive shaft and impeller assembly will follow. The drive shaft connects to the end of the motor, and the impeller connects to the opposite end of the drive shaft at the back of the hull.

Further research will be conducted in order to understand how to assemble each mechanical component for optimal performance of the whole system. The watercraft was left disassembled from last year's project, so our team will need some frame of reference to ensure every component gets installed correctly.

We have ordered all the propulsion system parts from the old 1997 Sea-Doo SPX model jet ski and are working on configuring the system back together. The coupler is a major aspect of our drive shaft/motor connection. Further analysis needs to be made on the coupler to determine if it is a type of connection between the motor and the shaft that will not fatigue under high RPM and torque.

The beginning of the physical assembly started in C-term. The impeller was removed from its housing and cleaned thoroughly. We assembled it back together and secured it airtight to the back through-hole of the hull. Once the impeller was secured, we attached the drive shaft. Since we secured the impeller to the hull, we needed to place the drive shaft from the inside of the hull and push it back into the impeller. We managed to match up the splines for a perfect fit and rotated the drive shaft by hand to confirm the fit.

The motor mount block holes were drilled into the hull from the start. However, we needed to clean up the inner hull as it was not level. The blocks need to be level for the mount to

be secured in the correct fashion. The inner hull is composed of fiberglass, which made it difficult to remove the excess material. We ended up cutting the fiberglass with sharp “X-acto” knives to level off the location for the blocks. This method avoids creating the dangerous microparticles of fiberglass that appear during drilling or sawing.

The next step was to bolt down the motor saddle. Once the metal was bent into the correct shape, we placed it in position and drilled down a bolt on each side rail into the hull. We had already machined the motor mount; however, we wanted to secure it to the blocks after implementing the motor. We used the crane in Higgins Machine Shop to hoist the motor into the hull of the jet ski. Unfortunately, the motor could not be placed in the correct position because it is too long. There are rails on the inner hull of the jet ski that would need to be cut out of the jet ski for it to fit. The 2020 Electric Jet Ski MQP team had designed the propulsion system with a shorter drive shaft (x in.). They wanted to cut the drive shaft’s external spline off and weld a coupling to the end. We realized the cut was not possible given the material was cold-hardened, so we were advised by machine shop managers to abort that plan. We ended up designing a custom coupling that added two more inches to the length of the drivetrain since we did not cut off any material.

The motor ended up being too long, and it could not sit on the saddle as we had hoped. The rails of the inner hull block the motor from becoming flush with the drive shaft. They are not able to perfectly align, which is a major issue.

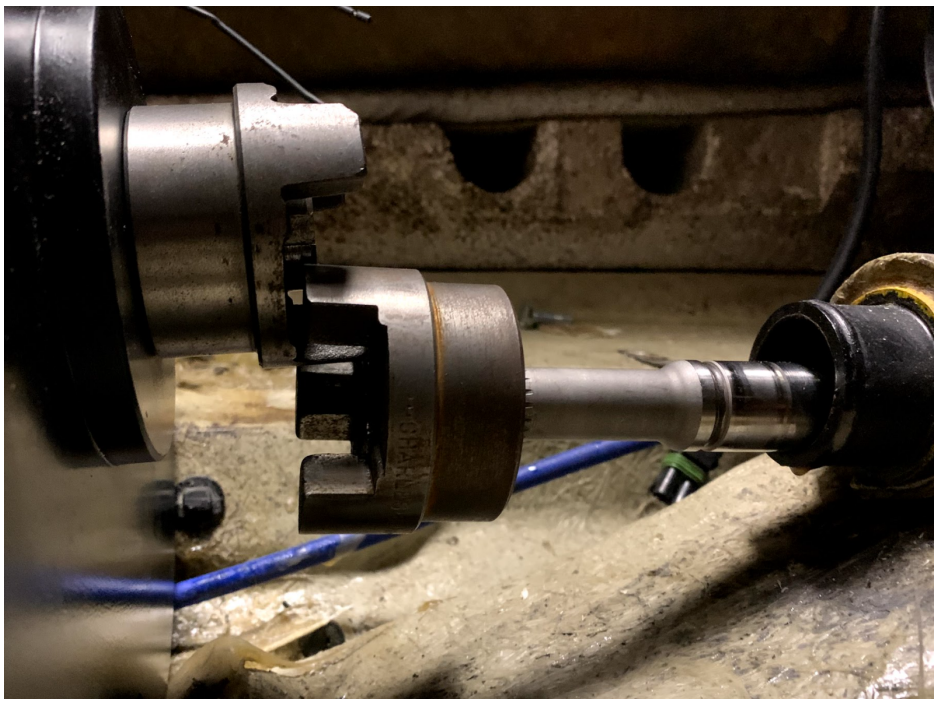

Figure 35: Motor/Drive Shaft Connection

Even though the current motor does not fit in the inner hull, there are a couple of different options. The drive shaft now has a custom coupling which allows it to adapt to many types of

electric motors. A new, smaller motor would work perfectly. If purchasing a motor is not an option, then the inner hull will need to be altered to allow the fit.

5. Discussion of Results

This chapter will discuss the outcomes and decisions following the testing described in chapter four. Due to COVID-19 restrictions, lab access and in-person collaborative work was limited. The high-power laboratories in Atwater Kent require key card access, and due to COVID restrictions, getting physical keys made was delayed; therefore, we never received access to the high-power lab, and most testing was done independently at home or in non-high-power Atwater Kent laboratories.

5.1. BMS

Each section of the battery management system was tested successfully. Due to limited lab access, the system was unable to be tested fully integrated. Batteries, EV Display, and BMS were all tested independently. The first test done was for the Nissan Leaf G2 Battery Modules. Each battery voltage was tested via a digital multimeter. Each module was successfully measured, and each range from 7.5-7.6V. At this voltage, a full load of batteries will produce 90-91.2V, which is ideal for powering and testing the current Motor Controller we have.

The display was tested isolated from the batteries but connected to the BMS. By connecting the display as described in the testing plan, it worked as expected. The user can scroll through the different screens via the touchscreen to monitor full battery pack power, individual cell voltages, and set high and low voltage cutoffs. The main screen of the EV display is shown below in Figure 36.

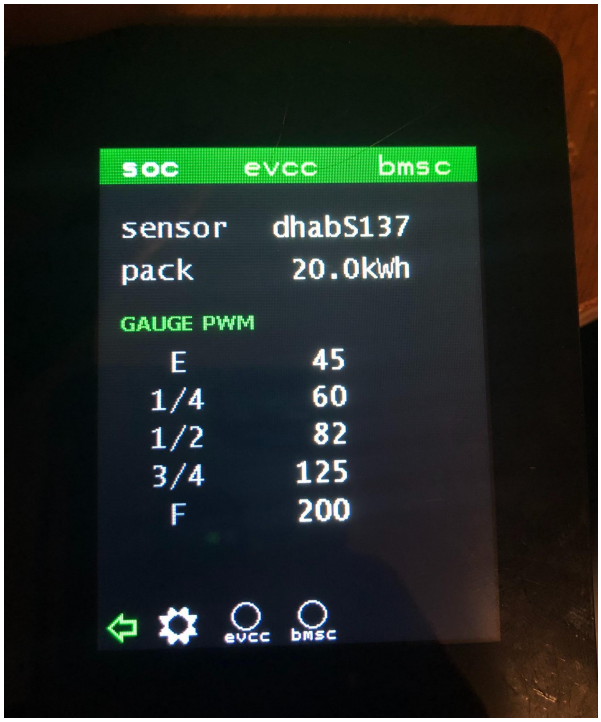

Figure 36: EV Display

The last portion of testing for the battery system was the BMS. The BMS connected as described in the testing plan was connected to a computer using the Thunderstruck software. Using this software, the BMS was successfully recognized, and the BMSC options were available, but the BMSC was not purchased. Using the correct serial line as connected via USB, the BMS can be configured using PuTTY. This PuTTY screen can be seen below in Figure x. Using this program, a command screen can be opened to input commands such as changing the high and low voltage cut-offs and minimum balancing voltage. In addition to this, the command “showmap” can be used to see the configuration of the battery modules to ensure the batteries are connected 12 in series in parallel with 12 in series.

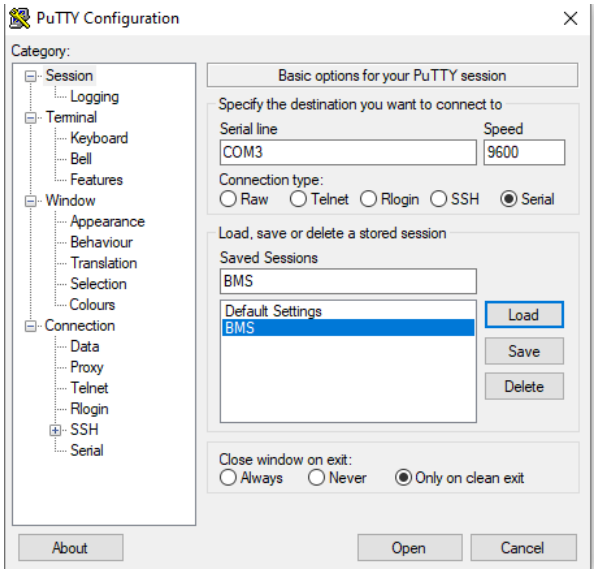

Figure 37. BMS PuTTY Screen

5.2. Motor Controller

The H-bridge was successfully designed and simulated in LTSpice, and it works as intended. Vbatt must remain below 100V, or Vbatt is shorted to ground due to exceeding the breakdown voltage of MOSFETS. Vbatt should be at least 16.67V with currently selected R_{BOT} and R_{TOP} values to guarantee PMOS operation, or the PMOS switches (the top two) may not be biased on when they should be. By adjusting the ratio of R_{BOT} to R_{TOP} , the circuit can be configured to work at a lower voltage.

Physical testing was limited due to never having MQP lab access, although some testing was still possible due to what team members had access to in their residences. The H-Bridge circuit was built on a breadboard and tested using a 15V power supply, current was limited to 20mA, with a low voltage (6V - 18V) motor. While the power supply is not 16.67V, the PMOS did work as intended (PMOS datasheet shows Vth range of 1.5 to 2.5 volts, yielding a range of 10V to 16.67V Vbatt). With no access to a function generator, PWM signals were left tied HIGH and pulsed LOW via manual button presses that shorted the PWM signal to 5 volts. Shorting PWM1 to 5V while PWM2 was grounded produced forward motor rotations, and shorting PWM2 to 5V while PWM1 was grounded produced reverse motor rotations, as intended. For both forward and reverse directions, a full 15V appeared across the load (in opposite directions, respectively), as measured by a DMM. This shows there is minimal drop across the switches of the H-Bridge, which will need to be verified at higher voltage operation. An Arduino was used to provide the 5V power rail.

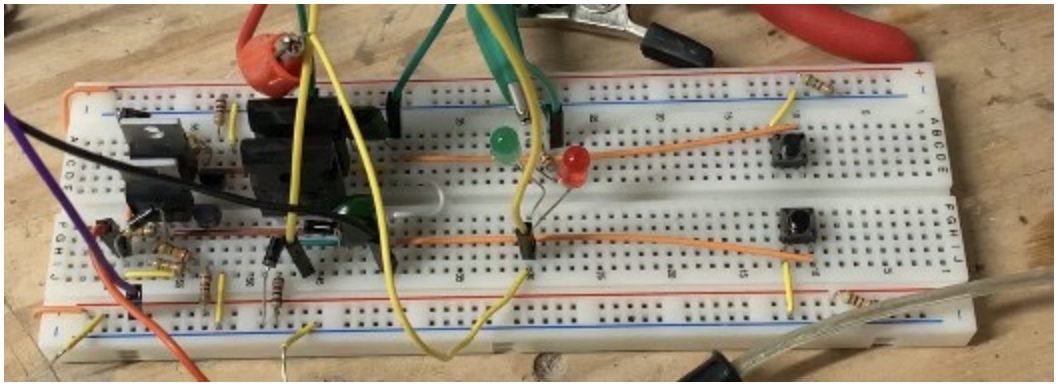

Figure 38 H-Bridge breadboarded for low power testing

The low-side switch delay circuitry could not be verified without an oscilloscope, and so before graduating to higher power testing, it should be verified that there are no shorts from power to ground on either the rising or falling edges of either PWM signal. Once this is completed with a breadboard circuit, the circuit should be soldered to the protoboard before increasing testing power.

RPM-estimation via ripple counting, the dead man switch, and the buck converter were not designed during this segment of the MQP and are left for future teams.

5.3. Throttle Control

With the Arduino set up, as shown in Figure 25, the tests were conducted in success. The twist grip was measured at a range of +5V to roughly 3mV when rotated. Through the Arduino code seen in Appendix F, the Arduino was able to map the twist grip on a rating scale of 0 to 1023. This range was chosen as it is large enough to allow slight changes for the noise, and it is regularly an Arduino scaling standard. The Arduino serial port reads the pulse width module using the pulseIn() function. This includes a delay in the function. The serial port will only print the PWM's value at a rapid pace when it is greater than zero. When the PWM is zero, the function sends a zero every second. This function will save space on the Arduino when the operator is not twisting.

When the twist grip is not moved, the LED is at a constant voltage of 3.1mV with no light showing. The twist grip is moved slightly with no change in value in the Arduino console. There is no noise sent to the motor or the LED for this testing scenario. Several iterations of the cut_off turn point had to be adjusted to find a solid value that implied the operator was twisting. As the twist grip is turned, the PWM is altered. This can be shown as the duty cycle of the PWM changes, as shown in Figure 39. The left image has a pulse width module with a shorter duty cycle than that of the image on the right for Figure 39. This is because the right twist grip has been rotated more than the left twist grip.

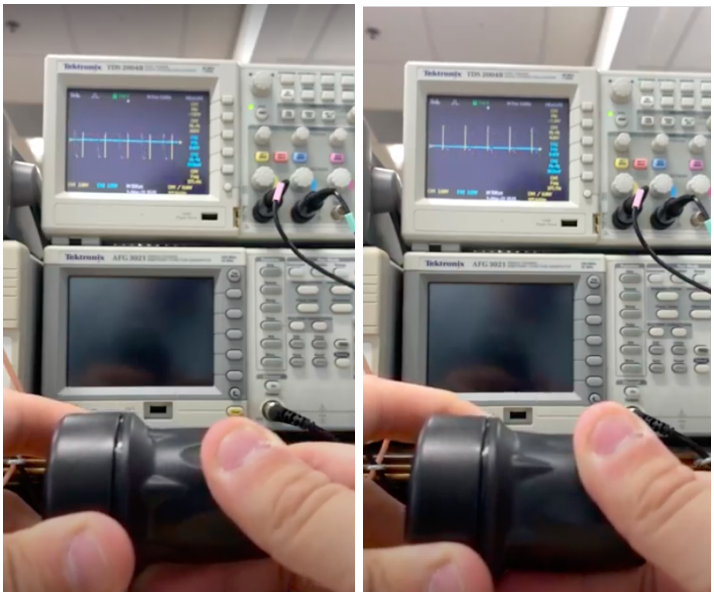

Figure 39: Moved PWM (Slighter twist left to right)

Through testing, the cutoff value for noise had to be adjusted several times. While most operators keep their right hand off the twist grip and on the extended part of the handle, this cutoff value was important to prevent motor operations unintentionally. This pulse width module at half-twist of the half-twist grip can be shown below in Figure 40. The duty cycle is approximately 50%.

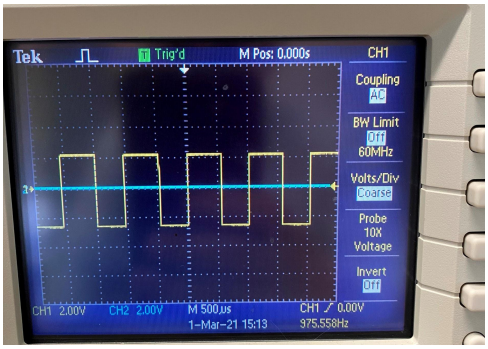

Figure 40. Pulse Width Module at Half Duty Cycle

- All three elements of the PWM process aligned when testing.
- The serial port proved to print the correct range of values based on the amount of twist.
- The oscilloscope displays an alternating PWM based on the amount of turn the twist grip was given.
- The LED appeared to alternate its brightness to the human eye.

5.4. User Display

Through the design and testing process, two user display components are operational: the speedometer and water safety sensor. The battery information display operation and progress are further discussed in the BMS section above, as the availability of battery testing directly influenced it. Both the speedometer and the water safety sensor are on the same display. The speedometer is in a larger font than the water sensor, as it is used more often, shown in Figure 41.

Figure 41. Display

During the initial testing of the GPS, there was an error that was run into. The first purchased GPS module was broken, so the expected NMEA data sentences were not being sent to the serial monitor, either due to a faulty antenna or the GPS module itself. When a new GPS module was ordered, the NMEA test was performed again, which now had full NMEA sentences being displayed to the serial monitor. Next, the example code from the TinyGPS++ package was run with a baud rate of 9600, with no errors. Once the speedometer itself was coded, the speedometer tests were performed.

After performing the three tests on the speedometer multiple times, data was gathered to determine how accurate it was. The results of the ‘steady speed test’ were that the speedometer displayed the same speed that the car's cruise control was set to; this was true for multiple speeds. When the ‘accelerating test’ was first performed, the speed was not incrementing fluently; it would jump by 15-20 mph. When the ‘hard stop test’ was also first performed, there was roughly a 10-second delay from when the car hit zero to when the speedometer hit zero. The code was adjusted to account for the delay and the lack of fluent incrementing. When the ‘accelerating test’ and ‘hard stop test’ were then reperformed, there were improvements in the speedometer. The delay is now roughly only one second, and the increment of the speed is much more fluent than before. The speedometer does still jump slightly when the car accelerates or decelerates very fast. Other speedometers that utilized the TinyGPS++ package were researched, and all appeared to have a similar delay in speed.

The two other tests involving the antenna were completed as well. When the GPS was tested at various locations in MA and NH, the antenna was able to make a connection. The current antenna is only effective outside or in a windshield. The GPS does not pick up a signal while inside a building or while being in the main body of the car; therefore, the recommendations made based on this testing is to install the antenna under the windshield of the jet ski or purchase a stronger antenna.

The water sensor is operational after designing and performing testing. In order to determine the lower threshold value of the water sensor, which then will display a warning to the user, the Arduino was first coded to display the analog reading that the water caused at various levels. To determine the lower threshold, a cup was first filled with water. The sensor was then slowly dipped into the cup and compared to the analog readings. When the sensor was submerged 1cm in water, the value was roughly 500 Arduino ratings; when removed from water (but still had water droplets), it was roughly 60; and with one water droplet, it was roughly 30. The lower threshold was set to 25 Arduino ratings to give a variance for humidity but low enough to catch the first signs of water within the jet ski hull. Once the lower threshold was determined, the Arduino was then coded to display "No water" when the value was below the lower threshold. When the level is above the lower threshold, the display warns the user, "Water On Board."

In the end, the water sensor can detect the initial signs of water of less than a drop. The water sensor was set up to check for water every eight seconds. The reason for not constantly checking for water was to reduce the corrosion rate of the water sensor and extend the life of the water sensors. Ten sensors were placed in parallel, as seen in Figure 42, and as a result of the testing, every sensor was operational and could detect the first signs of water. The recommendations for the next steps are to waterproof the connections of the water sensors, as well as to determine the optimal places for all ten sensors within the jet ski.

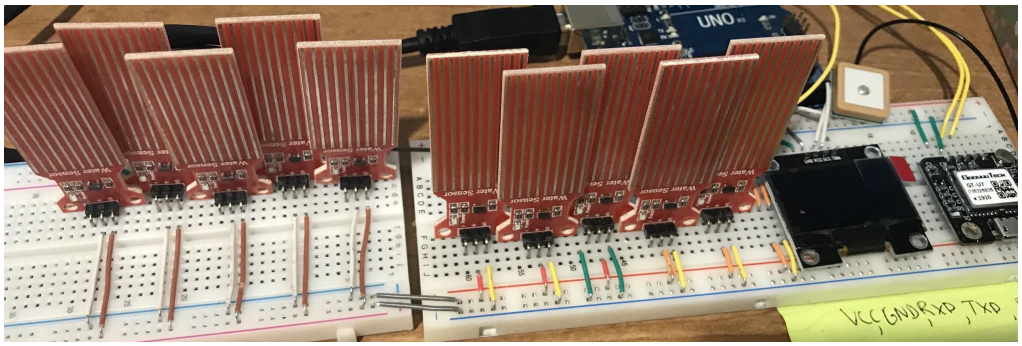

Figure 42. Water Sensors

After the speedometer and water sensors were operating individually, they were combined into one Arduino code, attached in Appendix I. The same tests were performed again, and the speedometer and water sensors work at the same time, with the same results. Even though both the speedometer and water sensors are operational, the process to get there didn't come without issues or difficulties. The discussion of issues and difficulties is important, as

another group will be continuing on constructing the electrical jet ski. Being aware of past troubles will speed up the process of implementation. Firstly, the original GPS purchased was faulty and could not read in the NMEA data. If this were to occur again, there is now code to test the NMEA data coming in. Without lab space, there were no soldiers available for use, so the pins repetitively continued to disconnect, and pieces had to be balanced to maintain their connections. Eventually, a solder was able to be located, and the pieces were properly connected, so going there should not be this issue. The memory space of the Arduino is limited; therefore, decisions and alterations had to be made to limit the amount of memory used, such as the library for the display. Due to multiple aspects of the jet ski utilizing an Arduino, another Arduino might need to be purchased, or increasing the memory space of the current Arduino might be necessary. When working with the GPS, the current antenna only receives a connection outdoors or in a windshield; therefore, it's recommended a stronger antenna be purchased. Some difficulties were faced when having to test outside. The weather has to be under certain conditions, as the electrical devices cannot get wet, and they do not operate when the weather is too cold. Finally, another next step is to perform waterproofing of the connections, wires, and electrical pieces.

5.5. Motor Mount

In order to test the mechanical components of our system, we relied on three-dimensional modeling and simulation software SolidWorks and Ansys. The motor mount connects directly to the motor, so it bears a lot of the weight and is an area of concern for simulation. Using SolidWorks simulation, the sides of the motor mount were fixed since this is where the mount is connected to the hull. Since this front plate is carrying the weight of the motor, a force was applied downward, as can be seen in the figures below. The first figure shows the Von Mises stress throughout the front plate as the load of the motor is applied, with the legend on the right indicating the proximity of the stress value at a certain location to the yield strength of the material. As can be seen in the figure, the majority of the stress is concentrated where the side extensions connect to the main body of the plate. The green color in this location indicates that the material is experiencing a small amount of stress compared to the yield strength of the material, and we can be confident the mount will not fail. The second figure shows the deformation of the front plate as the load of the motor is applied, with the legend on the right correlating colors to amounts of deformation. With the load being applied on top, the majority of the deformation can therefore be seen on the top of the plate. The maximum deformation experienced by the plate in this location is 5.272 X 10^-3 mm, a very minimal amount for this component.

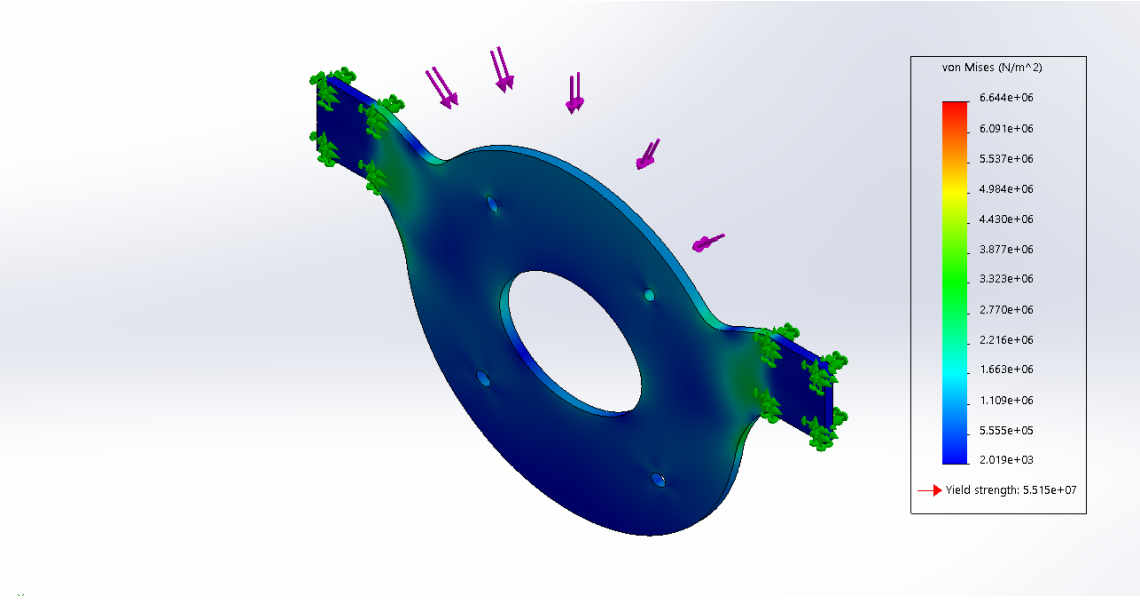

Figure 43: Stress simulation of Front Plate with load focused on top

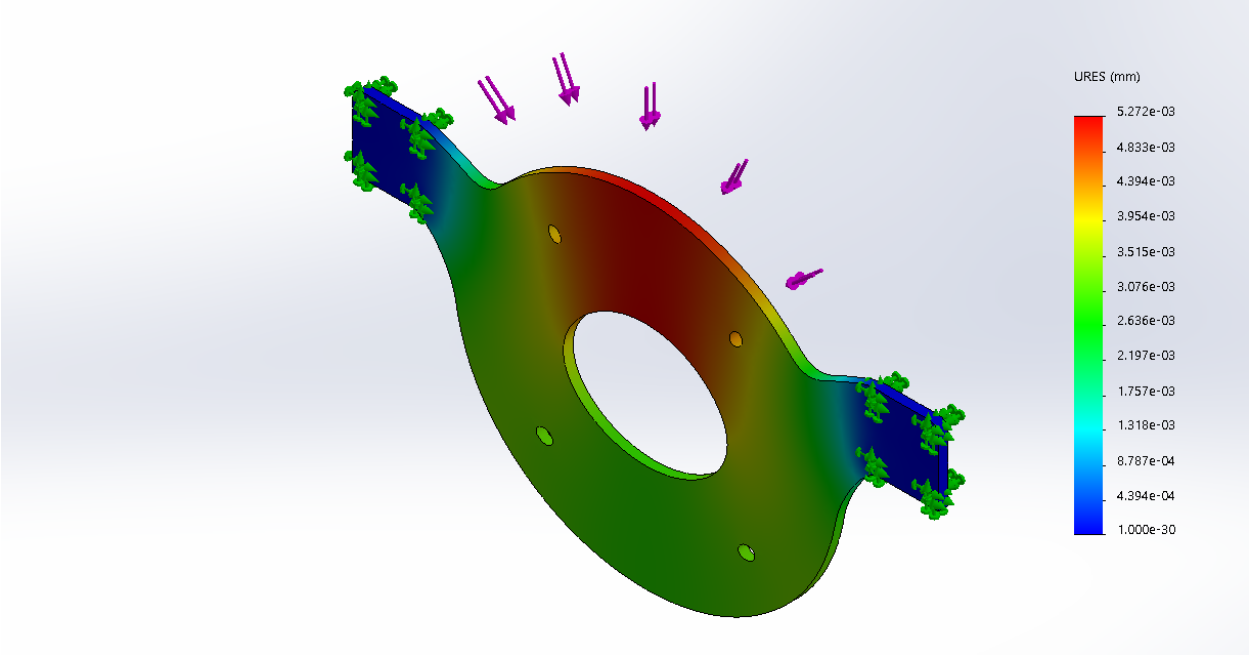

Figure 44: Deformation Simulation of Front Plate with load focused on top

As it was difficult to properly model the force on the front plate part, another simulation was created with the load focused on the bottom of the plate to get a good range of analysis. Again, the first figure shows the stress throughout the material, with the highest stress, experienced only being about half of the yield strength of the material, well within an acceptable range. The second figure below again shows the deformation of the front plate, with the largest amount of deformation occurring on the bottom as expected. This deformation is a maximum at a value of 4.587 X 10^-3 mm, which is a negligible amount for this part.

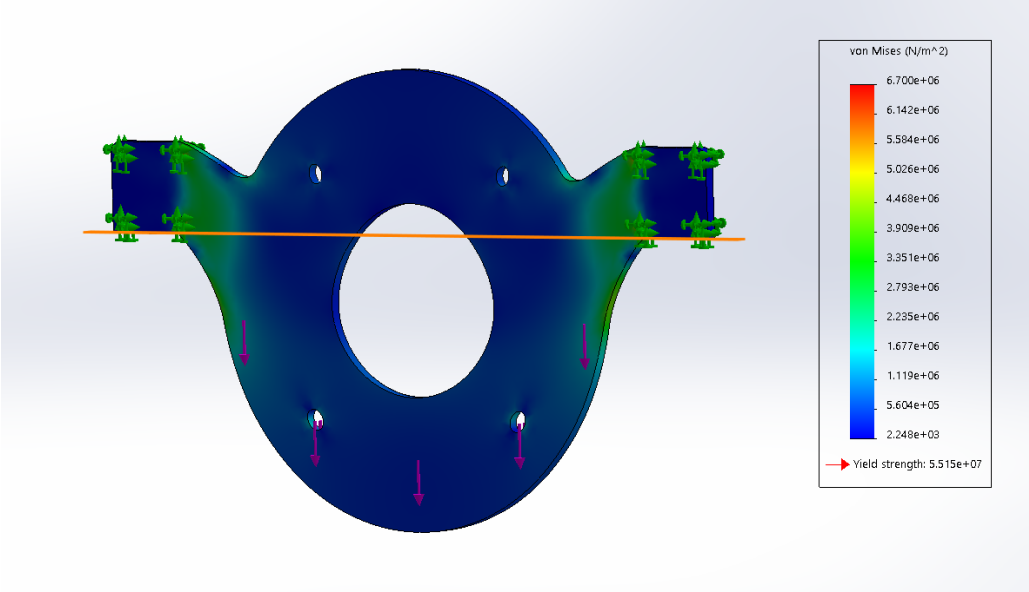

Figure 45: Stress Simulation of Front plate with load focused on bottom

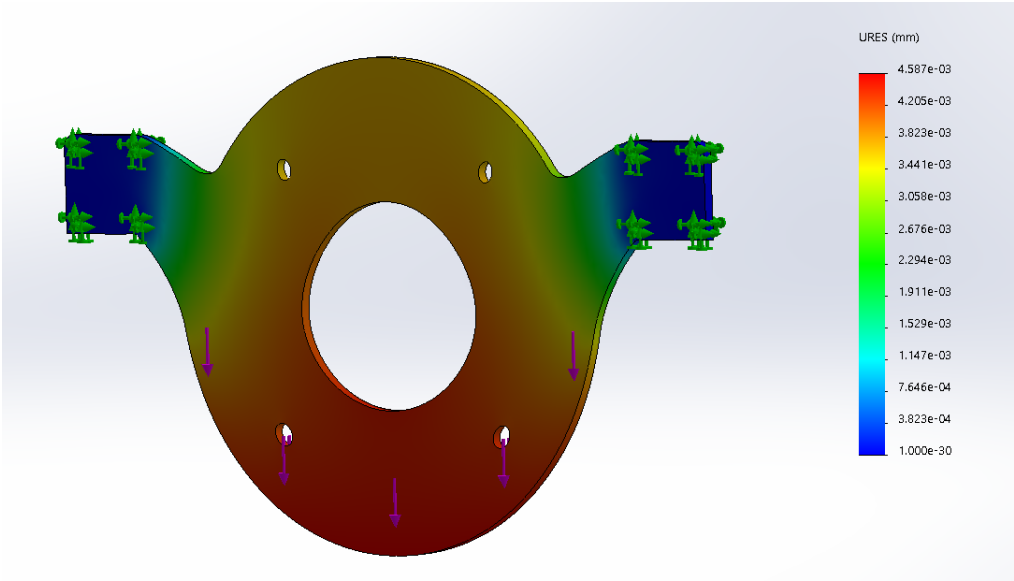

Figure 46: Deformation Simulation of Front Plate with load focused on bottom

5.6. Drive shaft

Another mechanical component that was of concern was the drive shaft, since this part is responsible for transmitting all the torque from the motor to the impeller. This part was simulated using Ansys, with one end of the drive shaft being fixed and with a moment being applied to the other end to simulate the torque that this part would experience. The first figure below shows the total deformation results of the simulation, with the maximum deformation being a little less than 0.7 mm. The second figure below shows the equivalent stress (Von-Mises stress) throughout the

drive shaft. The maximum stress experienced is 2.242 X 10^8 Pascals with the 316 annealed stainless steel. The drive shaft is made of a tensile yield strength of 2.521 X 10^8 Pascals, giving us a factor of safety of 1.124 for our drive shaft.

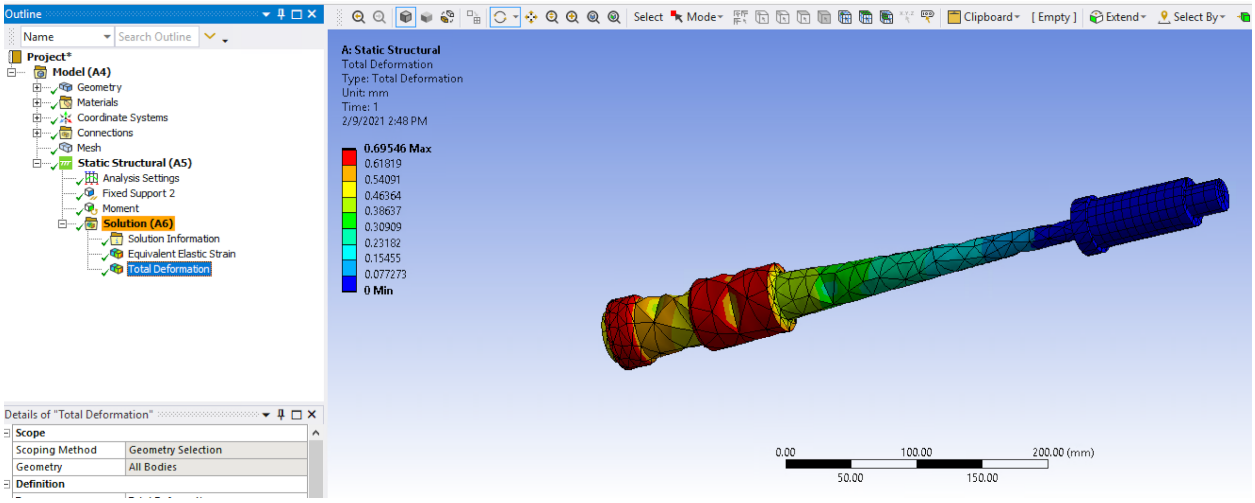

Figure 47: Total Deformation Simulation on Drive shaft

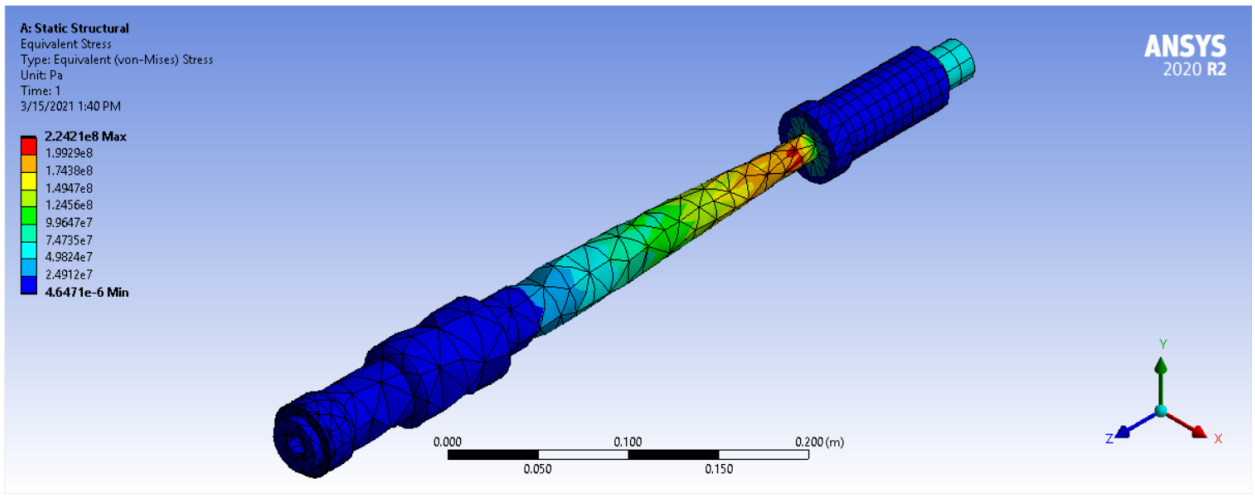

Figure 48: Equivalent Stress Simulation on Drive shaft

5.7. Battery Casings

The Von-Mises stress analysis of the battery casings were explored and analyzed using Ansys. We began with applying a force of 44 N of force for every battery inside of each casing. For the small 2-battery casing, we applied a total of 100 N of force from the weight of the batteries. Instead of applying 88 N of force we added an extra 12 N for safety measures. Our team wanted to test the casing against forces that it most likely will not encounter to ensure the casings will not fail under smaller, more realistic forces. We added constraints at the holes of the casing where the casing would be drilled into the hull. We also conducted random vibration

analysis on the casings. Each casing regardless of size and positioning within the hull was given the same random vibration analysis and similar battery weight forces. The 16-battery casing stress analysis was analyzed with taking on 750 N of force, 704 for 44 N per battery and an extra 46 N for testing a safe force that the battery casing normally will not encounter to ensure that it will be able to operate under normal circumstances. Figures 38A-D below show the Von-Mises stress analysis of the vibrations and the weight of the batteries on both the 2-battery casing and the 16-battery casing.

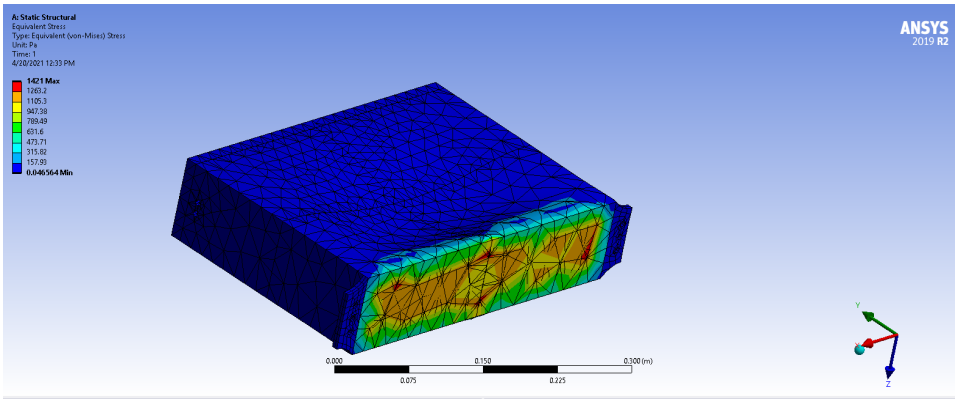

A

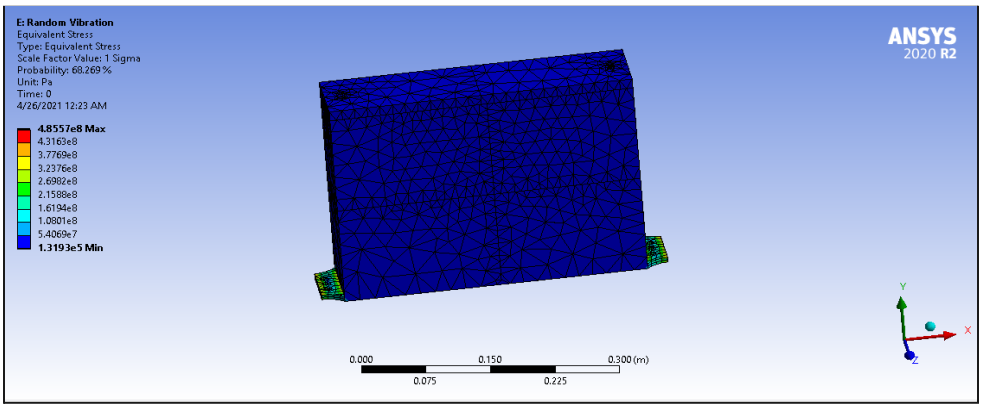

B

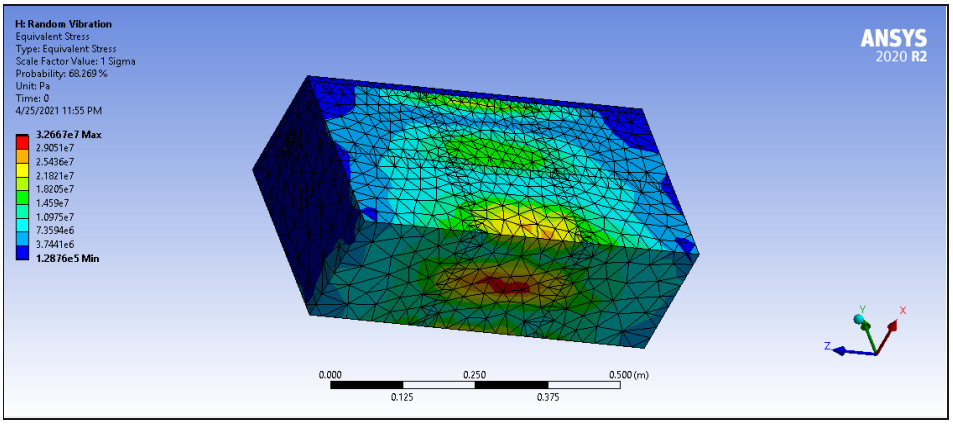

C

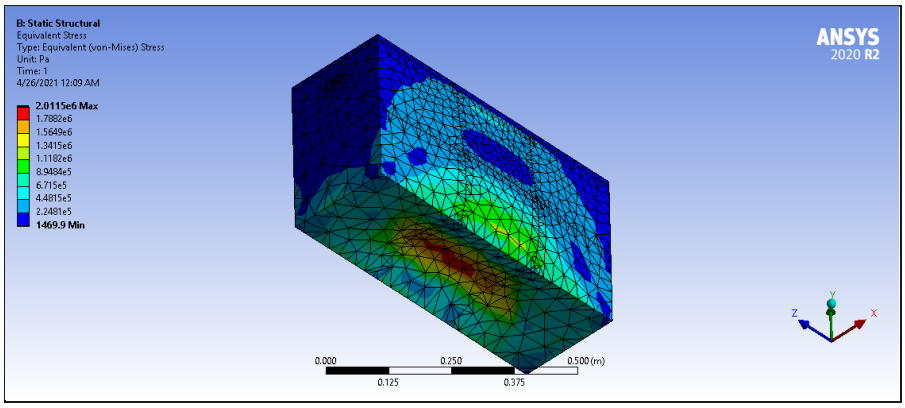

Figure 49A-D: Von-Mises Stress Analysis of Weight of Batteries (A,D) and Random Vibration (B,C)

Based on the results, the 2-battery casing total maximum equivalent stress of the random vibration and the weight of the batteries equates to 488.6 MPa. The random vibration stress accounted for nearly 99% of the total stress. The 16-battery casing total max stress rounded out to be equal to 37.7 MPa. The max stress from the batteries was around 2 MPa and the max random vibration stress on the casings was 32.67 MPa. The overall yield strength of the PLA material used for the battery casings is 52 MPa. The 16-battery casing design has a lower overall stress than the yield strength so therefore the PLA material and overall design is sufficient. For the 2-battery casing design, the overall stress is more than 10 times more than that of the 16-battery casing mostly due to the random vibration analysis. Based on these simulations the 2-battery casing design and PLA material is not sufficient for bearing the overall stress of the random vibrations experienced within the jet ski. Most of the stress is along the feet of the casing where the casing will be drilled into the hull and secured on the jet ski. This aspect of the design might need to be redesigned and reinforced so that the random vibrations does not distribute such great stress on that small area which would cause the casings to fail and detach from the inner hull.

The next steps for future teams should be to ensure that the batteries will not overheat in their casings while running the jetski at our current max capacity. Thermal steady state heat transfer analysis can be made in Ansys to determine whether the current material and design would keep the system cool and intact or fail. Our current design does not account for any ventilation and cooling of the batteries. Future teams can look into finding ways to keep the batteries from overheating. To run this test live, we would fully connect the entire BMS, Battery Casing, Propulsion System and Motor system together and connect thermal sensors to the inside of one of the battery casings. We would then power the jet ski for 15 minutes at full throttle and observe the data.

6. Conclusion

Over the academic year 2020-2021, significant progress was made towards the goal of a complete working electrically powered jet ski. Work this year on the electric components of the jet ski was primarily focused on designing and individually prototyping a number of the electrical subsystems: the throttle control, the motor controller, the user display, and the battery management system (BMS). Some testing was also performed on these prototypes, but testing abilities were significantly restricted due to the available testing equipment. For Mechanical components, the main focus was on the battery casing, motor mount, and drive shaft. Each of these components made significant progress throughout this academic year, with their progress thoroughly outlined in Chapter 5. The next steps for future work on this project are outlined below for each system.

6.1. Recommendations for Future Work

Significant amounts of progress were made on both the electrical and mechanical components. The mechanical lab space was open and was gained access to, but during much of the year, there was no physical access allowed into AK (ECE building). This prevented any testing that required the use of oscilloscopes, power supplies, or function generators. Additionally, while there were some tests run in the non-high-power AK labs once AK was opened, the high-power equipment needed to fully test the battery and motor controller systems is only located within a dedicated high-power MQP lab of AK210, which the team didn't receive access to prior to the end of the MQP. Access to this lab is a necessity for the next MQP team, and the process to gain access via being assigned physical keys by the ECE office should be pursued as soon as possible. Even with very limited equipment, the electrical team was able to perform a handful of tests on prototypes created in their own residences.

After manufacturing all the necessary parts to assemble the mechanical system inside the jet ski, many issues were noticed with the amount of space available inside the jet ski. The motor is too large to fit reasonably within the hull while still connecting properly to the drive shaft and impeller. Our group manufactured a coupling capable of connecting to the motor connection side of the drive shaft, with the impeller connection already being secured. In order to successfully complete this project, we think a new motor is necessary to help reduce overall weight and to fit properly inside the hull. With the new coupling for the drive shaft, a future team would simply have to purchase or find from Washburn shops, as we were able to, a coupling that connects to the new motor.

Our team chose to print our casings with PLA in the prototyping lab (3D printing) because it was the most cost-friendly and easily accessible option for our team. In the future, I would recommend teams to look into lighter, more heat resistant, and waterproof material. The biggest function that our team focused on was battery accessibility for the user. The inner hull lining has so many curving walls with low ceilings that interrupted our ability to place casings throughout the jet ski because the user would not be able to take the batteries out. Future teams

will be able to take our battery casing designs and configurations and find better ways to create a waterproofed case. One problem with our design is that if the batteries overheat, it can set the flex seal on fire due to the extremely flammable properties of flex seal, the rubber sealant our team chose to waterproof the system. We recommend that future teams look into ways to alter the layout of the inner hull. Electric Jet skis have different components compared to gas-powered jet skis, and the layout of the hull needs to be adjusted so that the components can fit inside well and have the jet ski perform at maximum potential.

The motor controller subsystem has a number of subcomponents: the H-Bridge circuit driving the motor; the PWM signals driving the H-Bridge circuit; the RPM estimation circuitry; and the dead man switch safety system. As the H-Bridge circuitry is the core component necessary to make the motor move, development time was focused on this subcomponent. The H-Bridge was fully designed and simulated within LTSpice over the 2020-2021 academic year. Parts were ordered, and a prototype was built on a breadboard and tested and verified at low power. Once lab access is acquired, the prototype should be transferred to perfboard, soldered, and tested at increasing power levels until it is verified at the voltage and current levels it is expected to use at full operation. High power supplies and a digital load will be vital for this testing. The PWM signals driving the H-Bridge circuit are created by the Throttle Control Arduino script, and so will be created during integration; in the meantime, a signal generator should be used to create testing PWM signals for the H-Bridge. The RPM estimation circuitry and the dead man switch safety system were not created during this academic year. High power testing and verification of the H-Bridge circuit should be the first priority of the next team, with RPM estimation circuitry being the next priority.

To create the PWM, the function analogWrite() was used in the Arduino. This function operates at a fixed frequency of 60 Hz. In order to get the required frequency needed for the motor controller, embedded registers need to be declared. This can easily be done after a short time of research on the Arduino forms. Another possible option is to operate two different Arduinos to all the Arduino to operate at the required frequency of the motor controllers, separate from that of the user display. From there, the PWM should be ready to connect to the motor controller and accept the PWM.

There are two main next steps for the user display. The first would be to add an RPM gauge. Through research, it was determined the least expensive but also accurate option would be to use ripple counting from the motor through the Arduino. This would then be tested by using a digital tachometer, or a tachometer could be created with an infrared LED and photodiode. The other main next step for the user display would be to waterproof and install the speedometer and water safety sensors. Recommendations to improve the current design would be to purchase a more robust antenna and test the GPS again in more locations.

The current BMS system has all been tested in parts but has not been fully integrated. Everything works as intended in isolation, but there are a few steps that need to be taken with lab access. The batteries should be connected 12 in series in parallel with another 12 in series to the BMS and Display to confirm the full battery module output voltage and power. In addition to

this, a charge controller is recommended. The easiest solution would be to use the Thunderstruck charge controller, which can be purchased for $300. With this charge controller, it can be directly connected to the BMS. A charger would also need to be purchased. Through research, there are many Nissan Leaf G2 battery chargers widely available. A waterproof charger is most recommended. In addition to this, the management system would also benefit from a buck converter. A buck converter should be used to convert the high battery voltage to a stable low voltage value that can be used as a power supply for the other electronics, such as the Arduino and User Display. This converter has not yet been designed; without it, a second power source is needed for these lower voltage components.

Final recommendations to the next group that continues the project are to document all data as the project is carried out. We also recommend writing Chapters 1-3 of the MQP report A-term, updating prior writing and adding Chapter 4 B-term, and finalizing the C-term report by updating past chapters and writing Chapters 5 and 6. Lastly, all of our inherited, newly purchased, and manufactured parts are stored and available to be passed on to the next group.

References

Asplund, T., (2000). The Effects of Motorized Watercraft on Aquatic Ecosystems Retrieved from https://dnr.wi.gov/lakes/publications/documents/lakes.pdf

Boating Tech Team. (2016). 60 great boating innovations. *Boating, 89*(9), 78-84. Retrieved from https://search.proquest.com/docview/1818007808?rfr_id=info%3Axri%2Fsid%3Aprimo

Deegoo-FPV. (n.d.). GPS module receiver,navigation satellite positioning NEO-6M (arduino GPS, drone microcontroller, GPS receiver) compatible with 51 microcontroller STM32 arduino UNO R3 with antenna high sensitivity. Retrieved from https://www.amazon.com/Navigation-Positioning-Microcontroller-Compatible-Sensitivity/dp/B084MK8BS2/ref=asc_df_B084MK8BS2/?tag=hyprod-20&linkCode=df0&hvadid=416672656770&hvpos=&hvnetw=g&hvrand=18338330377394274734&hvpone=&hvptwo=&hvqmt=&hvdev=c&hvdvcmdl=&hvlocint=&hvlocphy=9001843&hvtargid=pla-906486472275&psc=1&tag=&ref=&adgrpid=95587149724&hvpone=&hvptwo=&hvadid=416672656770&hvpos=&hvnetw=g&hvrand=18338330377394274734&hvqmt=&hvdev=c&hvdvcmdl=&hvlocint=&hvlocphy=9001843&hvtargid=pla-906486472275

Diymore. (n.d.). Diymore 2pcs OLED display module 1.3 inch 128x64 OLED display I2C IIC serial OLED module with SSH1106 for raspberry pi and microcontroller (white light). Retrieved from https://www.amazon.com/dp/B07X57CJHX/ref=sspa_dk_detail_6?psc=1&pd_rd_i=B07X57CJHX&pd_rd_w=63Zp7&pf_rd_p=7d37a48b-2b1a-4373-8c1a-bdcc5da66be9&pd_rd_wg=how1D&pf_rd_r=14EWHAR8YVVXF6T8A80D&pd_rd_r=f70a8092-bd20-4949-9f1a-b390b6b5db22&spLa=ZW5jcnlwdGVkUXVhbGlmaWVyPUExOEpXRFVRTE1NSk9BJmVuY3J5cHRlZElkPUEwMjA3MTIwMkY5TVJESkU2NFk0UiZlbmNyeXB0ZWRBZElkPUEwNjcxMjUxRVRaT1VRRFdRMTJMJndpZGdldE5hbWU9c3BfZGV0YWlsJmFjdGlvbj1jbGlja1JlZGlyZWN0JmRvTm90TG9nQ2xpY2s9dHJ1ZQ==#customerReviews

Domonoske, C. (2019). As more electric cars arrive, what's the future for gas-powered engines? Retrieved from https://www.npr.org/2019/02/16/694303169/as-more-electric-cars-arrive-whats-the-future-for-gas-powered-engines

Endless sphere. (n.d.). Retrieved March 16, 2021, from https://endless-sphere.com/forums/viewtopic.php?t=77735

Fields, S. (2003). “The Environmental Pain of Pleasure Boatings.” *Environmental Health Perspectives.* Retrieved from https://ehp.niehs.nih.gov/doi/pdf/10.1289/ehp.111-a216

Goouuu Tech. (n.d.). GT-U7 GPS modules. Retrieved from https://drive.google.com/file/d/15cIa03wqNB7sItn6I2s5xZ8PGOZ1Q0JF/view

Hart, M. (2013). TinyGPS++. Retrieved from http://arduiniana.org/libraries/tinygpsplus/

Hoffman, D. (2003). “Petroleum and Individual Polycyclic Aromatic Hydrocarbons.”

Handbook of Ecotoxico*logy.* 2, 341-360. Retrieved from https://books.google.com/books?hl=en&lr=&id=6U3MBQAAQBAJ&oi=fnd&pg=PA341&dq=hydrocarbon+emissions+impact+on+aquatic+life&ots=lWqVfsTkbX&sig=V3zUlcD639eJb_amaNlvoR0zr8U#v=onepage&q=%20aquatic%20life&f=false

Johnson, J. (2017, -08-10T15:37:19+00:00). Fatigue improvement techniques for welds. Retrieved from https://processbarron.com/fatigue-improvement-techniques-welds/

Kelly, R. T., & Kelly, S. L. (1991). In Kelly Roy T, Kelly Shawn L (Ed.), *Jet ski hull and method of manufacture* Retrieved from https://patents.google.com/patent/US5036789A/en

Koschinski, S. (2008). Possible Impact of Personal Watercraft (PWC) on Harbor Porpoises (Phocoena phocoena) and Harbor Seals (Phoca vitulina) Retrieved from https://www.researchgate.net/profile/Sven_Koschinski/publication/241217952_Possible_Impact_of_Personal_Watercraft_PWC_on_Harbor_Porpoises_Phocoena_phocoena_and_Harbor_Seals_Phoca_vitulina/links/555a042608ae6fd2d8281b67/Possible-Impact-of-Personal-Watercraft-PWC-on-Harbor-Porpoises-Phocoena-phocoena-and-Harbor-Seals-Phoca-vitulina.pdf

Lambert, Fred. (2020). “Taiga Unveils Cheaper Versions of Its Electric Watercraft.” Electrek, electrek.co/2020/07/15/taiga-orca-cheaper-electric-watercraft/. Accessed 7 Dec. 2020.

Last Minute Engineers. (n.d.). Water level sensor. Retrieved from https://lastminuteengineers.com/water-level-sensor-arduino-tutorial/

Liu, Yue & Zwingmann, Bernd & Schlaich, Mike. (2015). Carbon Fiber Reinforced Polymer for Cable Structures—A Review. Polymers. 7. 2078-2099. 10.3390/polym7101501.

Mackenzie, J. (2016). Air pollution: Everything you need to know. Retrieved from https://www.nrdc.org/stories/air-pollution-everything-you-need-know

McMaster-Carr. Retrieved from https://www.mcmaster.com/flexible-shaft-couplings/splined-to-keyed-flexible-shaft-couplings-6/

Morikawa, Koji, et al.(1999). “A Study of Exhaust Emission Control for Direct Fuel Injection Two-Stroke Engine.” *SAE Transactions*. 108, 1322–1329. Retrieved from https://www.jstor.org/stable/44716758?seq=1#metadata_info_tab_contents

Nikola Corp.Nikola wav. Retrieved from https://nikolamotor.com/reserve/wav

O'Kane, S. (2019). The nikola wav is an electric watercraft with a 4K display and cruise control. Retrieved from https://www.theverge.com/2019/4/17/18411541/nikola-wave-electric-jet-ski-4k-display-cruise-control

Pearce, J. (1998). Jet Skis Targeted as Polluters of Michigan's Great Lakes. The Detroit News. July 17. P.A1

Personal watercraft (PWC). (2016). In T. Riggs (Ed.), *How everyday products are made* (pp. 321-330). Farmington Hills, MI: UXL. Retrieved from https://link.gale.com/apps/doc/CX3233700042/MSIC?u=mlin_c_worpoly&sid=MSIC&xid=08227610

PWC inspection. (n.d.). Retrieved March 16, 2021, from https://www.usps.org/national/vsc/conductvsc_files/pwcvsc.htm#:~:text=EXAMINING%20PERSONAL%20WATERCRAFT%20The%20PWC,or%20kneeling%20ON%20the%20watercraft

Reducing pollution with electric vehicles. Retrieved from https://www.energy.gov/eere/electricvehicles/reducing-pollution-electric-vehicles

Reid, J. (2019). World's first electric hydrofoil jet ski. Retrieved from https://www.news.uwa.edu.au/2019080211532/research/worlds-first-electric-hydrofoil-jet-ski

REV electric jet ski. Retrieved from http://revproject.com/vehicles/jetski.php

The REV project. Retrieved from https://therevproject.com

Soltren, D., Duffy-Protentis, J., Quick, L., Hartwick, M., & Kolb, M. (2020). *Electric/Solar Powered Jet Ski* (Major Qualifying Project). Retrieve from Worcester Polytechnic Institute Electronic Projects Collection: https://digitalcommons.wpi.edu/mqp-all/7554/

Stacey, D., Braunl, T., Stott, M. & Knight, J. (2015). Australia's first electric jet ski. Retrieved from https://www.news.uwa.edu.au/201510238081/electric-jet-ski/australias-first-electric-jet-ski

Taiga Motors. (n.d.). Orca electric PWC. Retrieved from https://taigamotors.ca/watercraft/

Tinkercad. (2020). User display circuit. Retrieved from tinkered.com

The evolution of systems engineering. (2016, August 25). Retrieved March 16, 2021, from https://www.mitre.org/publications/systems-engineering-guide/systems-engineering-guide/the-evolution-of-systems

Thunderstruck. (2019). Battery Management System v2.2. Retrieved from http://www.thunderstruck-ev.com/images/companies/1/DD_BMSv2.2.pdf?1567717672490

Travis, J. (2015). Jet ski inventor with ties to parker recounts adventures. Retrieved from https://www.parkerpioneer.net/news/article_346c23ee-ed2e-11e4-ae89-f3072c730979.html

US EPA. (2016). Batteries. Retrieved from https://archive.epa.gov/epawaste/hazard/web/html/batteries.html#def

Appendix A: Inherited Electrical Parts

Motor Controller Bill of Materials

Index	Quantity	Part Number	Manufacturer Part	Description	Website	Unit Price	Total Price USD
1	5	PIC18F47Q10-I/	PIC18F47Q10-I/P	128KB FLASH 3.6KB RAM 1024B EEPR		1.8	9
2	5	MCP1826T-330:	MCP1826T-3302E/	IC REG LINEAR 3.3V 1A SOT223-5		0.68	3.4
3	3	MIC4606-2YTS-I	MIC4606-2YTS-TR	IC GATE DRVR HALF-BRIDGE 16TSSOP		2.1	6.3
4	3	MIC28514T-E/P	MIC28514T-E/PHA	IC REG BUCK ADJUSTABLE 5A 32VQFN		2.24	6.72
5	5	MCP6024-E/P-N	MCP6024-E/P	IC OPAMP GP 4 CIRCUIT 14DIP		1.91	9.55
6	5	MCP6541RT-E/(	MCP6541RT-E/OT	IC COMP 1.6V SNGL P-P SOT23-5		0.36	1.8
7	20	399-15252-1-NI	C410C100K1G5TA7	CAP CER 10PF 100V C0G/NP0 AXIAL		0.185	3.7
8	8	IRFP4468PBF-N	IRFP4468PBF	MOSFET N-CH 100V 195A TO-247AC		5.95	47.6
9	1	DM182029-ND	DM182029	PIC18F47Q10 CURIOSITY NANO EVALU		14.99	14.99
10	1	DM164136	DM164136	PIC MICRO MCU CURIOSITY HIGH PIN COUNT (HPC) DEVELOPMENT BOARD		55.35	55.35
						TOTAL	158.41

Battery Pack Accessories

Index	Quantity	Part Number	Manufacturer Part	Description		Unit Price	Total Price USD
1	1	43374573060	43374573060	1' x 2' DIAMOND TREAD ALUMINUM SHEET		17.98	17.98
2	3	887480023817	887480023817	WING NUT ZINC 5/16 10TPI		1.18	3.54
3	4	887480022278	887480022278	5/16 THREADED ROD 36''		3.38	13.52
4	1	37103136480	37103136480	WISS LEFT CUT SNIPS		13.97	13.97
						TOTAL	49.01

Motor Controller and Accessories

Index	Quantity	Part Number	Manufacturer Part	Description		Unit Price	Total Price USD
1	1			KLS-8080H - Sealed Sinusoidal Wave Brushless DC Motor Controller (96V) (500A)	https://www.k	$699.00	$699.00
2	1			Bluetooth Adapter	https://www.k	$29.00	$29.00
3	1			Controller Programming Cable USB to RS232 with Micro USB Adapter	https://www.k	$29.00	$29.00
						TOTAL	$757.00

Nissan Leaf Batteries

Index	Quantity	Part Number	Manufacturer Part	Description		Unit Price	Total Price USD
1	1			Nissan Leaf 48v Battery G1 Lithium Ion 7 kWh 500 watt per module (Lot of 14)	https://www.e	$746.64	$746.64
						TOTAL	$746.64

Battery Management System

Index	Quantity	Part Number	Manufacturer Part	Description		Unit Price	Total Price USD
1	1			BMS Controller (thunderstruck.com)	https://www.th	$450.00	$450.00
						TOTAL	$450.00

Throttle Control System

Index	Quantity	Part Number	Manufacturer Part	Description		Unit Price	Total Price USD
1	1			Dilwe Throttle Grips, Right Scooter Speed Control Twist Throttle	https://www.ama	$26.49	$26.49
2	1			Cylewet 5Pcs KY-040 Rotart Encoder Module with 15x16.5 mm with Knob Cap	https://www.ama	$8.99	$8.99
						TOTAL	$35.48
						PAGE TOTAL:	$2,196.54

Appendix B: Inherited Mechanical Part

				Steering System			
Index	**Quantity**	**Part Number**	**Manufacturer Part**	**Description**	**Website**	**Unit Price**	**Total Price USD**
	1	277000106		Rear Support			
	1	215686560		Cable Support			
	1	277000162		Thrust Support			
	1	277000291		Front Support			
	1	277000375400		Steering Stem			
	1	277000165		Steering Stem Arm			
	1	277000510		Thrust Arm			
	1	277000214		Throttle Handle			
	1	277000305		Handlebar			
	1	277000142		Steering Clamp			
	1	277000468		Throttle Cable			
	1	277000285		Throttle Handle Housing			
	1	295500111		Handle Grip Kit			
	2	XXX		Grip Insert			
	2	277000204		Grip Cap			
	1	277000257		Steering Cover			
	1	277000187		Foam (Top)			
	1	277000289		Steering Cable			
	1	277000153		Ball Joint			
	1	277000174		Rotule			
	1	277000038		Small Boot			
	1	277000039		Large Boot			
	1	277000167		Ajustment Knob			
	1	277000258		Plate			
	1	211100010		Retaining Ring			
	1	277000219		Retainer Plate			
	1	277000498		Left Housing Assembly			
	1	277000379		Left Housing			
	1	277000497		V.T.S. Knob			
	2	277000168		Half Ring			
	2	277000381		Pin			
	1	277000279		Lock-Tab			
	1	277000278		Boot-small			
	1	277000277		Boot-large			
	1	293900008		Spherical Cushion			
	1	293900009		Spherical Cushion			

Appendix C: Purchased Mechanical Parts

Propulsion System							
Index	**Quantity**	**Part Number**	**Manufacturer Part Num**	**Description**		**Unit Price**	**Total Price USD**
1	1	293300011	293300011	O-Ring for Impeller		$8.82	$8.82
2	1	271000703	271000703	Pusher		$10.45	$10.45
3	1	271000670	271000670	Impeller Cover (Sea-Doo New OEM Impeller Cover, Sportster GTS Challenger SPX, 271000670)		$21.87	$21.87
4	2	293300032	293300032	O-Ring for Drive Shaft		$5.18	$10.36
5	1	293650021	293650021	Oetiker Clamp		$12.99	$12.99
6	1	272000001	272000001	Rubber Boot		$26.99	$26.99
7	1	293650067	293650067	Oetiker Clamp		$7.99	$7.99
8	1	293650035	293650035	Tridon Clamp		$6.20	$6.20
9	1	272000042	272000042	Ring Carbone		$27.52	$27.52
10	1	272000096	272000096	Drive Shaft		$52.50	$52.50
11	2	272000019	272000019	Plug (Bumper)		$6.60	$13.20
12	2	218681000	218681000	Wing Nut M8		$1.82	$3.64
13	1	272000094	272000094	Flywheel Guard		$19.99	$19.99
14	1	293550010	293550010	Synthetic Grease 400g		$22.99	$22.99
15	1	292000075	292000075	Thru Hull Fitting		$21.95	$21.95
16	1	271000660	271000660	Impeller		$238.05	$238.05
						TOTAL	$505.51

Appendix D: Purchased Electrical Parts

User Display							
Index	**Quantity**	**Part Number**	**Manufacturer Part**	**Description**	**Website**	**Unit Price**	**Total Price USD**
1	1			Rain Water Level Sensor Module Depth of Detection Liquid Surface Height for Arduino（10pcs)	https://www.amazon.com/Sensor	$6.19	$6.19
2	1			GPS Module Receiver,Navigation Satellite Positioning NEO-6M (Arduino GPS, Drone Microcon	https://www.amazon.com/Navig	$10.99	$10.99
3	1			Diymore 2pcs OLED Display Module 1.3 inch 128x64 OLED Display I2C IIC Serial OLED Mod	https://www.amazon.com/dp/B0	$14.99	$14.99
						TOTAL	$32.17
BMS							
Index	**Quantity**	**Part Number**	**Manufacturer Part**	**Description**	**Website**	**Unit Price**	**Total Price USD**
4	1			Dilithium Design EV Motors	Thunder Struck Motors	$400.00	$400.00
						TOTAL	$400.00
						PAGE TOTAL:	$432.17

Appendix E: User Display Parts & Specifications

Display Module	
Brand	Diymore
Type	OLED
Size	1.3"
Resolution	128x64
Controlling Chip	SSH1106
Display Area	1.16"x0.58"
Voltage	3.3V-5V
Temperature	-40 to 70 ℃
Interface Type	IIC
Address	0X78
Address Compatible	0X3C
Color	Black/Blue

GPS Module Receiver	
Brand	Goouuu Tech
GPS Type	GT-U7
Antenna Type	IPX Antenna
Size	27.6x26.6mm
Voltage	3.3-5V
Compatibility	Neo-6M
Operating Baud Rate	9600
Rf Current	<50 mA
Antenna Gain	50 dB
Satellite Capability	>55

Rain Water Level Sensor	
Brand	Daoki
Type	Water Level Sensor
Sensor Type	Analog
Size	62x20x8mm
Detection Area	40x16mm
Operating Voltage	3-5V
Operating Current	<20 mA
Temperature	10-30 ℃
Humidity	10-90% non-condens

Appendix F: Arduino Code

```
//Twist Grip code

//Signal Cord -> Arduino Pin
//5v (Orange) -> 5V
//Speed adjusting Signal (Brown) -> A0
//Negative Electrode (Red) -> GND

int TwistGripPin = A0;          //The Arduino pin  for the twist grip
int Pin_to_motors = 6;          //Pin for the motors?
int Twist_Grip_val;            //The amount the twist grip is turned
int Value_to_motors;           //Value going to the motors
int PWM_val;

void setup()
{
 pinMode(TwistGripPin, INPUT);       //Declare Twistgrip Pin
 pinMode(Pin_to_motors, OUTPUT);      //Declare Motor Pin
 Serial.begin(9600);           //Start Serial Monitor
}

void loop()
{
 Twist_Grip_val = analogRead(TwistGripPin) - 170;  //Make the TwistGrip reads from 0 -> 705
 delay(100);                     //Delay readings
 Value_to_motors = map(Twist_Grip_val, 0, 705, 0, 255);   //Map from Weird range to standard
 if(Value_to_motors < 6)         //Omit "noise" or slight increases due to adjustment of grip
 {
  Value_to_motors = 0;
 }
 analogWrite(Pin_to_motors, Value_to_motors);    //Send a pulse width module to the motors
 PWM_val = pulseIn(Pin_to_motors, HIGH);   //Create PWM
 Serial.println(PWM_val);         //Print PWM
 delay(1);                 //Delay 1ms
```

Appendix G: SolidWorks CAD Models

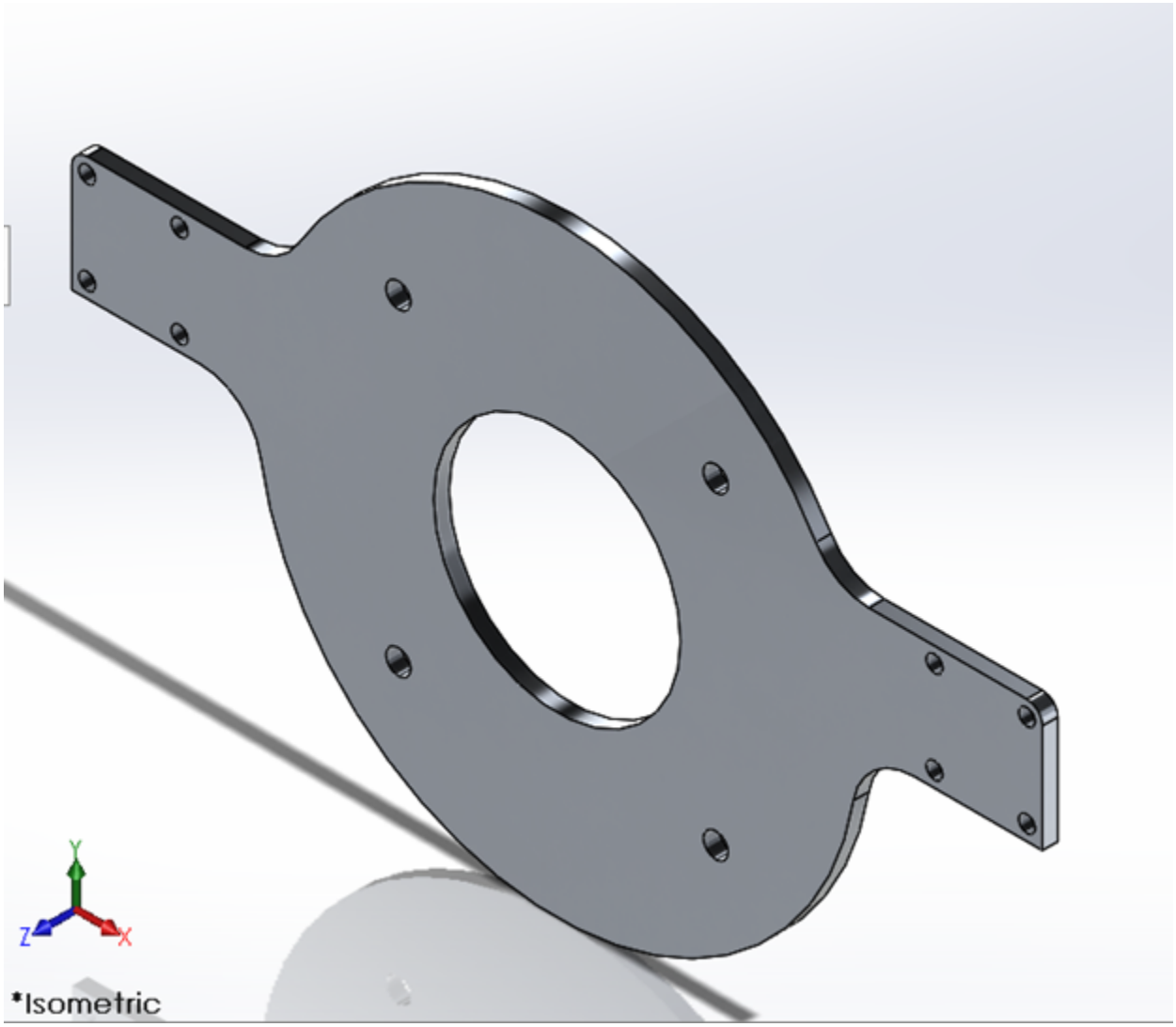

CAD Model of Front Plate for the ME1002 Motor Mount

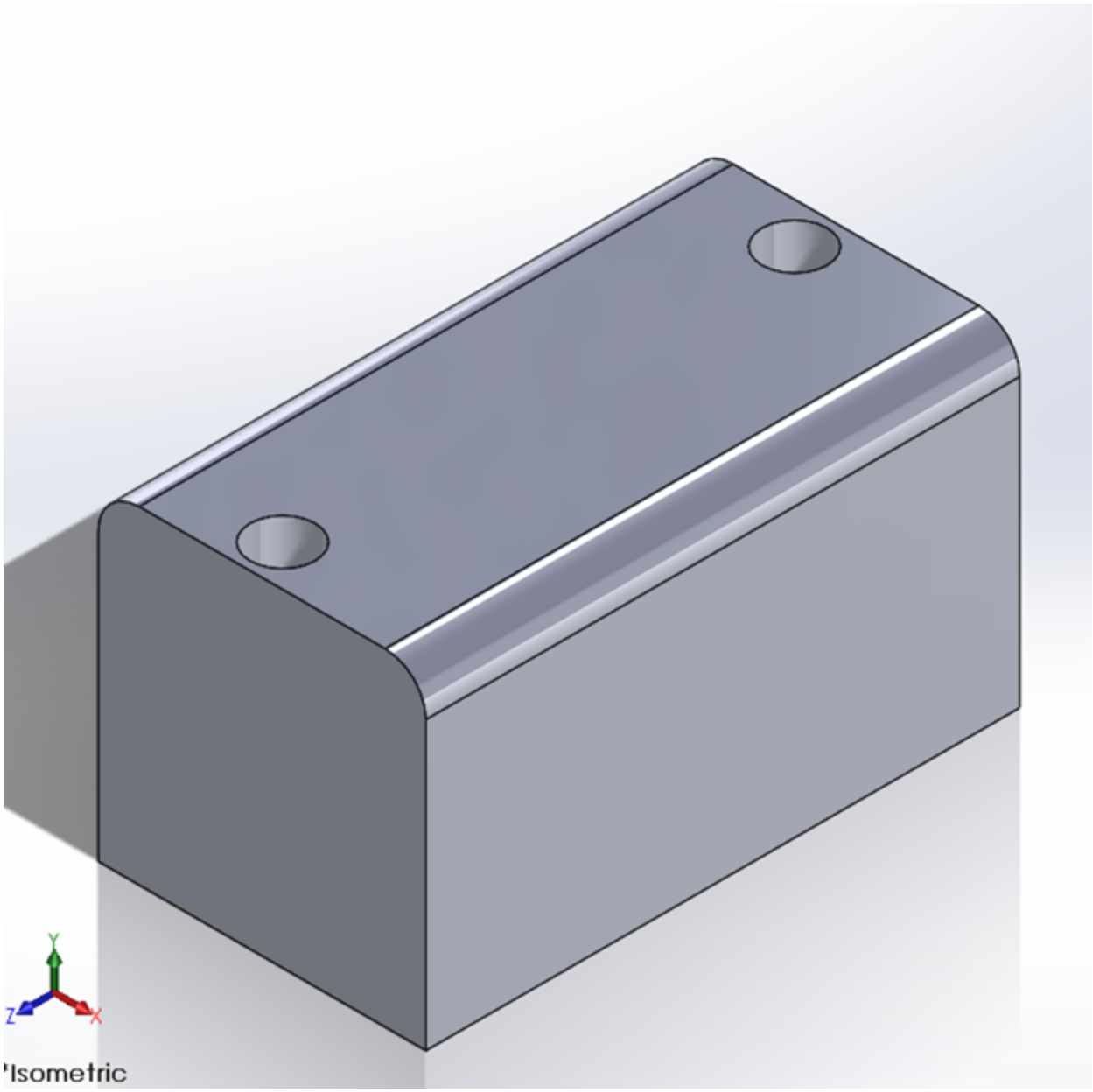

CAD Model of Side Block for ME1002 Motor Mount

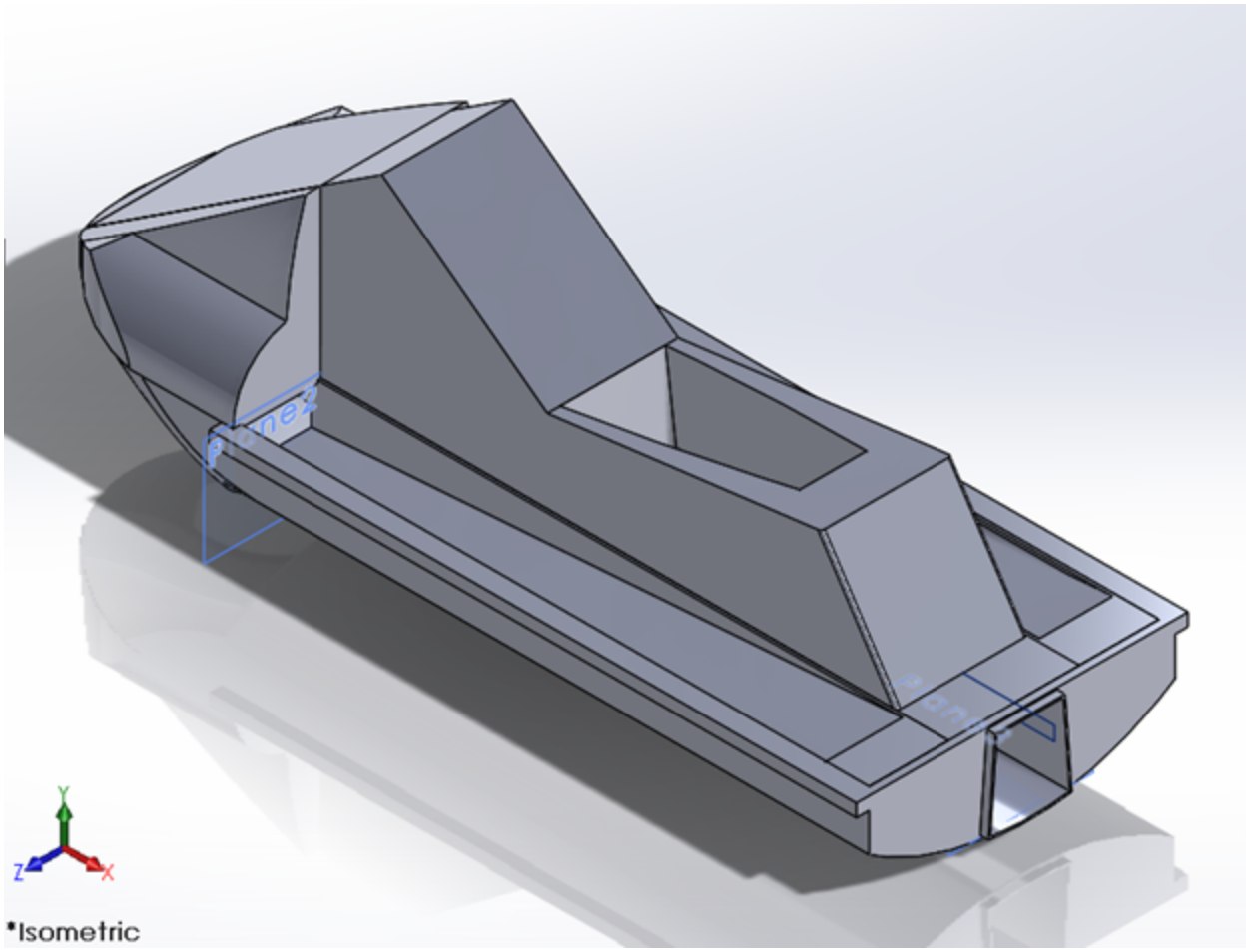

Preliminary Model of the Jet Ski Hull

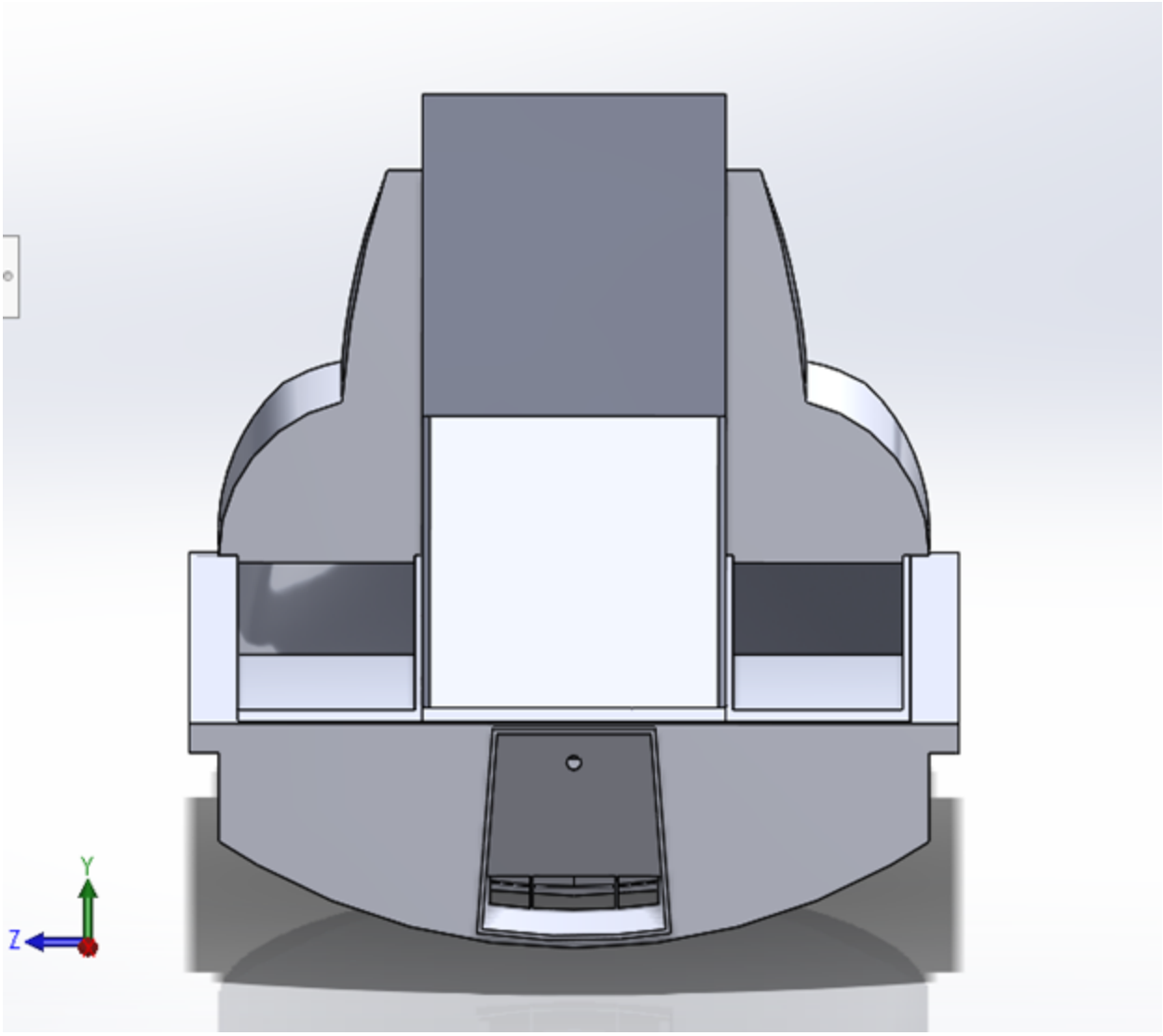

Rear View of Jet Ski CAD Model

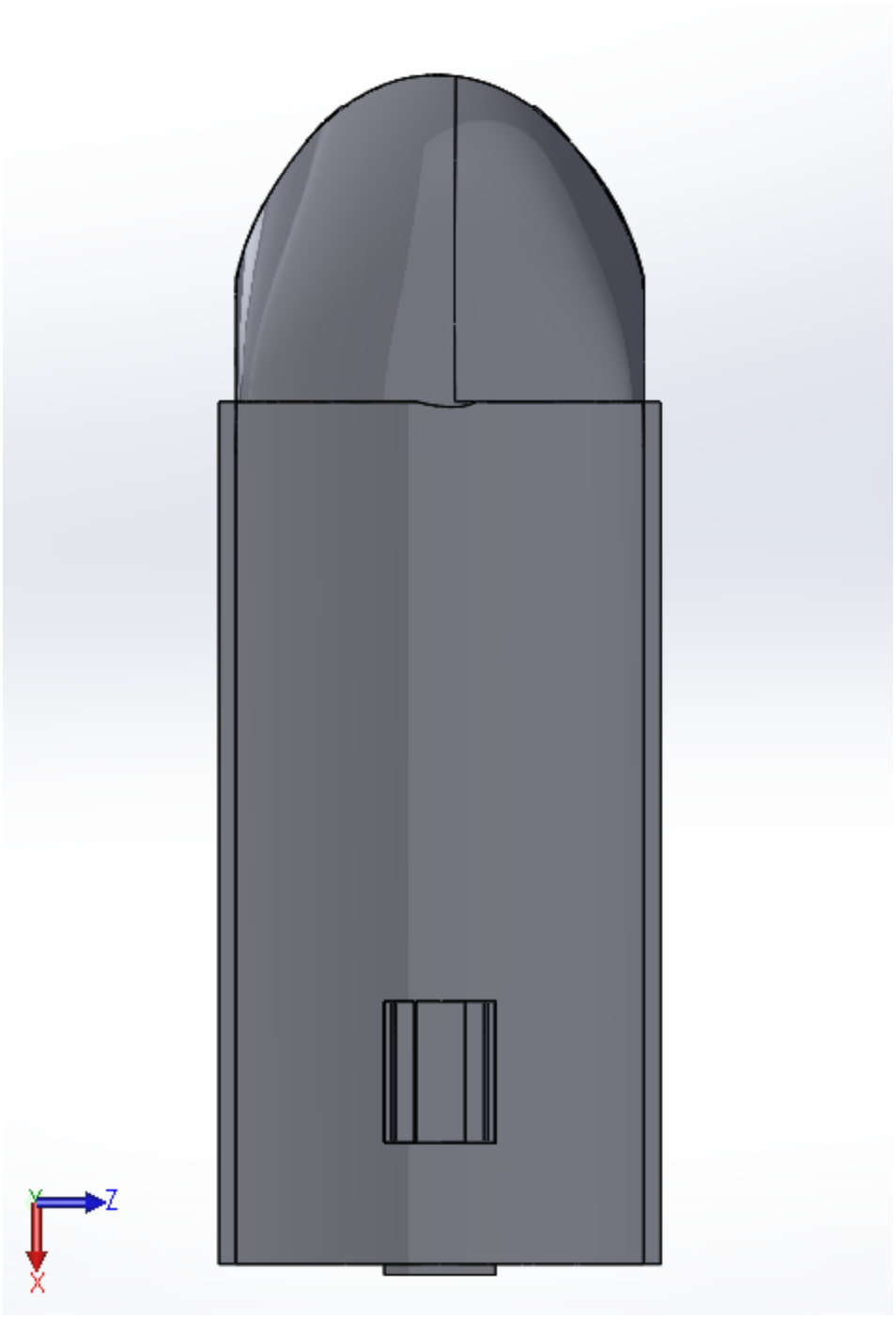

Bottom View of Jet Ski CAD Model

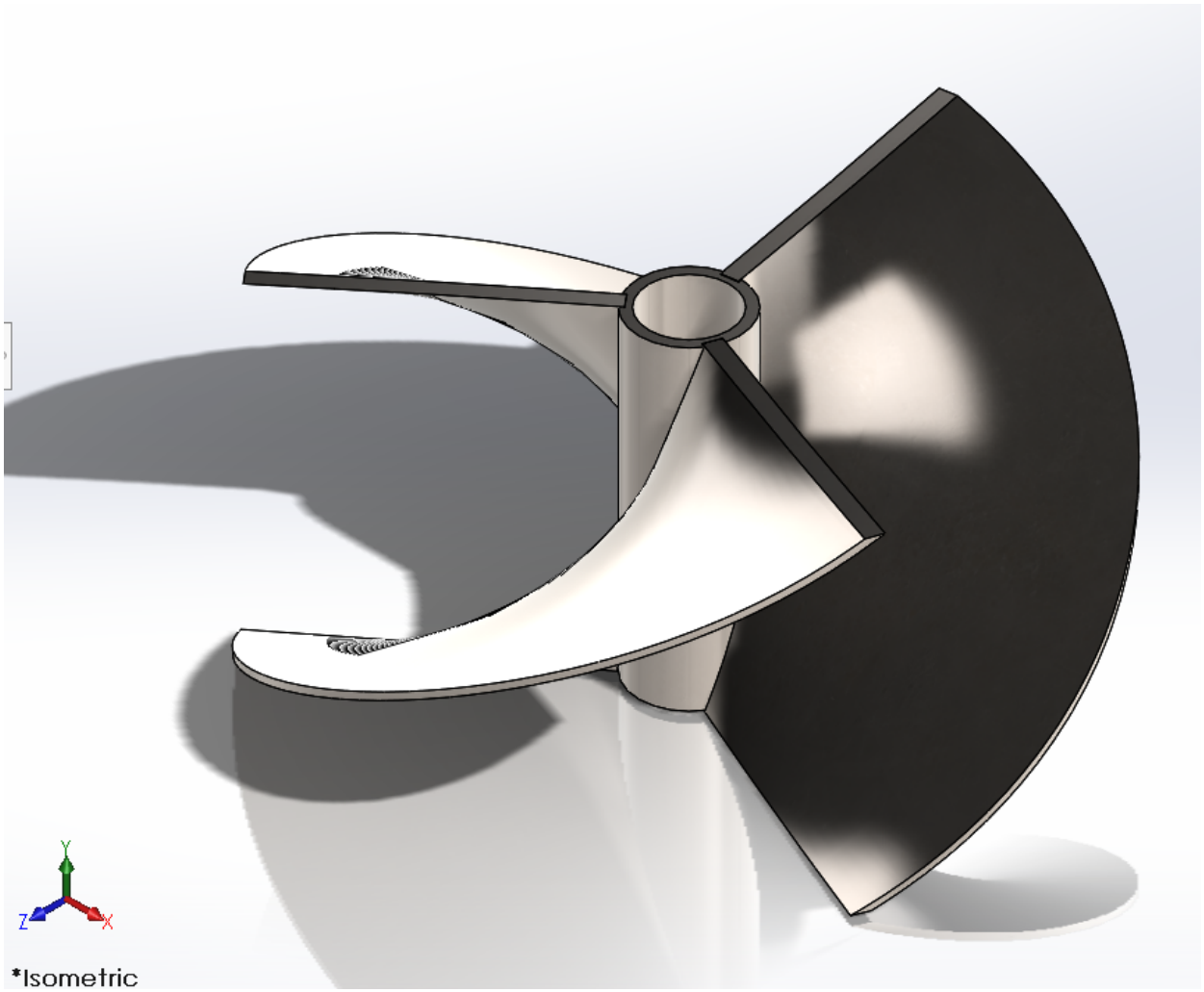

CAD Model of Impeller

CAD Models of 16-Battery Casing Parts

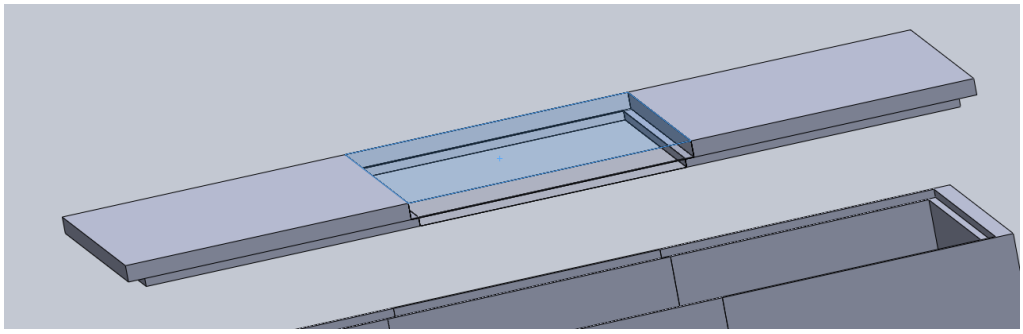

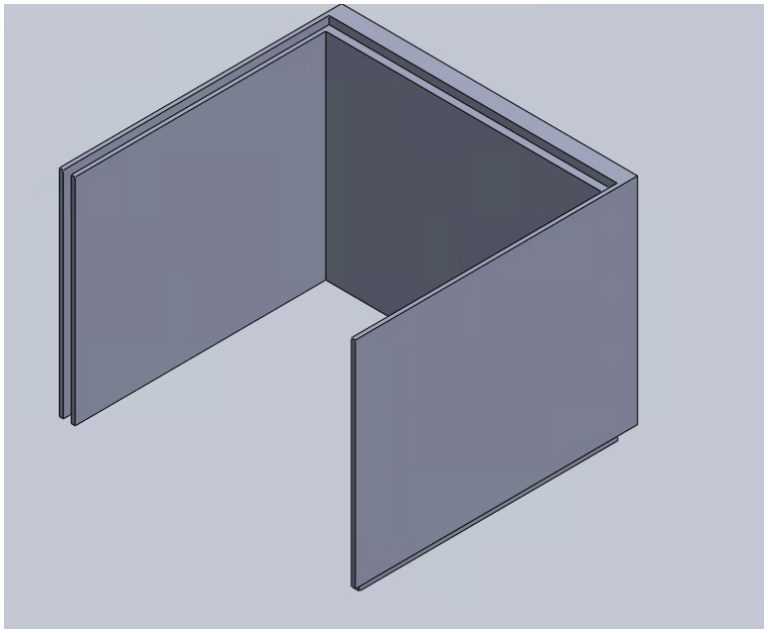

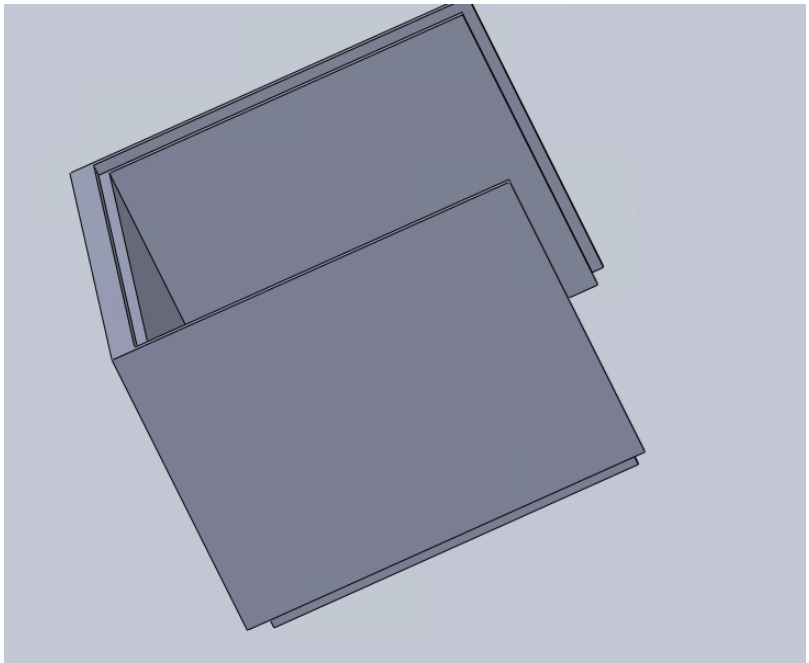

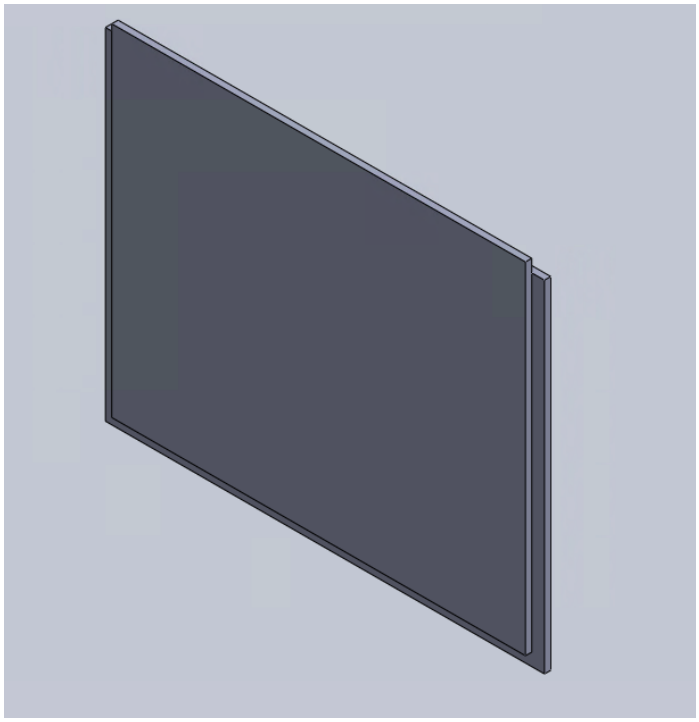

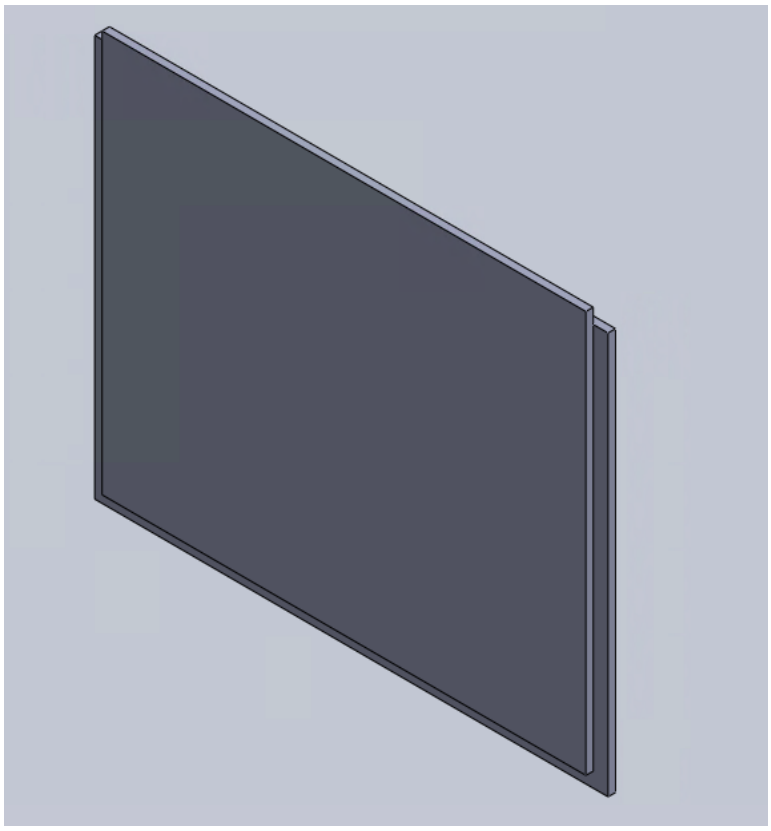

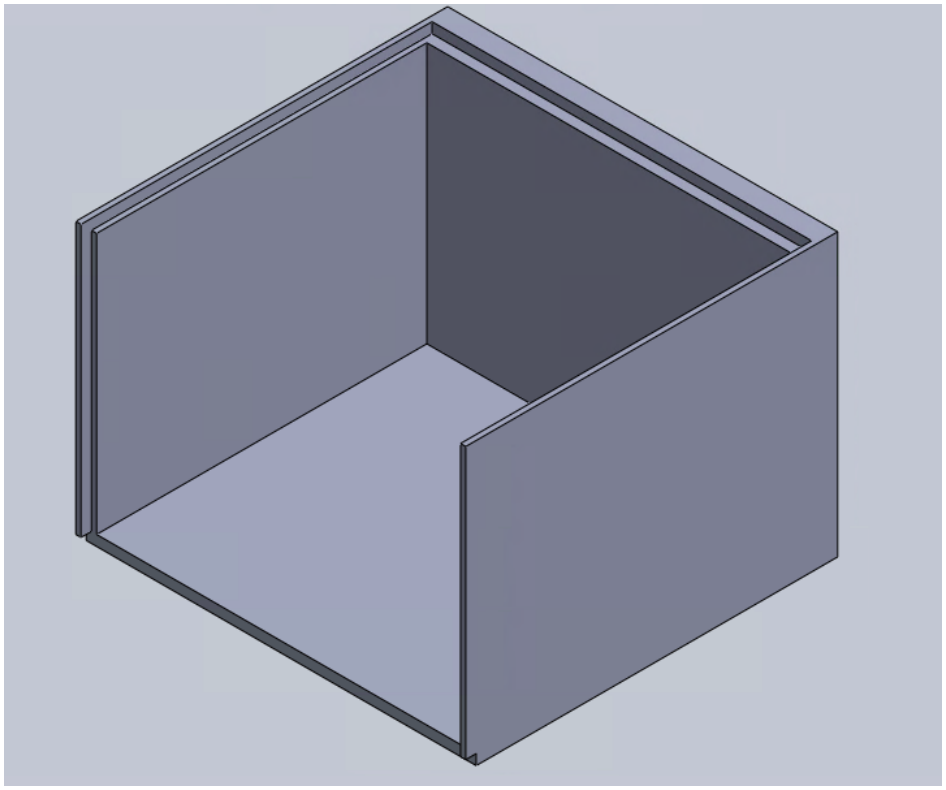

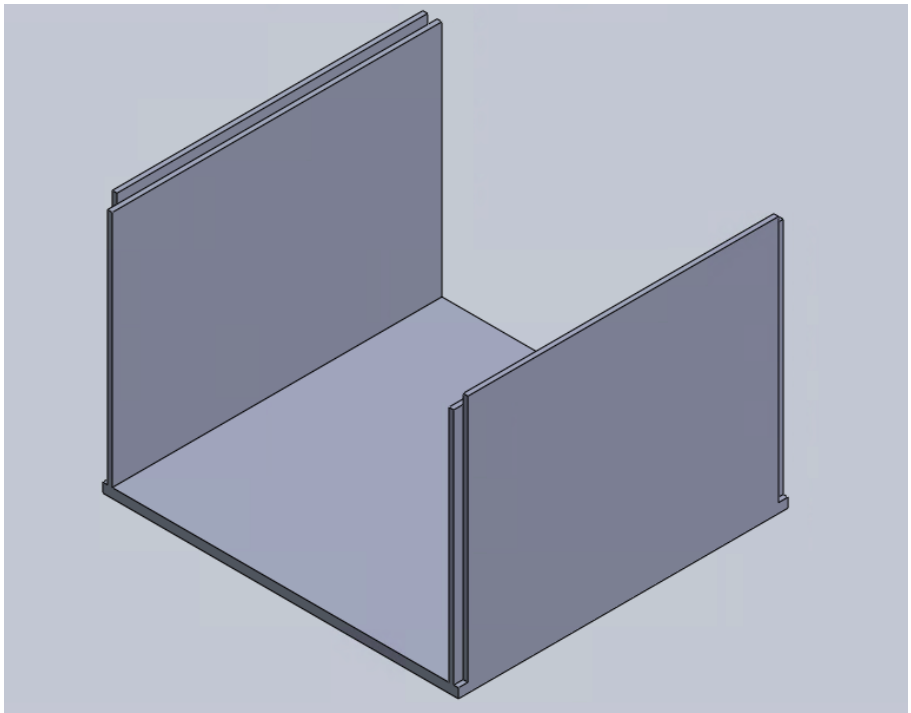

CAD Models of 2-Battery Casing Parts

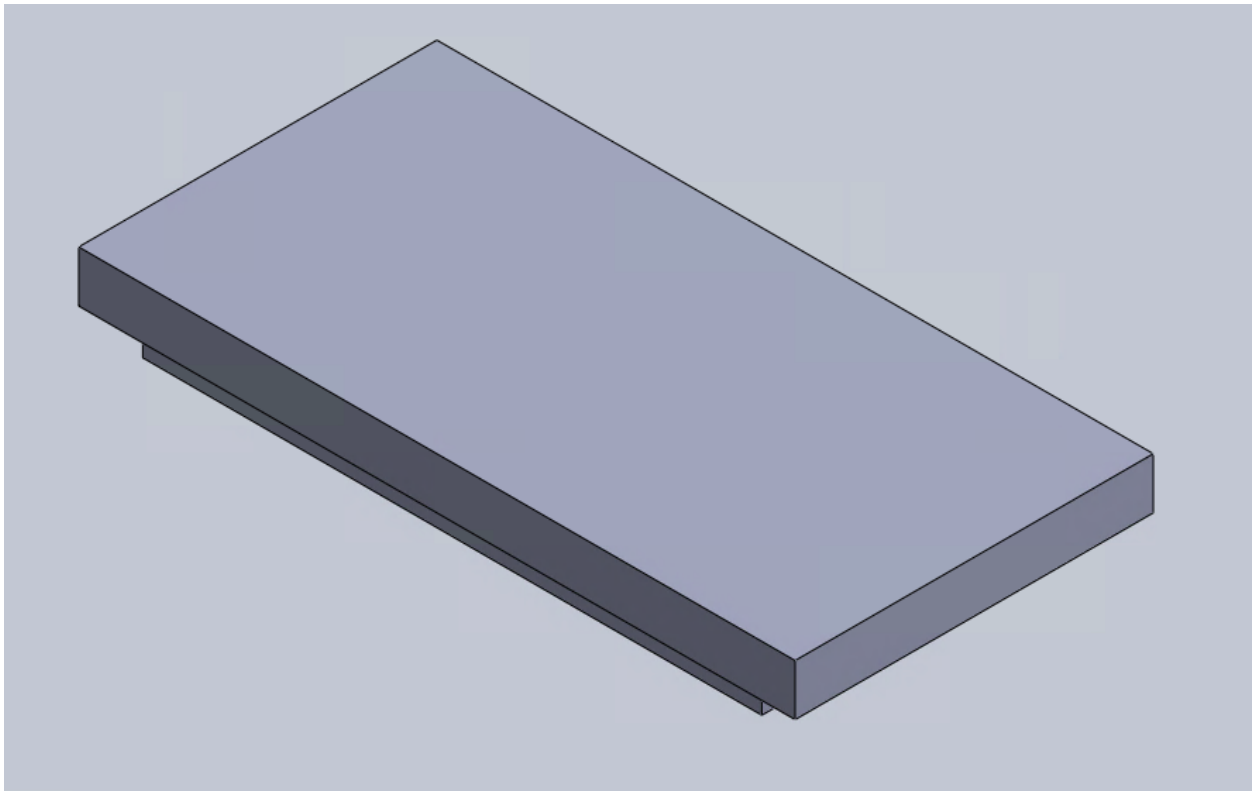

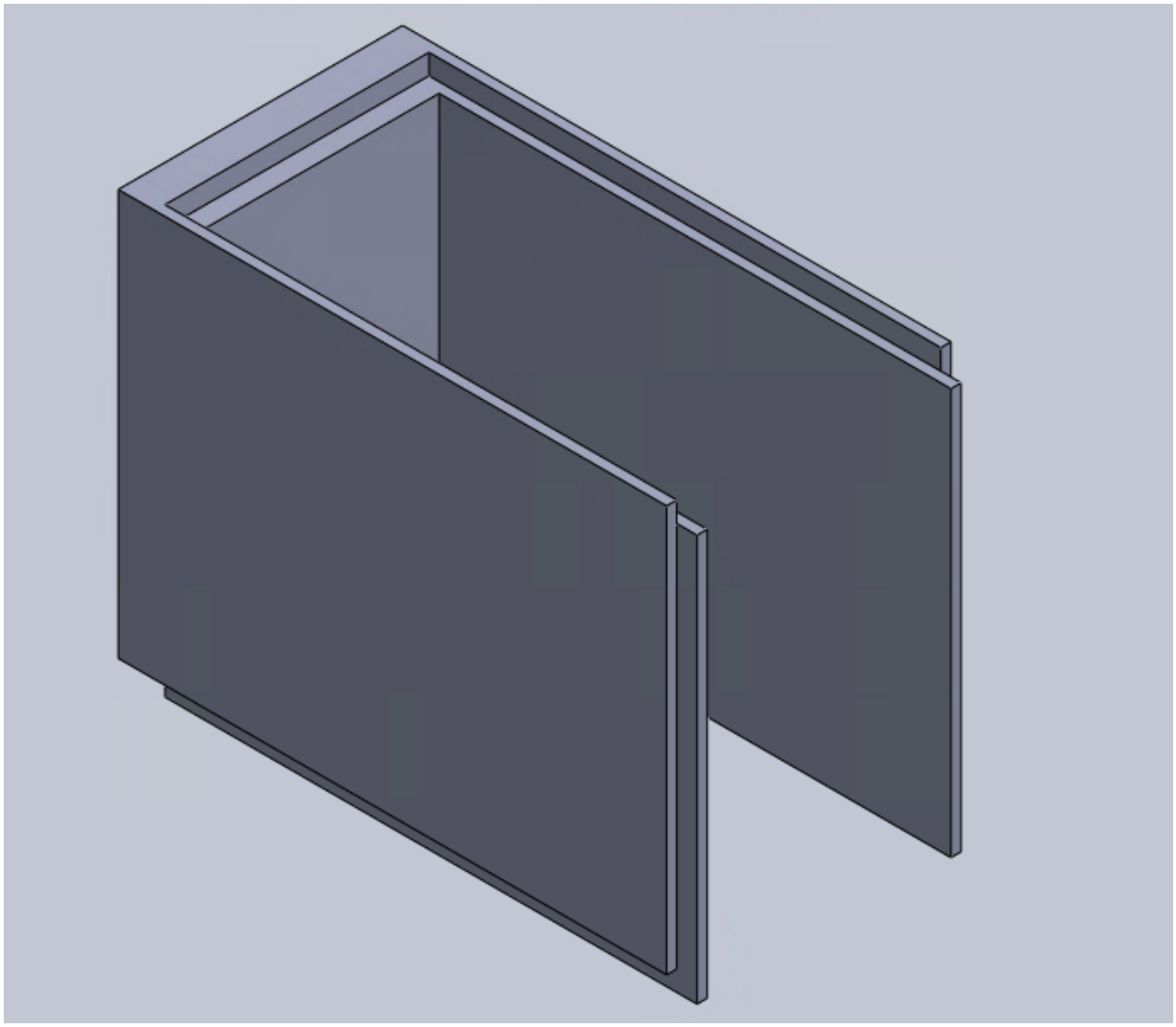

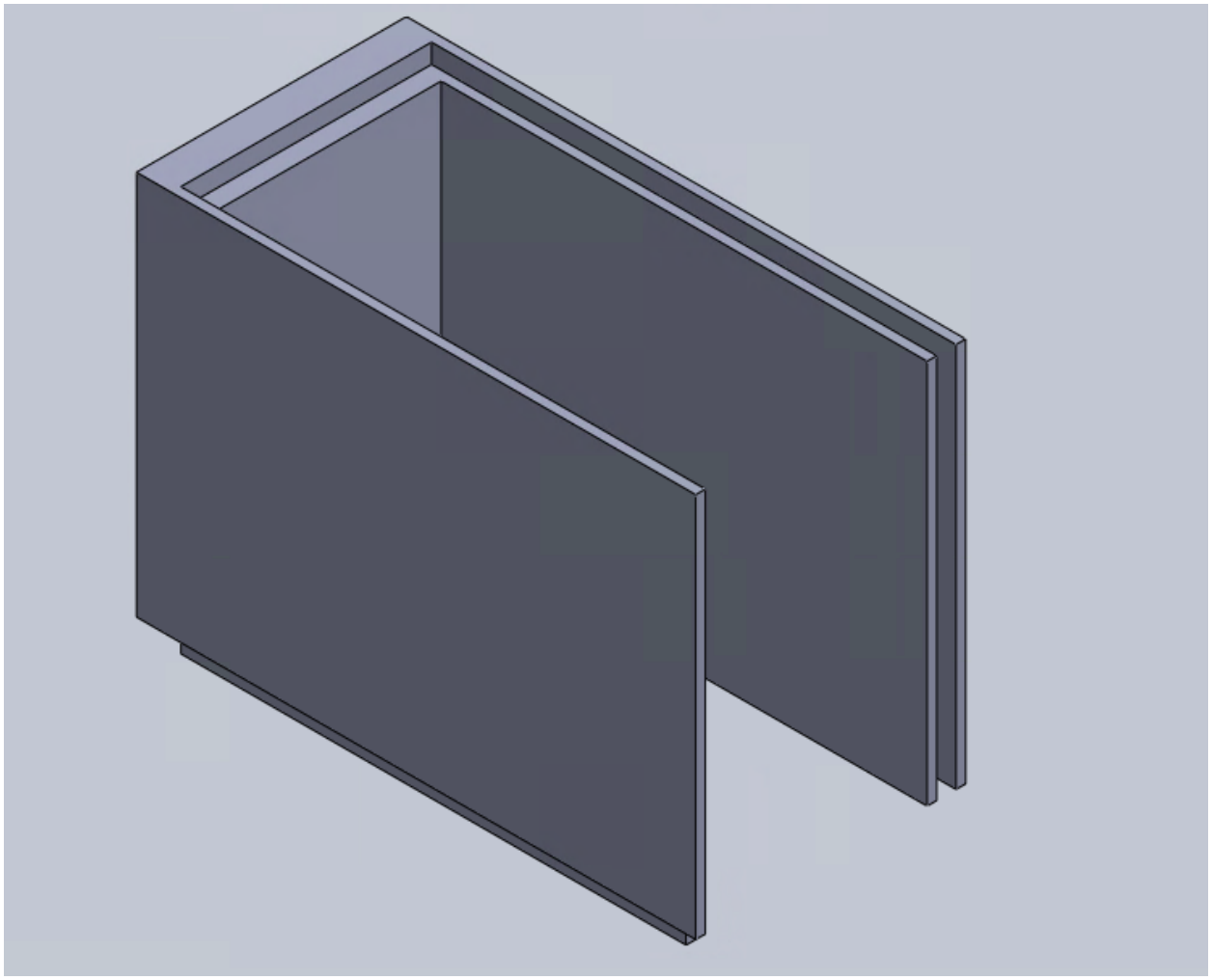

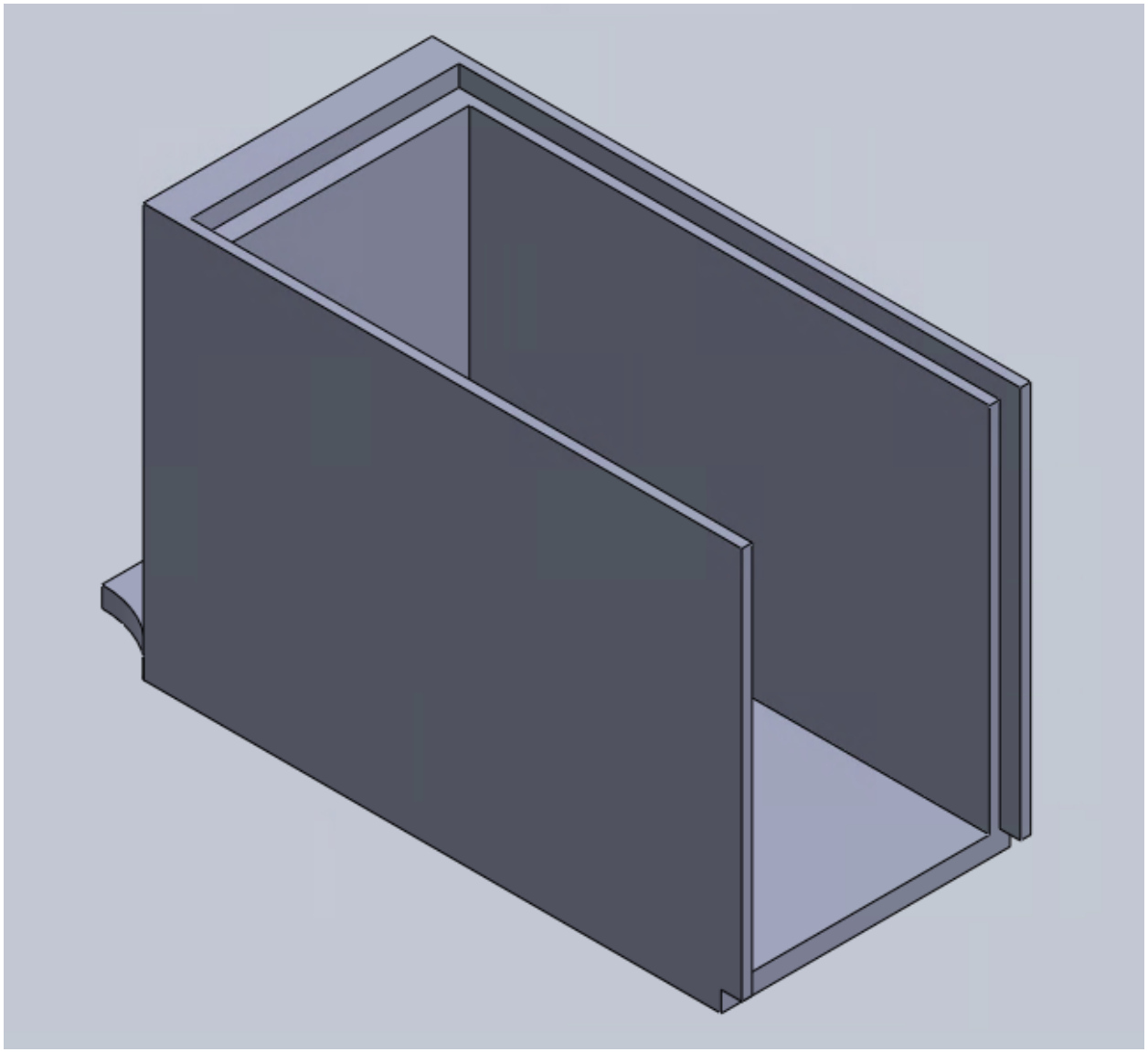

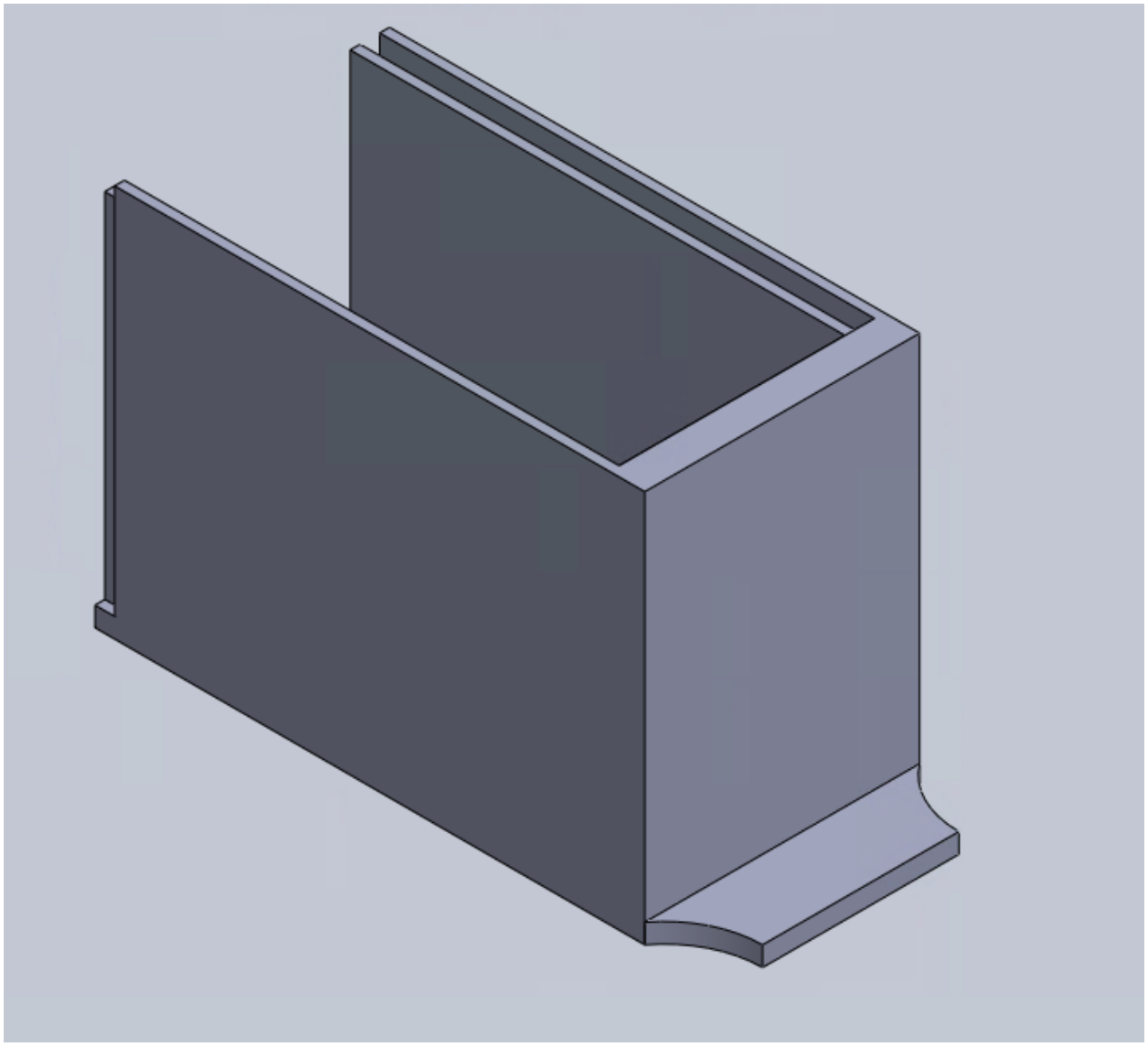

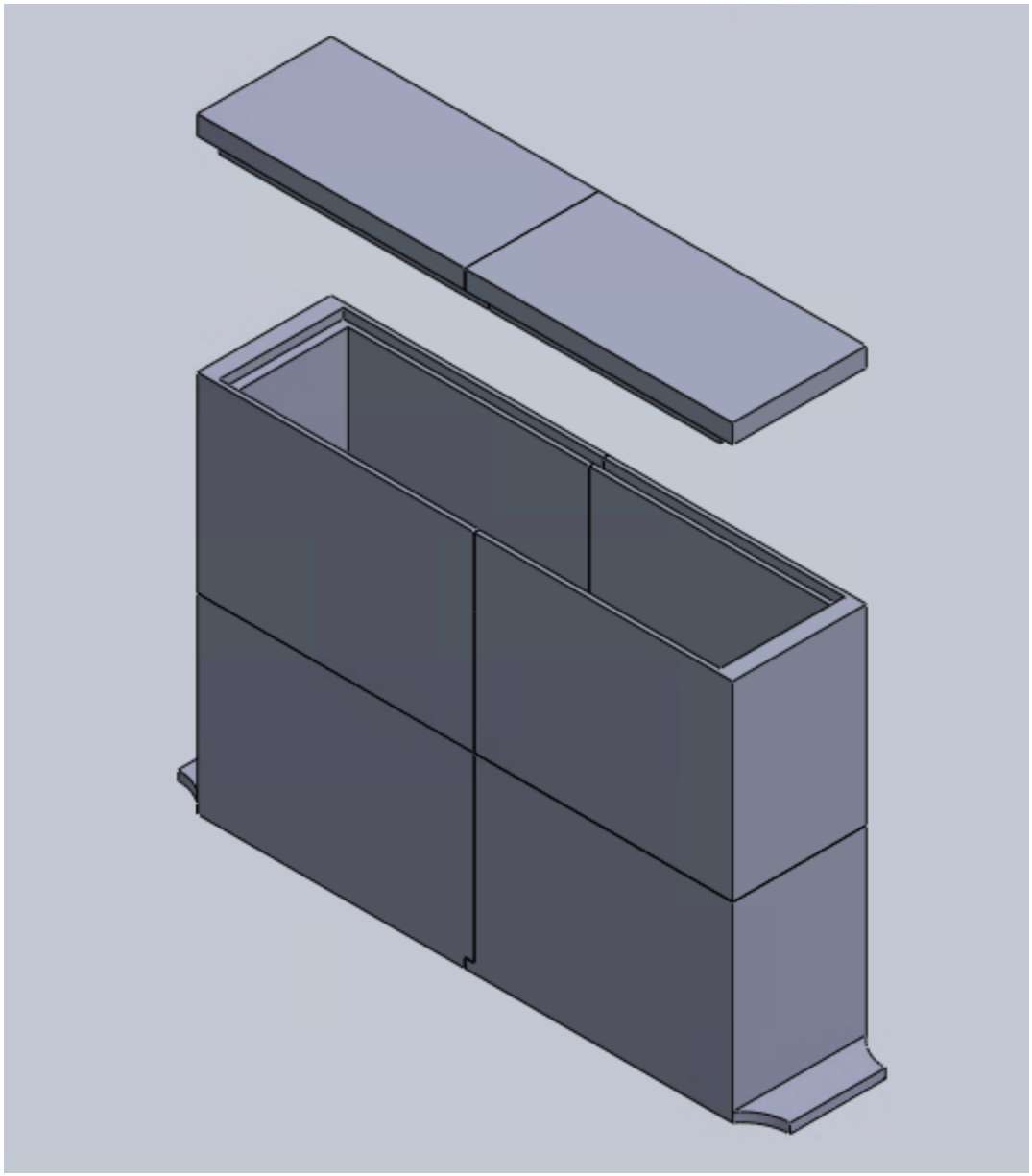

Appendix H: User Display NMEA Print Test (Arduino)

```
//#include <TinyGPS++.h>
//#include <SoftwareSerial.h>
//
//TinyGPSPlus gps;
//SoftwareSerial ss(4, 3);
//
//void setup()
//{
//  Serial.begin(9600);
//  ss.begin(9600);
//
//  Serial.println(F("Testing"));
//}
//
//void loop()
//{
//    while(!(ss.available())){}
//      Serial.write(ss.read());
//}
```

Appendix I: User Display Speedometer and Water Sensor Code (Arduino)

```
//////////////////////Water Level Inputs//////////////////////
//  // Define pins and variables
//#define powerPin 2
//#define waterlevelPin A3
//#define out OUTPUT
//#define off LOW
//#define on HIGH
//
//int waterLevel = 0;
//unsigned int i;
////////////////////////Speedometer Inputs//////////////////////
//#include "TinyGPS++.h"
//#include "SoftwareSerial.h"
//
//SoftwareSerial serial_connect(4, 3); //RX=pin 4 board/pin 3 gps, TX=pin 3 board/pin 4 gps
//TinyGPSPlus gps;
//
//int gpsspeed;
////////////////////////Display Inputs//////////////////////
//#include <Wire.h>
//#include "U8glib.h"
//U8GLIB_SH1106_128X64 u8g(U8G_I2C_OPT_DEV_0|U8G_I2C_OPT_FAST);  // Dev 0, Fast I2C / TWI
//
/////////////////////////////////////////////////////////////
//void setup() {
//  //Water Sensor Setup
//  pinMode(powerPin, out);
//  digitalWrite(powerPin, off);
//  //Speed Setup
//  Serial.begin(9600);
//  serial_connect.begin(9600);
//  Serial.println("GPS Start");
//}
/////////////////////////////////////////////////////////////
//void loop() {
//  print();
//  i++;
//}
//////////////////////Water Sensor Function//////////////////////
//
//void WaterSensor()
//{
//  ///Turns on for only 10 milliseconds to save power
//  digitalWrite(powerPin, on);
//  delay(10);
//  waterLevel = analogRead(waterlevelPin);
//  digitalWrite(powerPin, off);
//}
//
//////////////////////Speedometer Functions//////////////////////
```

```
//void GPSspeedometer()
//{
//  //collect NMEA data
//  delaying (200);
//
//  //get speed
//  if(gps.speed.isValid()==1)
//  {
//    Serial.println("Satellite Count:");
//    Serial.println(gps.satellites.value());
//    Serial.println("Speed MPH:");
//    Serial.println(gps.speed.mph());
//    Serial.println("");
//    gpsspeed=gps.speed.mph();
//  }
//
//  //Checks for error in connections
//  if (millis() > 5000 && gps.charsProcessed() < 10)
//  {
//    Serial.println("No GPS");
//    gpsspeed=9999;
//  }
//
//}
//
////Time to collect NMEA data
//static void delaying(unsigned long timems){
//  unsigned long timeRN = millis();
//  do{
//    while(serial_connect.available())
//      gps.encode(serial_connect.read());
//    } while (millis() - timeRN < timems);
//}
//
//////////////////////Printing to display////////////////////////////
//void print()
//{
//  int d=40;
//  if (i==25){
//     WaterSensor();
//     i=0;
//  }
//  GPSspeedometer();
//  if (gpsspeed<10){
//    d=50;
//  }
//  if (waterLevel <= 25) {
//    //Serial.print("No Water");
//    u8g.firstPage();
//    do {
//      u8g.setFont(u8g_font_fur35n);
//      u8g.setPrintPos(d, 40);
//      u8g.print(gpsspeed, DEC);
//      u8g.setFont(u8g_font_fur11r);
```

```
//      u8g.setPrintPos(30, 58);
//      u8g.print("No Water");;
//    } while( u8g.nextPage() );
//  }
//  else if (waterLevel > 25) {
//    //Serial.print("Water On Board");
//    u8g.firstPage();
//    do {
//      u8g.setFont(u8g_font_fur35n);
//      u8g.setPrintPos(d, 40);
//      u8g.print(gpsspeed, DEC);
//      u8g.setFont(u8g_font_fur11r);
//      u8g.setPrintPos(10, 58);
//      u8g.print("Water On Board");;
//    } while( u8g.nextPage() );
//  }
//}
```